This is to certify that the
dissertation entitled

MULTISTAGE TANDEM MASS SPECTROMETRY
STRATEGIES FOR THE TARGETED ANALYSIS OF
OXIDATIVE PROTEIN MODIFICATIONS

presented by

JENNIFER M FROELICH

has been accepted towards fulfillment
of the requirements for the

PhD degree in Chemistry

Major Professor's Signature

DEC. 8th, 2008

Date

MSU is an Affirmative Action/Equal Opportunity Employer

MULTISTAGE TANDEM MASS SPECTROMETRY STRATEGIES FOR THE TARGETED ANALYSIS OF OXIDATIVE PROTEIN MODIFICATIONS

By

Jennifer M. Froelich

A DISSERTATION

Submitted to
Michigan State University
in partial fulfillment of the requirements
for the degree of

DOCTOR OF PHILOSOPHY

Chemistry

2008

ABSTRACT

MULTISTAGE TANDEM MASS SPECTROMETRY STRATEGIES FOR THE TARGETED ANALYSIS OF OXIDATIVE PROTEIN MODIFICATIONS

By

Jennifer M. Froelich

The origin and control of *ex vivo* sample handling related oxidative modifications of methionine-, S-alkyl cysteine- and tryptophan-containing peptides obtained from typical in-solution or in-gel proteolytic digestion strategies, have been examined by capillary HPLC and MS/MS. The origin of increased oxidation levels was found to be predominately associated with the extensive *ex vivo* sample handling steps required for gel electrophoresis and/or in-gel proteolytic digestion of proteins prior to analysis by MS. Conditions for deliberately controlling the oxidation state (both oxidation and reduction) of these peptides, as well as for those containing cysteine, have also been evaluated using a series of model synthetic peptides and standard tryptic protein digests. Optimal conditions for oxidation and reduction were achieved via reaction with 30% hydrogen peroxide/5% acetic acid and reaction with 1 M dimethylsulfide/10 M hydrochloric acid, respectively.

The mechanisms for the gas-phase fragmentation reactions of singly and multiply protonated precursor ions of a series of model S-alkyl cysteine sulfoxide-containing peptides prepared by reaction with iodomethane, iodoacetamide, iodoacetic acid, acrylamide or 4-vinylpyridine, followed by oxidation with hydrogen peroxide have also been examined using multistage tandem mass spectrometry (MS/MS, MS^3 and MS^4), hydrogen/deuterium exchange and molecular orbital calculations (at the B3LYP/6-31 + G(d,p) level of theory). Dissociation of uniformly deuterated precursor ions of these

model peptides confirmed that the non-sequence neutral loss of alkyl sulfenic acid (XSOH) in each case occurred via a charge-remote five-centered *cis*-1,2 elimination reaction. Similarly, the charge state dependence to the mechanisms and product ion structures for the losses of CO_2, $CO_2 + H_2O$ and $CO_2 + CH_2O$ from S-carboxymethyl cysteine sulfoxide-containing peptides, and for the losses of $CH_2CHCONH_2$ and $CH_2CHC_5H_4N$, respectively from S-amidoethyl and S-pyridylethyl cysteine sulfoxide-containing peptide ions have also been determined.

A strategy involving the fixed-charge sulfonium ion derivatization, stable isotope labeling, capillary HPLC and automated neutral loss MS/MS and data dependent "pseudo MS^3" scans in a triple quadrupole mass spectrometer has also been developed for the targeted gas-phase identification, characterization and quantitative analysis of low abundance methionine-containing peptides present within complex protein digests. In contrast to MS-based quantitative analysis strategies, the neutral loss scan mode MS/MS method was able to achieve accurate quantification for individual peptides at levels as low as 100 fmol and at abundance ratios ranging from 0.1 to 10, present within a complex protein digest. Using a similar fixed-charge sulfonium ion derivatization and tandem mass spectrometry-based analysis strategy, methionine oxidation was successfully quantified following hydrogen peroxide treatment of the Ca^{2+}/calmodulin dependent serine/threonine phosphatase calcineurin.

ACKNOWLEGEMENTS

The road leading to the completion of my dissertation was not always an easy one for me and I know that I would not have made it to the end without the help of many people along the way. First and foremost, I would like to thank my advisor, Dr. Gavin Reid, for his constant support, dedication, creativity and unwillingness to let me give up. I would also like to thank the members of my committee, Dr. Merlin Bruening, Dr. Greg Swain and Dr. Jetze Tepe. I would like to thank the members of the Reid Research Group, both past and present, for all of their knowledge, friendship and support over the years and for helping me to enjoy my time here at MSU. I would especially like to thank Amanda "Pocahontas" Palumbo for always being there to listen and for helping me through all of those difficult times. I could never thank my family enough, especially my Mom, Ryan, Grandpa and Grandma Fritz and Aunt Debbie and Uncle Bob, for all of their support and encouragement, not only through graduate school, but through my entire life. My Mom, in particular, has been a constant source of strength for me and without her I would not be where I am today. Last, but certainly not least, I want to thank my husband Brad Cox for always believing in me, for making me a better person and for always being my biggest fan. I could not have done this without him.

I also wish to acknowledge the award of a U.S. Department of Homeland Security Fellowship, which is administered by the Oak Ridge Institute for Science and Education (ORISE) through an interagency agreement with the Department of Energy (DOE).

TABLE OF CONTENTS

LIST OF TABLES

TABLE **PAGE**

LIST OF FIGURES

LIST OF SCHEMES

SCHEME **PAGE**

CHAPTER ONE

Introduction*

1.1 An Overview of Mass Spectrometry-based Approaches for Proteome Analysis

The completion of several genome sequencing initiatives, particularly the Human Genome Project in 2003, has led to the identification of thousands of genes involved in cellular regulation. It has been demonstrated, however that mRNA transcript levels do not accurately reflect protein expression,[1] which is likely due to the vast number of transcriptional, translational and post-translational modifications associated with the proteome. Consequently, research efforts in the post-genomic era have shifted towards determining the unknown functional roles of proteins encoded by these genes, which has led to the field of proteomics. A major goal within the field of proteomics is to identify, characterize, and quantify changes in protein expression either at a particular time throughout the cell cycle or in response to a particular type of stimulation (e.g., disease). The outcome of this research should enable a more complete understanding of the processes which control normal cellular function and the changes in cell regulation that lead to the onset and progression of disease. Due to its speed, sensitivity and specificity, mass spectrometry (MS) has emerged as an integral technique in the field of proteomics.[2]

---

* The concepts discussed in this Chapter will be published in: Froelich, J.M.; Lu, Y.; Reid, G.E. Chemical Derivatization and Multistage Tandem Mass Spectrometry for Protein Structural Characterization. In: Practical Aspects of Ion Trap Mass Spectrometry. Vol. 5: Applications. CRC Press **2008**, *Submitted.* (invited chapter) and Froelich, J.M.; Reid, G.E. The Effect of Post-translational and Process-induced Modifications on the Multistage Gas-Phase Fragmentation Reactions of Protontated Peptide Ions. *Comb. Chem. High Throughput Screening* **2009**, *In Press.* (invited review article)

The "bottom-up" or "shotgun" tandem mass spectrometry (MS/MS) approach has emerged as one of the dominant methods employed for protein identification, characterization and quantitative analysis. In a typical bottom-up approach, unresolved protein mixtures, or individual proteins resolved by one- or two-dimensional electrophoretic or chromatographic methods, are subjected to proteolytic digestion, typically using trypsin. The resultant peptide mixture is then separated using one- or two-dimensional capillary liquid chromatography and introduced to the mass spectrometer by electrospray ionization (ESI), or by matrix-assisted laser desorption ionization (MALDI).[3-6] Following their mass analysis, individual protonated precursor ions are then automatically isolated and subjected to dissociation by tandem mass spectrometry, most commonly by using collision induced dissociation (CID).[7, 8] The identity of each peptide, and its protein of origin, is then subsequently achieved by *de novo* sequencing[7] or by database search algorithms which correlate the uninterpreted product ion spectrum with theoretically generated product ion spectra determined from peptides of the same mass contained within a known protein sequence database.[9-12]

Although the bottom-up approach has proven successful, there are several analytical challenges which limit its comprehensive application toward protein identification, characterization and quantitative analysis. Each of these challenges, as well as the strategies which have been developed to address them, will be described in more detail below.

1.2 Analytical Challenges Associated with Mass Spectrometry-based Approaches for Proteome Analysis

1.2.1 Mixture Complexity and Dynamic Range

The increase in sample mixture complexity resulting from proteolytic digestion, and the dynamic range associated with the proteome, present a formidable challenge for protein identification and characterization. To address these challenges, off- or on-line multidimensional chromatography (i.e., strong cation exchange followed by reversed-phase) is routinely employed to extensively fractionate proteolytically derived peptide mixtures prior to their analysis by mass spectrometry.[13] Numerous other strategies have also been used in conjunction with chromatographic separation to increase the number of unique peptide ions selected for analysis by MS/MS, particularly for those present at low abundance. Dynamic exclusion is one such approach, whereby the m/z values of precursor ions previously selected for fragmentation are automatically placed into an exclusion list for a defined period of time to prevent their reselection.[14-16] An iterative survey scan approach has also been described, which subjects peptide mixtures to multiple replicate LC-MS/MS analyses[14-16]. In each individual analysis, precursor ions are selected for fragmentation from a narrow m/z window rather than from the entire m/z range. In addition, Wang *et al.* recently described a strategy by which the m/z of peptide ions that are positively identified in an initial LC-MS/MS run are placed into an exclusion list in subsequent runs of the same peptide mixture to prevent these peptides from being re-selected for fragmentation.[17]

The identification of low abundance proteins present in complex biological samples (e.g., human serum or cerebrospinal fluid) can also be improved by removing

proteins which are present at high abundance. Traditionally, this has been achieved using dye-ligand affinity chromatography[18] or antibody-based methods such as immunoaffinity chromatography.[19, 20] In an alternative approach, combinatorial ligand library beads have recently been employed to increase the concentration of low abundance proteins while effectively reducing the concentration of high abundance proteins.[21-23] In this approach, a protein mixture is exposed to beads which have been synthesized with a library of diverse ligands. Each individual protein or peptide present within the sample will bind to the ligand exhibiting the strongest intermolecular interaction. Those proteins which are present at high abundance will continue to bind to the beads until a saturation limit is reached. However, low abundance proteins, which are present at concentrations below the saturation limits of the beads, will be extensively bound. Using this approach, the dynamic range of protein concentrations present within a complex biological sample can be significantly reduced.

Also in an effort to decrease sample mixture complexity and improve dynamic range, numerous "targeted" approaches have been described, which analyze only a subset of the peptides contained within a proteolytically derived peptide mixture. For example, affinity capture methods have been extensively employed to enrich for peptides containing specific post-translational modifications or selected amino acid residues. Immobilized metal ion affinity chromatography (IMAC) incorporating Fe^{3+}, Ga^{3+} or Al^{3+} has been used to isolate phosphorylated peptides,[24, 25] while the enrichment of histidine-containing peptides has been achieved using IMAC columns loaded with Cu^{2+}.[26] In an analogous approach, organomercurial agarose beads have been employed to isolate

cysteine-containing peptides from a tryptic digest of yeast cell lysates.[27] Metal oxide affinity chromatography (MOAC) methods utilizing titanium dioxide (TiO_2), zirconium dioxide (ZrO_2) and aluminum oxide (Al_2O_3) have also been used for the highly selective enrichment of phosphopeptides as an alternative strategy to IMAC.[28-30] The enrichment of glycosylated peptides prior to mass spectrometry analysis has also been achieved using lectin affinity chromatography.[31]

As an alternative "targeted" approach, peptide subsets may be enriched via the chemical derivatization of specific functional groups within a peptide (i.e., amino acid side chains) followed by isolation using affinity capture, covalent capture or chromatographic strategies.[14, 32-48] Specific examples include the biotinylation of cysteine residues within a peptide and subsequent enrichment using streptavidin affinity chromatography,[14, 32, 33] or the introduction of a quaternary amine tag to the side chain of cysteine residues followed by their isolation using strong cation exchange (SCX) chromatography.[38] Thiol-specific covalent resins have also been employed to enrich for cysteine-containing peptides.[41-44] For example, Wang *et al.* have used a cysteine covalent capture strategy to characterize the mouse brain proteome.[44]

1.2.2 Quantitative Analysis

In addition to protein identification and characterization, another major goal of proteomics research is to quantify protein expression levels. However, mass spectrometry is not inherently quantitative. Thus, the intensity of a peptide ion introduced to the mass spectrometer via ESI or MALDI does not necessarily reflect the amount of peptide

present in the sample, due to the strong dependence of ionization on the physical and chemical nature of the analyte. To overcome this challenge, numerous quantitative analysis strategies have been developed which measure the differences in protein abundances between two different cellular states of a biological system (e.g., normal and diseased cells).

Differential quantitative analysis has previously been performed at the protein level using two-dimensional differential gel electrophoresis (2D DIGE).[49-51] In this approach, individual protein populations are covalently labeled with structurally similar, but spectrally distinct fluorophores. The protein populations are then combined and separated by 2D polyacrylamide gel electrophoresis (PAGE). Protein quantitation is achieved via imaging of the gel using different fluorescence excitation wavelengths. To determine the identity of those proteins which are either up- or down-regulated, gel spots are individually excised, subjected to enzymatic in-gel digestion then the resultant peptide mixture is subsequently analyzed by mass spectrometry. Although this technique overcomes many of the disadvantages associated with protein quantitation via traditional 2D PAGE, it still suffers from limited dynamic range (10^4), as well as a limited ability to resolve proteins with extremes of molecular weight and pI. Additionally, accurate quantitative analysis is precluded when two or more proteins are present in the same gel spot.

The quantitative analysis of protein expression levels from different protein populations has also been achieved using "label free" mass spectrometry-based approaches.[52-55] In the label free approach, control and experimental samples are enzymatically digested and analyzed individually by LC-MS and MS/MS. Protein

abundances are then determined by summing the extracted ion chromatographic peak areas,[52, 55] peptide identification scores obtained from database analysis[53] or MS/MS spectral counts[54, 55] for all the peptide ions identified for a single protein. However, in order to achieve accurate quantitation, highly reproducible LC-MS analysis is required to minimize shifts in retention time and fluctuations in MS signal intensity. Furthermore, protein quantitation may be precluded when peptides are present at low abundance or the MS signals of peptide ions with identical m/z values elute at the same retention time.

Differential quantitative analysis has also been achieved via the incorporation of differential stable isotope labels between control and experimental samples. To date, the majority of stable isotope labeling methods have involved either *in vivo* metabolic labeling[56-58] or *in vitro* chemical derivatization.[32, 33, 35, 41-43, 58-60] *In vivo* metabolic labeling approaches such as SILAC (Stable Isotope Labeling by Amino acids in Cell culture)[57] incorporate a differential stable isotope label by growing one population of cells in normal media and a second population of cells in media enriched with an isotopically encoded amino acid. Following protein extraction, the two protein populations are combined and enzymatically digested. Protein expression levels are then determined by MS analysis via comparison of the relative abundances of intact peptide precursor ions derived from the "light" and "heavy" isotopically labeled samples.

In vitro chemical derivatization approaches employed for differential quantitative analysis either label all peptides within a proteolytically derived peptide mixture (i.e., at the N- or C-terminus), or target specific amino acid side chains or post-translational modifications. A general overview of commonly employed chemical derivatization strategies is shown in Figure 1.1. A more detailed discussion of each of these chemical

derivatization approaches can be found in a review article by Julka *et al.*[58] and the references cited therein. Although numerous chemical derivatization and quantitative analysis strategies have now been described, one of the earliest of these involved use of the isotope coded affinity tag (ICAT) reagent.[32] The first generation ICAT reagent, designed by Gygi *et al.*, consisted of an iodoacetyl thiol-specific reactive group, a biotin tag and an oxyethylene linker region which contained either eight hydrogen atoms (light ICAT reagent) or eight deuterium atoms (heavy ICAT reagent).[32] In this approach, all cysteine residues from control and experimental samples are labeled with the light and heavy ICAT reagent, respectively. After labeling, the two protein populations are combined, subjected to enzymatic digestion and then the ICAT labeled peptides are isolated from non-labeled peptides using avidin affinity chromatography. Relative protein expression levels are then determined by measuring the peak ratios of peptide pairs in MS mode, while peptide identification is achieved by MS/MS analysis of individual peptide precursor ions. Using the ICAT approach, protein quantitation and a reduction in sample mixture complexity are achieved simultaneously.

Figure 1.1 Generic summary of the stable isotope labeling strategies currently employed for mass spectrometry-based relative protein quantitation. All reactions shown to occur on the amino terminus also apply to the ε-amino group of lysine residues. The numbers in parentheses indicate the respective references cited in the review article by Julka *et al. J. Proteome Res.* **2004**, *3*, 350-363. [Reproduced from reference 58]

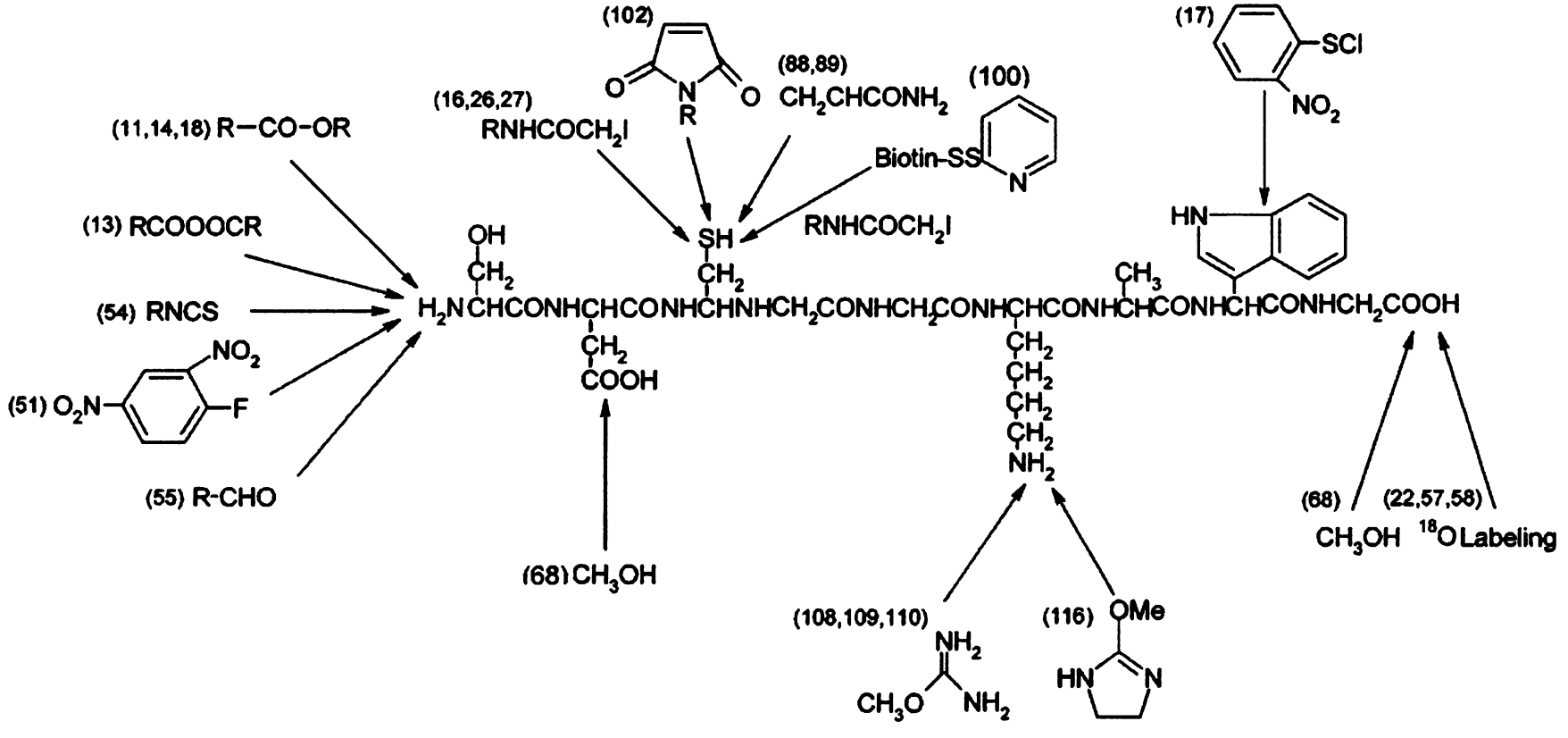
(102)
(88,89)
CH2CHCONH2
(100)
(17)
SCl
NO2
(16,26,27)
RNHCOCH2I
(11,14,18) R—CO—OR
Biotin-SS
N
(13) RCOOOCR
RNHCOCH2I
HN
(54) RNCS
H2NCHCONHCHCONHCHNHCH2CONHCH2CONHCHCONHCHCONHCHCONHCH2COOH
(51) O2N
F
(55) R-CHO
(68) CH3OH
(108,109,110)
(116) OMe
(68)
(22,57,58)
CH3OH 18OLabeling

Despite the initial success of this approach, a number of disadvantages associated with the first generation ICAT reagent have been noted. For example, the presence of deuterium atoms in the linker region of the heavy ICAT reagent may result in the chromatographic separation of light and heavy ICAT labeled peptides during reversed-phase chromatography, thereby precluding their accurate quantitation. To ensure that light and heavy labeled peptides co-elute, a second generation ICAT reagent was designed to include ^{13}C rather than ^{2}H in the linker region.[33] In addition, fragmentation of the bulky biotin tag has often been observed during CID-MS/MS analysis, which complicates interpretation of the resultant MS/MS spectra for peptide identification. Thus, an acid-cleavable group, which connects the biotin moiety with the thiol-specific isotope tag, was also incorporated into the second generation ICAT reagent to cleave the biotin moiety from modified peptides.[33] In contrast to the first generation ICAT reagent, the small size of the remaining tag results in minimal fragmentation following CID-MS/MS.

As an alternative to the solution-phase ICAT approach, a number of solid-phase isotope labeling strategies have also been developed.[33, 41-43] Solid-phase covalent capture methods enable more stringent wash conditions to be employed in an effort to remove non-specifically bound peptides. In addition, peptide labeling and isolation can be achieved in a single step. Zhou *et al.* have described a method for solid-phase stable-isotope labeling of cysteine-containing peptides from *Saccharomyces cerevisiae* using controlled-pore glass beads containing an *o*-nitrobenzyl-based photocleavable linker, a stable isotope tag incorporating either seven hydrogen or seven deuterium atoms and a thiol-specific iodoacetyl group.[41] Proteins from control and experimental samples were

individually proteolyzed and then cysteine-containing peptides were captured by d_0- or d_7-beads, respectively. The beads were then combined, washed and photolytically cleaved to release the differentially labeled cysteine-containing peptides. Following LC-MS/MS analysis in a quadrupole ion trap it was determined that more proteins were able to be identified and quantified using the solid-phase isotope labeling approach than when the samples were prepared using the first generation solution-phase ICAT reagent. A similar solid-phase isotope labeling approach termed acid-labile isotope-coded extractants (ALICE) has also been developed by Qiu *et al.*[42] In this approach, cysteine-containing peptides are captured using a nonbiological polymer which has been chemically modified to contain a maleimido thiol-reactive group and an acid-labile linker in both heavy and light isotope-encoded forms.

For the majority of stable-isotope labeling approaches, including those described above, quantitative analysis is achieved in MS-mode. Limitations are encountered however, when one or both of the differentially labeled peptide ions are present at or below the level of chemical noise in the MS spectrum, thereby precluding quantitative analysis. Furthermore, accurate quantitation may be precluded when the m/z values of differentially labeled peptide ions overlap with non-labeled or other labeled components present in the peptide mixture.

To address these challenges, several differential quantitative analysis strategies have been recently described whereby quantitation is performed by MS/MS, rather than by MS.[61-67] The commercially available iTRAQ approach, which utilizes a multiplexed set of reagents to quantitate relative expression levels for multiple protein populations, is one example.[64, 65] The initial reagent employed in this approach consists of a reporter

group, a balance group and an amine specific peptide reactive group. Differential stable isotope labels are incorporated into the balance and reporter groups of four iTRAQ reagents in such a way that the tag generated upon reaction with a peptide has the same overall mass (+145.1 Da). To use this approach for quantitative analysis, peptide mixtures are individually labeled with one member of the multiplexed set after which the labeled peptide mixtures are combined and subjected to mass spectrometry analysis. In MS-mode, identical tagged peptides from each of the four samples are present at the same m/z value, therefore the MS-mode sensitivity is maximized. Upon CID-MS/MS of the peptide precursor ions, the balance group is lost as a neutral, while the reporter group retains a charge to generate low m/z product ions at m/z 114, 115, 116 or 117, which are subsequently used for quantitative analysis. The product ions that can be used to identify the sequence of the labeled peptide may also be generated during the MS/MS experiment and remain isobaric. Compared to conventional MS-based approaches, increased sensitivity and greater specificity is achieved due to the reduction in chemical noise associated with the MS/MS experiment. To increase the number of protein populations which can be analyzed via this approach, an 8-plex version of the iTRAQ strategy was recently introduced.[66]

Recently, Li *et al.* described a similar MS/MS-based quantitative analysis strategy termed Cleavable Isobaric Labeled Affinity Tag or CILAT.[67] Essentially a hybrid of the ICAT and iTRAQ approaches, the CILAT reagent includes an isobaric tag consisting of a reporter group and a balance group. The reagent also incorporates a biotin moiety for the enrichment of modified peptides via avidin affinity chromatography and an acid cleavable linker to remove the biotin moiety prior to MS/MS analysis. The thiol group

employed in this reagent is used to modify tyrosine residues within peptides which have been converted to ortho-quinone via oxidation with tyrosinase.

1.3 Tandem Mass Spectrometry and Gas-Phase Chemistry of Protonated Peptide Ions

The utility of the tandem mass spectrometry based approaches for protein identification and characterization described above, particularly for the analysis of peptides containing process-induced or post-translational modifications, is highly dependent on the ability to derive sufficient information from the peptide product ion spectrum to enable its subsequent database analysis, as well as on the ability to accurately predict *in silico* the types and abundances of the various product ions that will be generated.[68, 69] The successful development and application of these methods, therefore, have been greatly facilitated by the concurrent development of an improved understanding of the mechanisms and other factors (e.g., precursor ion charge state, amino acid composition, peptide conformation, product ion structures, etc.) that influence the gas-phase fragmentation reactions of protonated peptide ions,[70] and the development of methods for controlling the fragmentation reactions of peptide ions in the gas-phase.

1.3.1 Concepts and Terminologies Associated with the Gas-phase Fragmentation Reactions of Protonated Peptide Ions

A central concept underlying the mechanisms currently proposed for the gas-phase fragmentation reactions of protonated peptide ions under low-energy collision induced dissociation (CID) conditions[71] is that of the "mobile proton", originally

described by the groups of Wysocki and Gaskell.[72-75] **"Proton mobility"** has been divided into three categories.[76] Peptides are classified as "mobile" when the total number of ionizing protons is greater than the total number of basic residues (i.e., combined number of arginine, lysine and histidine residues), and as "non-mobile" when the total number of ionizing protons is less than or equal to the number of arginine residues. Those peptides which fall outside of these two categories (i.e., when the total number of ionizing protons is greater than the number of arginine residues, but less than or equal to the total number of basic residues) are classified as "partially mobile".

Depending on the proton mobility of the precursor ion, the gas-phase fragmentation of protonated peptide ions may proceed via **"charge-directed"** (i.e., an ionizing proton initiates or is directly involved in the fragmentation reaction) or **"charge-remote"** (i.e., an ionizing proton is not directly involved in the fragmentation reaction) reaction mechanisms. The product ions formed from these reactions can be classified as **"sequence ions"** (i.e., those resulting from fragmentations along the peptide backbone from which information regarding the amino acid sequence can be derived) or **"non-sequence ions"** (e.g., those resulting from fragmentation at the side chains of certain amino acids, from which diagnostic information regarding the composition of the peptide can be derived), and can be further classified as **"non-selective"** (i.e., those resulting from fragmentation at multiple sites within the peptide ion) or **"selective"** (i.e., those that result from fragmentation at a single site within the peptide ion).

A variety of approaches have been employed to provide evidence for the mechanisms and other factors that influence the gas-phase fragmentation reactions of protonated peptide ions. These include the use of multistage tandem mass spectrometry

(MS^n) coupled with isotopic and structural labeling, comparison of the MS^3 spectra of product ions with the MS/MS spectra of "authentic" product ion structures formed via independent synthesis, gas-phase ion-molecule reactions, determination of activation energies either through the measurement of dissociation kinetics or via energy-resolved dissociation experiments, theoretical molecular orbital modeling techniques, and the statistical analysis of large experimentally derived datasets.[77-85]

1.3.2 Overview of the Mechanisms Responsible for the Formation of "Sequence" Ions from the Gas-Phase Fragmentation of Protonated Peptides

The formation and types of sequence ions resulting from the gas-phase fragmentation of protonated peptide ions are highly dependent on the proton mobility of their precursor ions.[76, 86, 87] Under mobile proton conditions, both non-selective and selective sequence ions are typically observed. Non-selective fragmentation reactions typically result in the formation of a series of complementary b- and y-type sequence ions,[88, 89] via cleavage of amide bonds along the peptide backbone (Scheme 1.1). This type of fragmentation is generally accepted to proceed via a charge-directed neighboring group participation mechanism, in which localization of an ionizing proton at either the carbonyl oxygen or the amide nitrogen of the amide bond initiates nucleophilic attack from an adjacent amide carbonyl.[77, 90-92] The pathway shown in Scheme 1.2 for dissociation of the second amide bond in a protonated tetrapeptide can be regarded as a general mechanism for the formation of $b_{(n\geq 2)}$ and y_n product ions. Dissociation of this bond results in an initial ion-molecule complex between the b-type product ion consisting

of a cyclic oxazolone structure containing the two N-terminal amino acid residues,[93-96] and a truncated neutral peptide. Direct separation of this ion-molecule complex would result in observation of the b_2 ion (pathway A of Scheme 1.2), while intermolecular proton transfer prior to its separation would yield the y_2 ion containing the two C-terminal amino acid residues (pathway B of Scheme 1.2). The relative abundances of these b- and y-type product ions have been shown to be dependent on the proton affinities of their respective N- and C-terminal fragments,[97] as well as the lifetime of the ion-molecule complex[7]. Subsequent fragmentation and rearrangement of the initial product ions can also occur, particularly for the oxazolone-containing b-type ions, thereby complicating the appearance of the resultant product ion spectrum.[98]

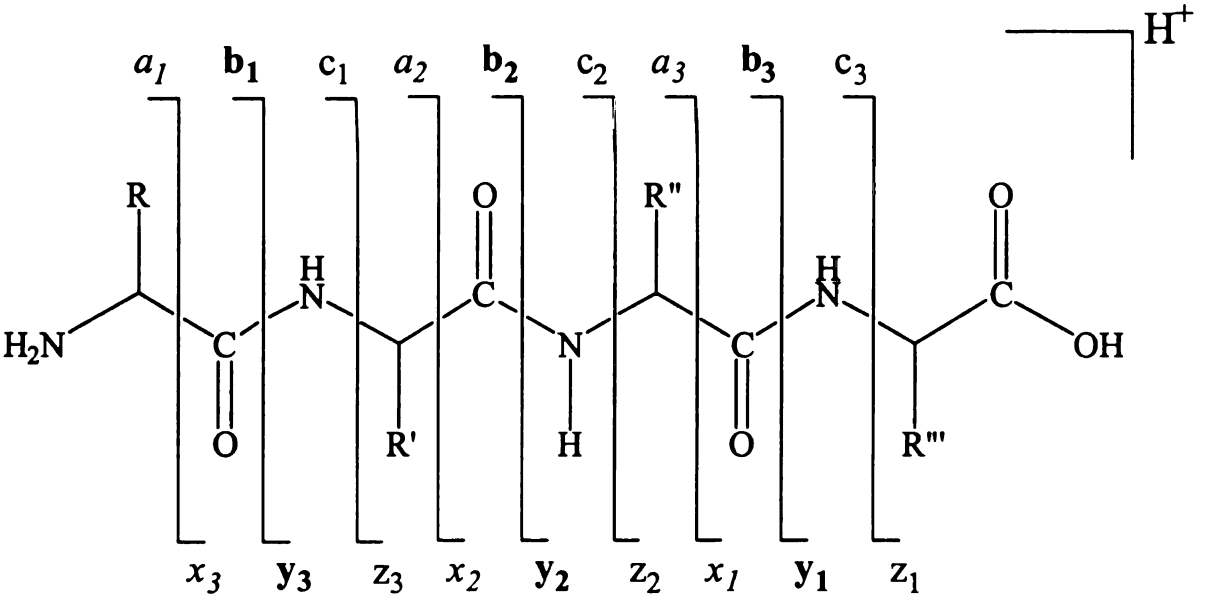

Scheme 1.1 Nomenclature for peptide fragment ions.

Note that while Scheme 1.2 shows the amide bond fragmentation reaction proceeding via an amide nitrogen protonated precursor,[99-101] an alternative dissociation

mechanism initiated by protonation at the thermodynamically preferred carbonyl oxygen[102] could also be considered, involving a simple intramolecular "proton shuttle" mechanism within the tetrahedral cyclic intermediate that would result from the initial nucleophilic attack process, analogous to that proposed for intramolecular proton transfer within protonated precursor ions, prior to amide bond cleavage. Indeed, previous results from the literature indicate that product ions formed via initial protonation at the carbonyl oxygen can be observed experimentally, at least under certain conditions.[103, 104]

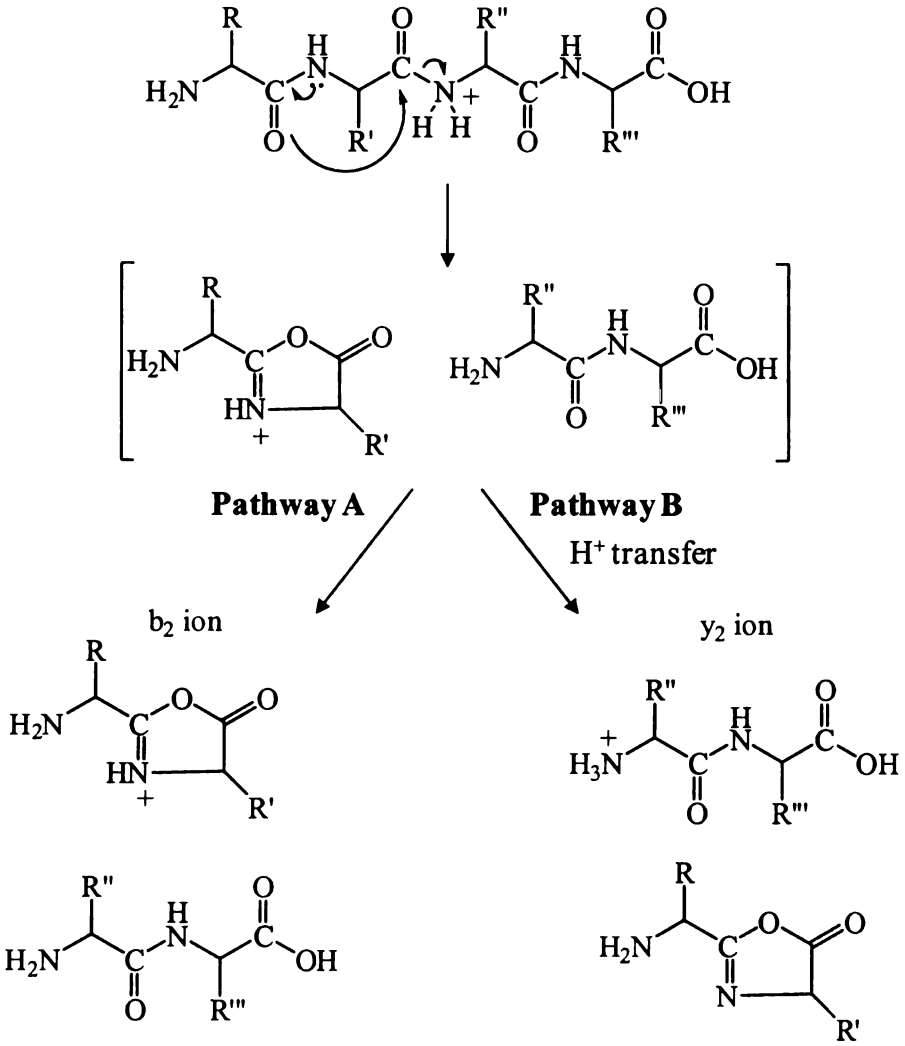

Scheme 1.2 Generally accepted mechanism for the formation of b- and y-type sequence product ions following CID-MS/MS.

Selective fragmentation reactions can also be observed under mobile proton conditions, typically when proline residues are present within a protonated peptide ion. These reactions often result in the formation of dominant b- or y- type sequence ions by fragmentation of the imide bond N-terminal to the proline residue, presumably due to the higher local proton affinity of the imide bond, therefore leading to a greater degree of

localization of the ionizing proton, compared to that of a conventional amide bond.[7, 76, 86, 87, 105]

Under non-mobile proton conditions, selective fragmentation reactions typically dominate the appearance of the product ion spectrum. For example, dominant b- or y-type sequence ions are typically observed under these conditions as a result of selective cleavage C-terminal to aspartic acid residues, via either a charge-remote or salt bridged mechanism, whereby the acidic proton of the aspartic acid side chain facilitates cleavage of the amide bond.[84, 106-113] Notably, it has been demonstrated that the specificity associated with the formation of selective b- and y-type sequence ions can be used to significantly enhance the utility of database search methods for the identification of aspartic acid-containing peptides.[114, 115]

1.3.3 Overview of the Mechanisms for the Formation of "Sequence" and "Non-Sequence" Ions from the Gas-Phase Fragmentation of Protonated Peptides containing Post-Translational or Process-Induced Modifications

The presence of post-translational or process-induced modifications of certain amino acids can also influence the observation of selective sequence ions from the fragmentation of protonated peptides. For example, the oxidation of cysteine to cysteine sulfinic acid (Cys-SO_2H) or to cysteine sulfonic acid (Cys-SO_3H) has been observed to result in selective fragmentation C-terminal to the oxidized cysteine residue under conditions of limited proton mobility.[106, 116-120] Conversely, while the presence of histidine within a peptide sequence has previously been shown to result in some

enhancement in selective cleavage C-terminal to the histidine residue,[86, 112] a recent study by Bridgewater *et al.* has found that oxidation of histidine, presumably to 2-oxohistidine, eliminates this selective fragmentation behavior.[121]

The dissociation reactions of protonated peptides containing post-translational or process-induced modifications under non-mobile proton conditions are also often observed to result in the formation of dominant non-sequence product ions via selective fragmentation of the side chains of the modified amino acid.[122, 123] Examples include the neutral loss of phosphoric acid (H_3PO_4, 98 Da) from phosphoserine- or phosphothreonine-containing peptides,[80, 124-126] the loss of HPO_3 (80 Da) from phosphotyrosine-containing peptides,[124-127] the loss of SO_3 (80 Da) from O-sulfonoserine-, O-sulfonothreonine-[128, 129] or thiosulfate- (-S-SO_3H) containing peptides,[130] the loss of a glycan moiety from O-linked N-acetylgalactosamine-containing peptides,[131, 132] the loss of alkyl sulfenic acid (RSOH) from methionine sulfoxide- (i.e., CH_3SOH, 64 Da)[81] and S-alkyl cysteine sulfoxide-containing peptides,[133-135] the loss of H_2O from cysteine sulfenic acid (Cys-SOH)-containing peptides,[135, 136] the loss of H_2SO_2[118-120] or H_2SO_3[106, 117-119] from cysteine sulfinic acid- and cysteine sulfonic acid-containing peptides, respectively, the loss of SO_2+NH_3 from N-terminal cysteine sulfinic acid-containing peptides,[120] and the loss of H_2O from peptides containing oxidized tryptophan.[78]

The formation of these non-sequence ions can often provide useful diagnostic information regarding the presence of a particular modified amino acid residue within a

peptide, and may therefore be attractive for use as "targets" for selective proteomic analysis. However, their formation in high relative abundance can result in the loss of sequence information, potentially compromising peptide identification. Under such circumstances, isolation and further dissociation of this initial product ion (by MS^3 in a quadrupole ion trap mass spectrometer, or by energy resolved "pseudo" MS^3 in triple quadrupole or hybrid quadrupole-time of flight mass spectrometers), may be required in order to unambiguously identify the peptide or to localize the modification to a specific amino acid residue within the peptide sequence.[25, 28, 137-140]

1.3.4 Alternative Dissociation Methods and Chemical Derivatization Strategies for Controlling the Formation of "Sequence" versus "Non-Sequence" Product Ions

It is clear from the above discussion that the mechanisms responsible for the gas-phase fragmentation reactions of protonated peptide ions, and the appearance of the resultant product ion spectrum, are all highly dependent upon the proton mobility of the peptide precursor ion. This results in a generally limited ability to control or direct the low energy CID-MS/MS fragmentation reactions of protonated peptide ions toward a particular fragmentation pathway (e.g., sequence ion backbone fragmentation versus non-sequence ion side chain cleavage), thereby placing limitations on the ability of these methods to be selectively employed for either comprehensive or targeted proteome analysis. To address these limitations, alternative dissociation techniques have recently been developed in order to provide more extensive non-selective sequence ion information, while a number of chemical derivatization strategies have also been developed to control or direct the fragmentation reactions of protonated peptide ions

toward the formation of either non-selective sequence-ions, or selective non-sequence ions.

1.3.4.1 Alternative Dissociation Techniques

The recently developed alternative dissociation methods of electron capture dissociation (ECD)[129, 135, 141-146] and electron transfer dissociation (ETD)[120, 129, 147-152] have proven to be particularly successful for the characterization of protonated peptide ions containing post-translational or process-induced modifications. ECD involves the capture of an electron with near thermal energy by a multiply protonated ($[M+nH]^{n+}$) precursor ion, while ETD occurs via electron transfer to a multiply protonated precursor ion from an anion of low electron affinity. In both cases, an odd electron reduced charge state ($[M+nH]^{(n-1)+\bullet}$) product is formed, that undergoes fragmentation to yield a series of non-selective c- and z-type sequence ions (Scheme 1.1). In contrast to the fragmentation processes typically observed by CID, the formation of product ions from ECD and ETD is generally indifferent to the proton mobility of the precursor ion, or to the presence of otherwise labile amino acid modifications, such as phosphorylation,[141, 147, 148, 152] glycosylation,[143, 146, 149] oxidation[120, 135] or sulfonylation.[129]

1.3.4.2 Chemical Derivatization Strategies for Protein Identification and Characterization

In an effort to improve peptide identification and characterization by *de novo* sequencing or database search algorithm strategies, numerous chemical derivatization approaches have been developed to direct the fragmentation reactions of peptides toward

the formation of a series of non-selective sequence product ions. One such approach involves chemical derivatization of the side chains of basic amino acid residues within a peptide to alter proton affinity.[153-156] For example, the reagents acetylacetone[153] and malondialdehyde[154] have been employed to chemically modify guanidino groups on the side chain of arginine residues in an effort to decrease the proton affinity of these sites. By decreasing the proton affinity of the arginine side chain, an ionizing proton is less likely to be sequestered and is therefore available to initiate cleavage of the amide bonds along the peptide backbone. It has been demonstrated that CID-MS/MS of these chemically modified arginine-containing peptides results in an increased number and intensity of b- and y-type sequence product ions compared to their non-derivatized counterparts, thereby improving peptide identification.[154] In a similar approach, the ε-amino group of C-terminal lysine residues have been converted to an imidazole derivative via chemical modification with 2-methoxy-4,5-dihydro-1H-imidazole.[155, 156] In contrast to producing both b- and y-type sequence ions, the increased proton affinity resulting from this chemical modification predominantly results in the formation of a series of y-type ions, yielding a simplified MS/MS product ion spectrum for interpretation, particularly for *de novo* peptide sequencing.

The chemical derivatization of peptide N- or C-termini to incorporate a fixed positive or negative charge is yet another approach that has been extensively employed to direct peptide ion fragmentation toward the formation of a desired series of non-selective sequence product ions.[146, 157-166] For example, it has been shown that the chemical derivatization of peptide N-termini with S-pentafluorophenyl [*N*-tris(2,4,6-trimethoxyphenyl)phosphonium]acetate bromide (TMPP-AcSC_6F_5 bromide)[158, 159] or

with [tris(2,4,6-trimethoxyphenyl)phosphonium]acetic acid N-hydroxysuccinimide ester (TMPP-Ac-OSu)[160] to form [tris(2,4,6-trimethoxyphenyl)phosphonium]acetyl (TMPP-Ac) derivatives directs the gas-phase CID fragmentation reactions of protonated peptides toward the formation of a series of a- or b-type sequence product ions. Adamczyk *et al.* have also demonstrated that N-terminal b- and a-type ions are predominately formed following CID-MS^3 analysis of the TMPP-Ac containing b-type ions produced in the first stage of tandem mass spectrometry analysis,[160] which can be particularly useful for the analysis of larger peptides, whereby incomplete sequence information is often obtained following CID-MS/MS alone. Recently, fixed-charge chemical derivatization of peptide N-termini with (N-succinimidyloxycarbonylmethyl)tris(2,4,6-trimethoxyphenyl)phosponium acetate to form an acetylphosphonium derivative has also been used to increase the sequence coverage obtained by electron capture dissociation of *o*-phosphorylated and *o*-glycosylated peptides.[146]

Peptide N-termini have also been chemically modified with 4-sulfophenyl isothiocyanate and various other sulfonic acid derivatives to incorporate a fixed negative charge.[163-166] The introduction of a fixed negative charge on the N-terminus of the peptide, and the localization of an ionizing proton on the side chain of arginine or lysine residues contained within the peptide sequence, results in the formation of a neutral peptide molecule. To analyze the peptide via mass spectrometry, a second ionizing proton is therefore required. Since the arginine or lysine side chains are already protonated, the second ionizing proton is able to move along the peptide backbone and initiate cleavage of the amide bonds. Using this approach, a single series of y-type sequence product ions are generated.

Numerous chemical derivatization strategies have also been developed to direct the fragmentation reactions of protonated peptides toward the selective formation of single characteristic sequence type product ions.[113, 167, 168] For example, Summerfield and coworkers have demonstrated that N-terminal derivatization with phenylisothiocyanate to form the corresponding phenylthiocarbamoyl (PTC) derivative results in exclusive fragmentation of the amide bond between the first two amino acid residues under mobile proton conditions to generate a b_1 ion and the complementary y_{n-1} ion.[167, 168] The incorporation of a fixed-charge TMPP-Ac tag to the N-terminus of aspartic acid-containing peptides has also been employed to promote enhanced cleavage C-terminal to aspartic acid residues.[113] The specific information obtained regarding the presence and location of an aspartic acid residue within a peptide sequence has been shown to improve the specificity of database search analysis strategies employed for protein identification.[114]

Recent work in our laboratory has also examined the potential for controlling the formation of non-sequence product ions for use in selective protein identification and characterization via the introduction of fixed-charge derivatives to peptides containing certain amino acid side chains.[169-172] For example, it has been demonstrated that CID-MS/MS of peptide ions containing fixed-charge sulfonium ions on the side chains of methionine- or cysteine-containing peptides, formed by reaction with the alkylating reagents phenacylbromide ($BrCH_2COC_6H_5$)[169-171] or (3-[*N*-bromoacetamido]propyl)-methylphenacylsulfonium bromide (BAPMPS),[172] respectively, results in exclusive fragmentation of the derivatized side chain and the formation of a single "diagnostic"

product ion via the neutral loss of methylphenacylsulfide ($CH_3SCH_2COC_6H_5$) (Scheme 1.3A and 1.3B, respectively). The mechanisms for these selective fragmentation reactions have been demonstrated, by using multistage tandem mass spectrometry of regioselectively deuterated sulfonium ion containing tryptic peptides and by molecular orbital calculations, to occur via S_N2 neighboring group participation reactions.[170, 172] Notably, the selective fragmentation reactions of the side chain sulfonium ion derivatized peptides have also been shown to occur independently of the proton mobility of the precursor ion. Additional structural information on peptide ions initially identified from the selective fragmentation reactions is readily achieved by subjecting the characteristic MS/MS product ion to further dissociation by MS^3 in a quadrupole ion trap mass spectrometer or by energy resolved "pseudo" MS^3 in a triple quadrupole mass spectrometer.

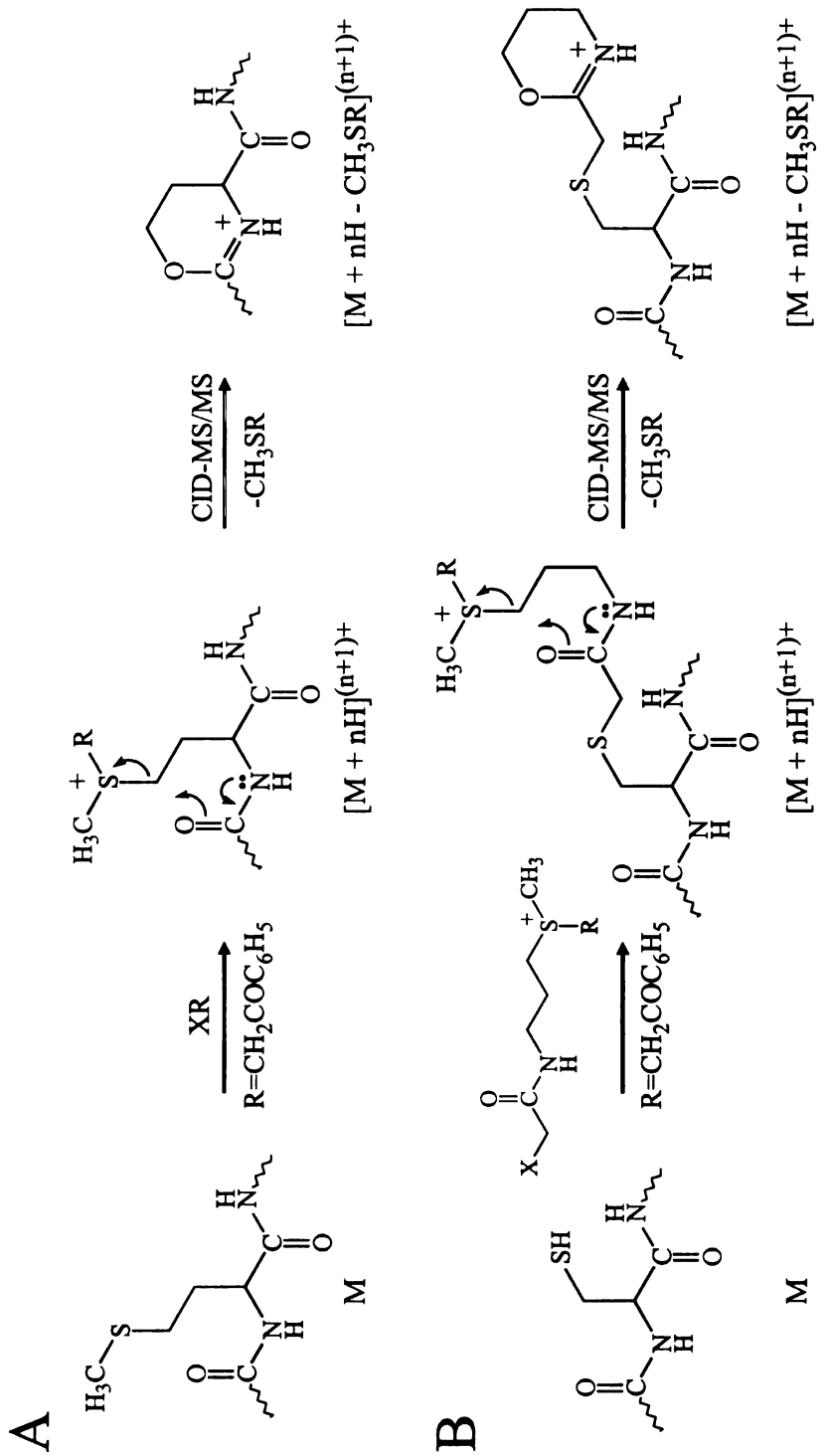

Scheme 1.3 Gas-phase fragmentation reactions of phenacylsulfonium ion derivatized methionine- and cysteine-containing peptides.

A number of approaches described in the literature have also demonstrated that selective dissociation can be achieved by first generating a radical site within a peptide or protein.[173-176] For example, Ly *et al.* recently described an approach whereby reactive tyrosine residues within individual proteins were converted to 3-iodotyrosine under natively folded conditions.[175] The modified tyrosine-containing proteins were ionized via ESI, introduced to a linear quadrupole ion trap and subsequently subjected to UV photodissociation which resulted in the formation of a radical site on the aromatic ring of the modified tyrosine residues. Following re-isolation and low-energy CID, radical-directed selective cleavage adjacent to the tyrosine residues was observed, resulting in the formation of a-type sequence product ions. Similar results were also obtained for proteins containing exposed histidine residues, which were also shown to be susceptible to iodination. The information generated via this site-specific fragmentation could potentially be used to reduce the computational time associated with database search analysis strategies.

1.3.4.3 Chemical Derivatization Strategies for Quantitative Analysis of Protein Expression

Numerous chemical derivatization approaches have also been described to direct the fragmentation reactions of peptides toward the selective formation of isotopically encoded low mass product ions for quantitative peptide analysis (see Section 1.2.2). Although the MS/MS-based quantitative analysis strategies described in Section 1.2.2 above overcome the limitations associated with MS-based approaches, the low m/z product ions required for quantitation are generally observed below the low mass cut-off

introduced during MS/MS in quadrupole ion trap mass spectrometers, thereby precluding their use for quantitative analysis in this type of instrumentation. Thus, to date, the majority of proteomic experiments utilizing these reagents have been performed using quadrupole time-of-flight (QTOF), time-of-flight/time-of-flight (TOF/TOF), and to a lesser extent, hybrid triple quadrupole/linear ion trap mass spectrometers.[177-181] However, a new "High Amplitude Short Time Excitation" (HASTE) dissociation technique (an analogous method is termed Pulsed Q Collision Induced Dissociation (PQD) in the commercially available ion trap mass spectrometry platforms available from Thermo Scientific), has been recently implemented which enables the low m/z product ions normally excluded from CID spectra to be observed.[182] Using the iTRAQ approach coupled with PQD-MS/MS on a Thermo linear quadrupole ion trap, Meany and coworkers were able to successfully quantify carbonylated proteins enriched from rat skeletal muscle mitochondria.[183] Griffin *et al.* also compared PQD-MS/MS in a linear quadupole ion trap mass spectrometer with MS/MS in a quadrupole time-of-flight mass spectrometer for the quantitative analysis of iTRAQ labeled peptides derived from a standard yeast lysate mixture.[184] It was determined that similar quantitative accuracy could be achieved using both instrumentation platforms, although careful tuning of the relative collision energy was required for efficient fragmentation by PQD. Protein kinases extracted from cells which had been incubated with various drugs have also been quantified using the iTRAQ approach and PQD-MS/MS in a linear quadrupole-Orbitrap mass spectrometer.[185]

It has also been demonstrated that the iTRAQ MS/MS based quantitative analysis strategy can be used in conjunction with the quadrupole ion trap by performing multiple

stages of mass analysis (i.e., MS^3).[186] For example, chemical derivatization with the iTRAQ reagent not only labels the N-terminus of a peptide, but also the lysine side chain. Thus, tryptic peptides with a modified lysine residue present at the C-terminus will produce a y_1 product ion at m/z 291 following CID-MS/MS. To generate the low m/z iTRAQ reporter ions required for quantitation, the y_1 product ion can be isolated and subjected to data dependent CID-MS^3. Using this approach peptide identification is achieved in the MS/MS scan, while quantitation is achieved via MS^3.

Regardless of the instrumentation platform employed for analysis, each of the quantitative MS/MS based derivatization strategies requires an ionizing proton to initiate cleavage of the stable-isotope containing label to generate the low m/z reporter ions required for quantitation. Therefore, the fragmentation reactions associated with these strategies are expected to be highly dependent upon the proton mobility of the precursor ion, such that the characteristic isotopically encoded low mass reporter ions may often be observed at sufficient levels in only a sub-set of the total peptide ions selected for MS/MS to enable their use for quantification. Another limitation is that the desired fragmentation pathway giving rise to the low m/z reporter ions of interest is typically only one of many dissociation channels, including those resulting in the formation of b- and y-type sequence product ions, thereby "diluting" the spectrum and limiting the dynamic range for quantitative analysis.

To overcome some of these challenges, the SELECT approach described in Section 1.3.4.2 above has been applied to quantitative analysis, via the incorporation of light and heavy isotopically encoded labels into the fixed-charge chemical derivatization reagents. In the initial report by Reid *et al.*, methionine-containing peptides were

alkylated with either "light" $^{1}H_5$-phenacylbromide or "heavy" $^{2}H_5$-phenacylbromide to form a fixed-charge sulfonium ion on the side chain of methionine residues.[169] The light and heavy phenacyl sulfonium ion fixed-charge containing peptides were subsequently combined and subjected to LC-MS/MS analysis. The relative abundances of the neutral loss product ions $CH_3SCH_2COC_6H_5$ (166 Da) and $CH_3SCH_2COC_6{}^{2}H_5$ (171) generated by CID-MS/MS were then used for quantitative analysis. In contrast to the MS/MS based quantitative analysis strategies described above, the neutral loss product ions required for quantitation via the SELECT approach are formed independent of the proton mobility of the precursor ion such that these product ions will be observed all of the time. Furthermore, formation of the neutral loss product ions at a m/z value close to that of the selected precursor ion circumvents the low mass cutoff limitation of the ion trap. Characterization of the identified and quantified methionine peptides may readily be achieved by subjecting the common neutral loss product ion formed from the light or heavy labeled peptides to MS^3 analysis. One of the potential disadvantages to this initial approach, however is that some, albeit limited, chromatographic separation of the $^{1}H_5$ and $^{2}H_5$ forms of the fixed-charge sulfonium ion derivatives was observed following reversed-phase chromatography of these peptides. Although not investigated to date, light and heavy isotopically encoded labels could also be readily incorporated into the previously described alkylating reagent (3-[N-bromoacetamido]propyl)-methylphenacylsulfonium bromide[172] to enable the selective MS/MS based quantitative analysis of cysteine-containing peptides.

1.4 Aims of this Dissertation

The aims of this dissertation are:

1. to examine the origin of *ex vivo* sample handling related oxidative modifications of methionine-, S-alkyl cysteine- and tryptophan-containing peptides obtained from typical in-solution or in-gel proteolytic digestion strategies and evaluate conditions for deliberately controlling the oxidation state of these peptides;
2. to investigate the mechanisms and proton mobility dependence to the fragmentation reactions of model S-alkyl cysteine sulfoxide-containing peptides;
3. to develop an automated electrospray ionization (ESI)-HPLC neutral loss MS/MS and date dependent pseudo MS^3 analysis method in a triple quadrupole mass spectrometer for the selective gas-phase identification, characterization and differential quantitative analysis of fixed-charge sulfonium ion-containing peptides, and;
4. to identify and quantify methionine oxidation in the Ca^{2+}/calmodulin dependent serine/threonine phosphatase calcineurin using a fixed-charge chemical derivatization and tandem mass spectrometry-based approach similar to that outlined in aim 3.

CHAPTER TWO

Instrumentation

2.1 Mass Spectrometry

Mass spectrometry is an analytical technique that involves the ionization of a sample to generate gas-phase ions, separation of the resultant ions based on their individual mass-to-charge (m/z) ratios, and measurement of the m/z and abundance of each ion reaching a detector. Optionally, individual gas-phase ions can be isolated and subjected to fragmentation, followed by mass analysis of the resultant product ions. The main components of a mass spectrometer are illustrated in Figure 2.1.

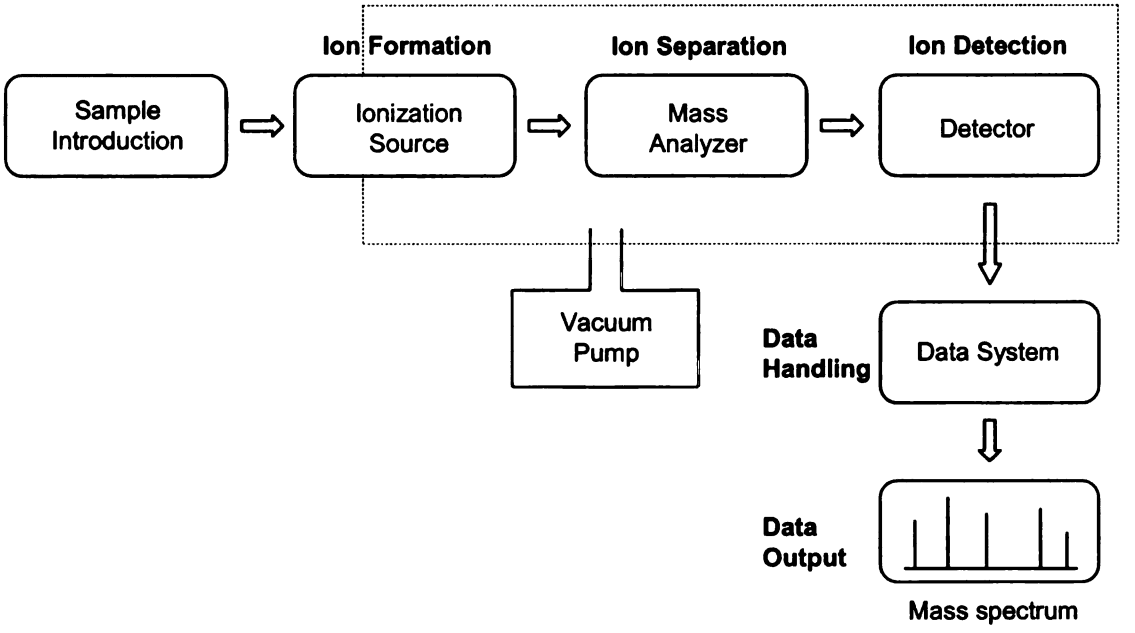

Figure 2.1 Components of a mass spectrometer (adapted from "What is mass spectrometry". www.asms.org).

2.1.1 Ionization

The ionization source is responsible for converting a sample of interest into gas-phase ions. Numerous ionization techniques are currently employed for mass spectrometry analysis including electron impact (EI), chemical ionization (CI), fast atom bombardment (FAB), electrospray ionization (ESI) and matrix-assisted laser desorption ionization (MALDI). ESI and MALDI are generally used for the analysis of biological molecules, such as peptides and proteins, and therefore are described in more detail below.

2.1.1.1 Electrospray Ionization (ESI)

Electrospray ionization (ESI), an atmospheric pressure ionization technique, was first introduced by Fenn and coworkers in the late 1980's.[187] ESI results in minimal analyte fragmentation, is suitable for analyzing polar and ionic compounds, and produces multiply charged pseudomolecular ions ($[M+nH^+]^{n+}$), which enable high molecular weight species, such as peptides and proteins, to be readily analyzed by many types of mass analyzers. ESI can be performed in direct infusion mode, whereby a sample of interest is dissolved in an appropriate liquid solvent and then introduced to the mass spectrometer via a syringe pump. However, ESI can also be readily coupled with high performance liquid chromatography (HPLC) to directly ionize an analyte as it elutes from a chromatographic column. The ability to couple ESI directly with HPLC is particularly advantageous for the analysis of complex mixtures, whereby separation prior to mass spectrometry analysis is required. When sample quantity is limited, the use of

nanoelectrospray ionization (nESI), which is typically operated at flow rates of less than 1 μL/min, may be beneficial.[188]

In ESI, a sample is initially pumped through a small diameter stainless steel or fused silica capillary tubing, the tip of which is maintained at atmospheric pressure in the source region of the mass spectrometer. A high potential is applied between the capillary tip and a counter electrode, which results in charge accumulation at the surface of the liquid. A combination of charge repulsion at the surface, and the presence of an electric field, enables the surface tension of the liquid to be overcome and the liquid subsequently expands into a Taylor cone. The tip of the Taylor cone then elongates into a liquid filament, which breaks to yield an electrostatic spray of charged droplets. Finally, solvent evaporation, in the presence of high temperature and/or a sheath gas, and charge repulsion, result in a series of coulomb fission events to yield gas-phase ions.

The mechanism by which gas-phase ions are produced from the charged droplets has been explained by two competing theories, the charge residue model (CRM)[189] and the ion evaporation model (IEM).[190, 191] In the CRM, successively smaller droplets are produced when the surface charge density of the droplet exceeds the Rayleigh stability limit (i.e., the force due to the repulsion of the surface charges becomes equal to the surface tension force of the liquid). The result of this process is the formation of droplets which contain only a single analyte molecule. A free gas-phase ion is then produced as the remaining solvent evaporates. In the IEM, it is also proposed that a series of Rayleigh instabilities produce successively smaller droplets. However, in contrast to the CRM, the surface electric field of the droplet becomes strong enough to overcome the solvation forces, causing direct emission of the analyte ions from the droplet surface into the gas-

phase. Experimental evidence suggests that large molecules, such as proteins, ionize according to the CRM, while small molecules ionize according to the IEM.[192]

2.1.1.2 Matrix-assisted Laser Desorption Ionization (MALDI)

Matrix-assisted laser desorption ionization (MALDI) was developed by Karas and Hillencamp in the late 1980's for the purpose of analyzing large molecular weight proteins.[193] MALDI is performed by dissolving an analyte of interest in an excess of matrix containing a UV absorbing chromophore. After the analyte-containing matrix has been spotted onto a metal target and allowed to crystallize, the target is placed under vacuum in the source region of the mass spectrometer. The target is then bombarded with short duration laser pulses, which induces rapid heating of the crystals and sublimation of both the analyte and matrix into the gas-phase. Although formation of analyte and matrix ions can occur at any time during this process, the exact mechanism of ionization is still the subject of much debate.[194]

Similar to ESI, MALDI results in limited analyte fragmentation and is suitable for analyzing polar and ionic compounds. Although MALDI is used for the analysis of high molecular weight species, the formation of singly charged pseudomolecular ions via this technique limits the types of mass analyzers that may be employed. Also, due to the nature of the ionization process, MALDI cannot be coupled on-line with HPLC. For this reason, MALDI was not explored as a potential ionization technique in the studies reported herein.

2.1.2 Mass Analyzers

The mass analyzer component of the mass spectrometer separates gas-phase ions according to their individual m/z ratios. A number of mass analyzers are currently employed in the field of proteomics including the quadrupole, quadrupole ion trap, time-of-flight (TOF) and Fourier transform ion cyclotron resonance (FT-ICR) mass analyzers[195]. The quadrupole and quadrupole ion trap mass analyzers were exclusively used in the studies reported here and are described in more detail below.

2.1.2.1 The Quadrupole Mass Analyzer

The ideal quadrupole mass analyzer consists of four parallel hyperbolic shaped electrodes; however, electrodes of circular cross-section are typically employed for both economic and practical reasons. Ions entering the quadrupole along the z-axis experience an electric field which is created by applying separate potentials to each pair of diagonally opposite electrodes. The applied potentials are expressed in equation (1), where U is the direct current (DC) potential, V is the zero-to-peak amplitude of the radio frequency (RF) voltage, ω is the angular frequency ($\omega = 2\pi\upsilon$, where υ is the frequency of the RF field), and t is time.

$$\Phi_0 = +(U - V\cos\omega t) \quad \text{and} \quad -\Phi_0 = -(U - V\cos\omega t) \qquad (1)$$

As the ions travel along the z-axis, the force induced by the electric field also accelerates the ions in the x and y dimensions. The force experienced by the ions along the x- and y-

axis is expressed in equations (2) and (3), respectively, where m is the mass of an ion, z is the number of charges on a given ion, and e is the charge of an electron (1.60×10^{-19} C).

$$Fx = m\frac{d^2x}{dt^2} = -ze\frac{\partial \Phi}{\partial x} \tag{2}$$

$$Fy = m\frac{d^2y}{dt^2} = -ze\frac{\partial \Phi}{\partial y} \tag{3}$$

In equations (2) and (3), Φ is expressed as a function of Φ_0 as shown by equation (4), where r_0 is the distance from the center of the quadrupole mass analyzer to the electrodes.

$$\Phi_{xy} = \Phi_0(x^2 - y^2)/{r_0}^2 = \frac{(x^2 - y^2)(U - V\cos\omega t)}{{r_0}^2} \tag{4}$$

Derivatizing and rearranging the terms in equations (2) and (3) provides the equations of ion motion within a quadrupole which are given by equations (5) and (6) below.

$$\frac{d^2x}{dt^2} + \frac{2ze}{m{r_0}^2}(U - V\cos\omega t)x = 0 \tag{5}$$

$$\frac{d^2y}{dt^2} - \frac{2ze}{m{r_0}^2}(U - V\cos\omega t)y = 0 \tag{6}$$

The similarities between these two equations and the Mathieu equation, given by equation (7), enable the working equations of ion motion in a quadrupole to be derived. In equation (7), u represents either x or y in equations (5) and (6), respectively, q_u and a_u are dimensionless parameters, and $\xi = \omega t/2$.

$$\frac{d^2u}{d\xi^2} + (a_u - 2q_u \cos 2\xi)u = 0 \tag{7}$$

The working equations of ion motion, expressed in the form of the Mathieu equation, are given by equations (8) and (9). According to these equations, an ion will only have a stable trajectory (i.e., pass through the quadrupole without discharging against an electrode) if the position of the ion in the x and y dimensions does not exceed r_0, the distance from the center of the quadrupole to the electrodes.

$$a_u = a_x = -a_y = \frac{8zeU}{m\omega^2 {r_0}^2} \tag{8}$$

$$q_u = q_x = -q_y = \frac{4zeV}{m\omega^2 {r_0}^2} \tag{9}$$

Equations (8) and (9) may also be rearranged to yield equations (10) and (11).

$$U = a_u \frac{m\omega^2 r_0^2}{8ze} \tag{10}$$

$$V = q_u \frac{m\omega^2 r_0^2}{4ze} \tag{11}$$

In equations (10) and (11), e is a constant, and r_0 and ω are fixed values for a given quadrupole, while U and V are variables. Thus, the regions where ions of different masses have a stable trajectory through the quadrupole is obtained by plotting U as a function of V as shown in Figure 2.2 for positively charged ions with increasing m/z values from m_1 to m_4. As can be seen from Figure 2.2, only one m/z ion will have a stable trajectory through the quadrupole for a certain combination of U and V when operating near the apex of the stability diagram (a_u = 0.237; q_u = 0.706). All other m/z ions will have an unstable trajectory and will discharge against the electrodes. A mass spectrum may therefore be acquired by linearly scanning U and V near the apex of the stability diagram while maintaining a constant ratio of U/V. In an effort to increase resolution, the slope of the scan line can be increased. However, increasing the slope of the scan line will result in a decrease in the number of ions which have a stable trajectory through the quadrupole, and therefore decrease sensitivity. As a result, most commercial instrument platforms operate at point just below the apex as a compromise between good sensitivity and high resolution.

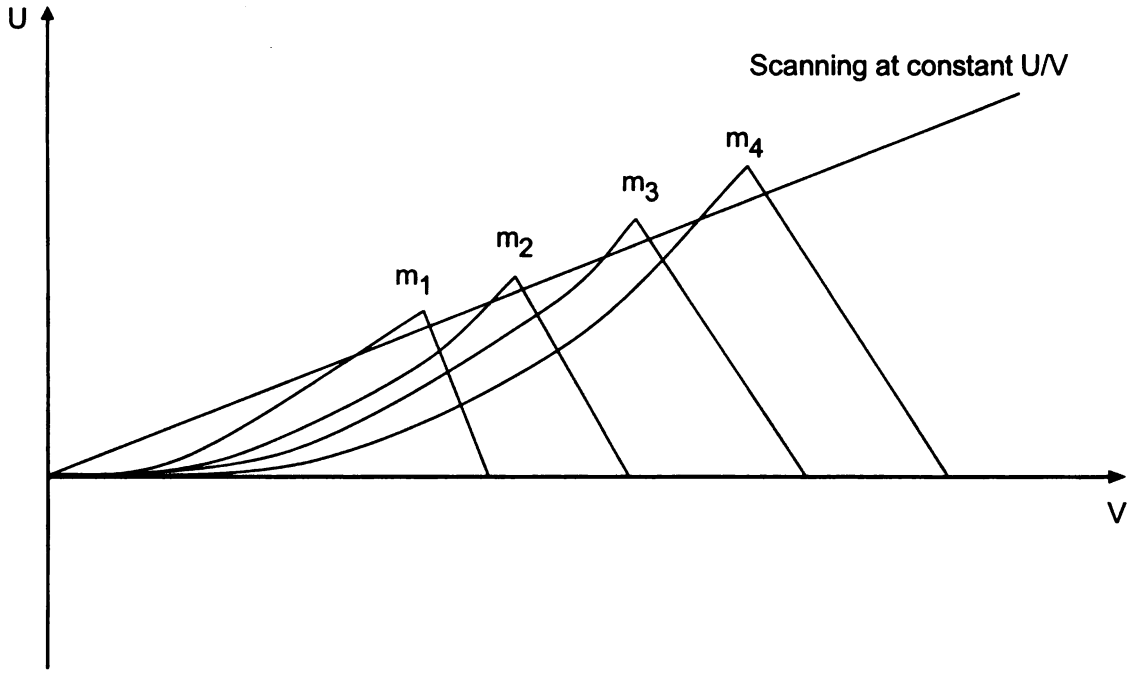

Figure 2.2 Stability regions as a function of U and V for positively charged ions with different masses ($m_1 < m_2 < m_3 < m_4$). Each ion can be observed successively by changing U linearly as a function of V while maintaining a constant ratio of U/V. (Reproduced and modified from reference 195)

To perform tandem mass spectrometry, three quadrupole mass analyzers can be coupled in series. In this configuration, the first and third quadrupoles are used to mass select or scan ions, while the second quadrupole is used as a collision cell via the addition of an inert gas such as argon. Using a triple quadrupole mass spectrometer, three types of tandem mass spectrometry scan modes are commonly employed. In the product ion scan mode, a precursor ion of interest is mass selected in the first quadrupole, fragmented in the second quadrupole and the resultant product ions are then detected by scanning the third quadrupole. In the precursor ion scan mode, the first quadrupole is scanned to sequentially transmit all m/z ions through to the second quadrupole for subsequent fragmentation. A fragment ion with a specified m/z value is then mass selected in the third quadrupole in order to detect all of the precursor ions which give rise to the

fragment ion of interest. Finally, in the neutral loss scan mode, the first and third quadrupoles are both scanned, but with a constant mass offset between them. Any precursor ion which gives rise to a characteristic neutral loss upon fragmentation in the second quadrupole will then be detected.

2.1.2.2 The Quadrupole Ion Trap Mass Analyzer

The three-dimensional quadrupole ion trap mass analyzer, illustrated in Figure 2.3, consists of a hyperbolic ring electrode with an internal radius r_0, and two hyperbolic end-cap electrodes each positioned at a distance z_0 from the center of the trap.[196] In most commercial instrument platforms, the end-cap electrodes are maintained at ground, and a high voltage RF potential is applied to the ring electrode to create a three-dimensional (3D) quadrupolar electric field within the trap. As ions are injected into the trap, via a small hole in the entrance end-cap electrode, ions of all m/z values with stable oscillating trajectories (i.e., trajectories which do not exceed the dimensions of the trap) are stored. To help focus ions toward the center of the trap, and therefore improve the overall trapping efficiency, a continuous flow of helium bath gas is introduced to the trap at a pressure of approximately 1 mTorr. Ion focusing is achieved via collisions between the stored ions and the helium gas.

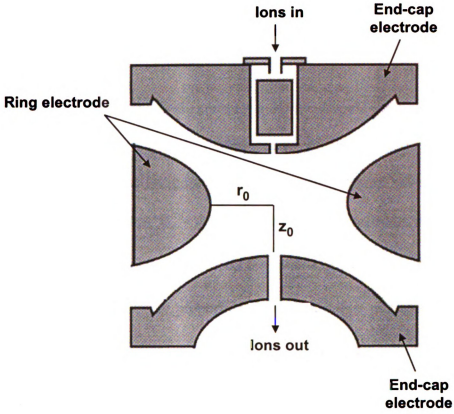

Figure 2.3 Cross-section of a three-dimensional quadrupole ion trap. (Reproduced and modified from reference 196)

Similar to the quadrupole mass analyzer, the working equations of ion motion in the 3D quadrupole ion trap can also be expressed in the form of the Mathieu equation and are given by equations (12) and (13) below. According to these equations, an ion will only have a stable trajectory if the motion of the ion does not exceed z_0 an r_0 for a defined set of operating conditions (i.e., U, V and ω).

$$a_u = a_z = -2a_r = \frac{-16zeU}{m(r_0^2 + 2z_0^2)\omega^2} \tag{12}$$

$$q_u = q_z = -2q_r = \frac{8zeV}{m(r_0^2 + 2z_0^2)\omega^2} \tag{13}$$

The Mathieu stability diagram for a 3D quadrupole ion trap is depicted in Figure 2.4. Ions located within the bounded region of the stability diagram have stable trajectories, while those lying outside of the bounded region have unstable trajectories. Typically, a DC potential, U, is not applied to the ring electrode, therefore a_z is equal to zero, and the ion trap is operated along the q_z axis. According to equation (13), the m/z value of an ion is inversely proportional to q_z, thus low m/z ions (represented by the smaller balls in Figure 2.4) have larger q_z values, and high m/z ions (represented by the larger balls) have smaller q_z values. In equation (13), the term *e* is a constant, and r_0, z_0 and ω are fixed values, therefore the q_z value of an ion with a particular m/z increases as the amplitude of the applied RF potential, V, increases. When q_z reaches a value of 0.908 (stability limit), the ion no longer has a stable trajectory and is ejected from the trap in the z_0 dimension for detection. A mass spectrum can therefore be acquired by linearly scanning V to progressively destabilize ions of increasing m/z value. This method of mass analysis is referred to as ion ejection at the stability limit.

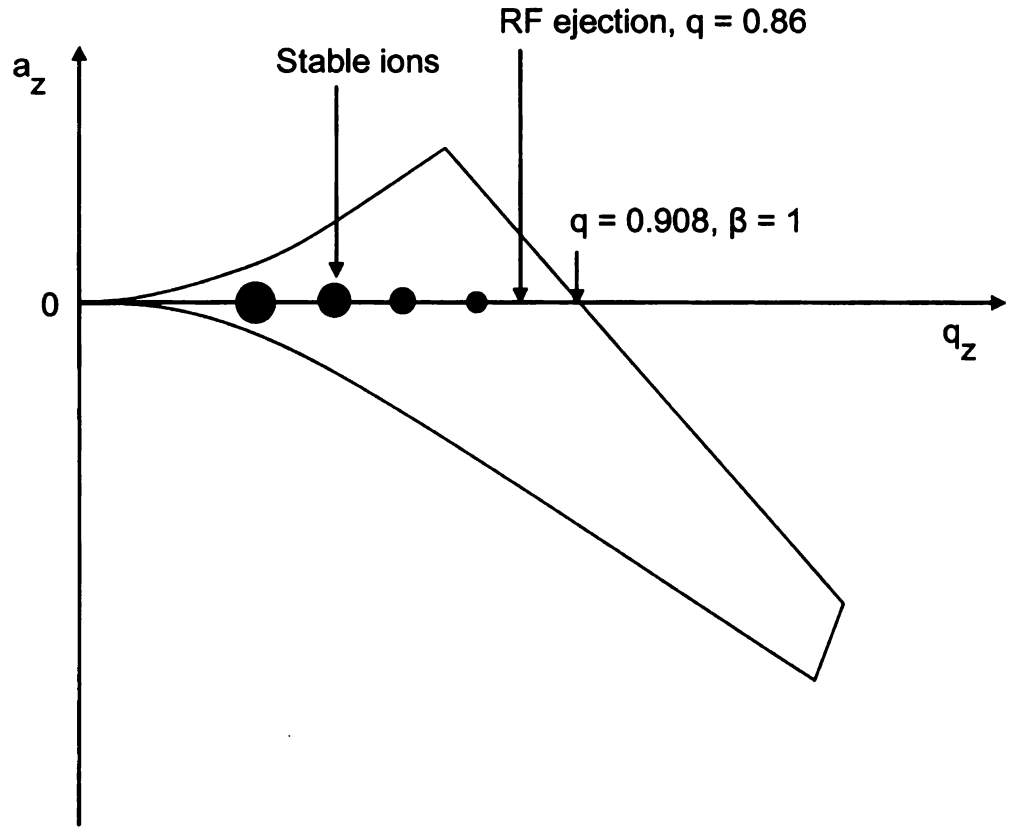

Figure 2.4 Typical Mathieu stability diagram for the quadrupole ion trap. The larger balls represent high mass ions whereas the smaller balls represent low mass ions. (Reproduced and modified from reference 195)

Mass analysis however, is typically achieved by resonance ejection. In this technique, a supplementary high amplitude RF potential is applied to the end-cap electrodes, typically at a q_z value of 0.86. The amplitude of the RF voltage applied to the ring electrode is then linearly scanned, which causes the secular frequency at which an ion oscillates in the trap, f_z, to slowly increase. The secular frequency of an ion, which due to its inertia, is not equal to the fundamental frequency, v, of the applied RF potential, is expressed by equation (14)

$$f_z = \frac{\beta_z v}{2} \tag{14}$$

where β_z is a fundamental stability parameter and is approximated by equation (15) for q values less than 0.4.

$$\beta_z = \left[a_z + \left(\frac{q_z^2}{2} \right) \right]^{1/2} \tag{15}$$

When the secular frequency of an ion matches the applied frequency of the end-cap electrodes, the kinetic energy of the ion will rapidly increase to the point where the ion's trajectory becomes unstable and the ion is ejected from the trap, resulting in higher mass resolution when compared to mass analysis via ion ejection at the stability limit.

One of the main advantages to using a quadrupole ion trap mass analyzer is the ability to perform multiple stages of mass analysis to obtain detailed structural information for an ion of interest. Tandem mass spectrometry in a quadrupole ion trap involves the isolation of a precursor ion, fragmentation of the precursor ion via energetic collisions with an inert gas, and mass analysis of the resultant product ions. A precursor ion of a selected m/z ratio is typically isolated by applying a supplementary high amplitude, broadband resonance ejection RF signal to the end-cap electrodes to eject all ions except for the precursor ion of interest. The isolated precursor ion is then activated by applying a low amplitude RF resonance excitation signal to the end-cap electrodes with a frequency corresponding to the secular frequency of motion of the isolated ion.

The applied potential increases the axial motion and kinetic energy of the precursor ion and energetic collisions with the background helium buffer gas converts a fraction of the kinetic energy into internal energy. This enables the ion to reach a vibrationally excited state, and fragmentation is induced. The secular frequencies of motion of the resultant product ions are not in resonance with the supplementary RF signal, therefore the product ions are focused to the center of the trap following collisions with the helium gas. A mass spectrum is acquired by sequentially ejecting the product ions from the trap in the same manner as described above. Multistage tandem mass spectrometry (MS^n) experiments are performed by incorporating additional ion isolation and fragmentation events following initial MS/MS analysis.

Although the 3D quadrupole ion trap is considered a relatively high sensitivity mass analyzer, it suffers from low injection and trapping efficiencies and limited ion storage capacity. To address these disadvantages, the two-dimensional linear quadrupole ion trap was recently introduced.[197, 198] The linear quadrupole ion trap, illustrated in Figure 2.5, stores ions in a two-dimensional electric field, which is created by applying an RF potential to four hyperbolic rods, and static DC potentials applied to the electrodes located at each end of the rods. The linear quadrupole ion trap has a greater ion storage capacity, because ions can be stored along the entire length of the trap. The extent to which ions experience the applied RF potential in the axial dimension is also minimal, therefore resulting in greater ion trapping efficiencies. In the studies reported herein, a three-dimensional quadrupole ion trap and a two-dimensional linear quadrupole ion trap were both employed.

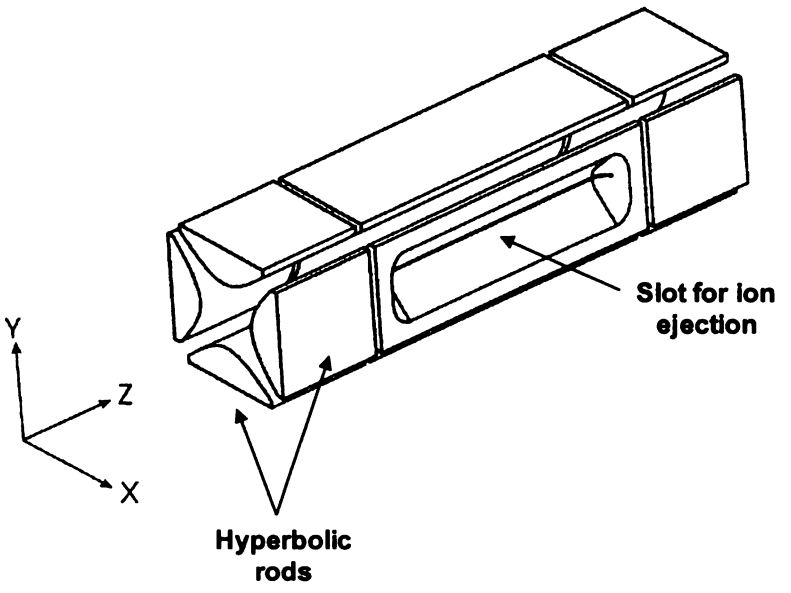

Figure 2.5 Diagram of a two-dimensional linear quadrupole ion trap. (Reproduced and modified from reference 198)

2.1.3 Detectors

The ion detection system of the mass spectrometer is responsible for converting the ion beam exiting the mass analyzer into a measurable electrical current. The ion detection system used in the instrumentation employed in the studies described herein consists of a continuous-dynode electron multiplier coupled with a conversion dynode. When an ion strikes the surface of the high voltage conversion dynode, secondary particles are emitted, which are then accelerated into the electron multiplier. Secondary electrons are ejected from the electrically resistive surface of the electron multiplier following collisions between the surface and the secondary particles. As the electrons travel further into the electron multiplier, repeated collisions with the surface cause additional electrons to be expelled due to the presence of a positive electrical field along the surface. The data acquisition system then plots the amplified electric current, which

corresponds to the abundance of the ion, as a function of ion m/z to obtain a mass spectrum.

CHAPTER THREE

Experimental

3.1 Materials

Unless stated otherwise, all reagents were of analytical reagent (AR) grade and were used as supplied without further purification. The synthetic model "tryptic" peptides GAILMGAILK (MK), GAILMGAILR (MR), VTMAHFWNFGK (MWK), VTMGHFCNFGK (MCK) and GAILCGAILK (CK) were purchased from GenScript (Piscataway, NJ, USA) and were washed with ether prior to use in order to remove residual scavengers remaining from their synthesis. GAILCGAILR (CR) was obtained from New England Peptide, Inc. (Gardner, MA, USA). VTMGHFDNFGR (MDR) and VTMSHFWNFGK (MSK) were from Auspep (Melbourne, Australia). Iodoacetamide, iodomethane, iodoacetic acid, 4-vinylpyridine, dimethyl sulfide, tris(2-carboxy-ethyl)phosphine hydrochloride, N-(methyl)mercaptoacetamide, calcium chloride, HEPES, ethylene glycol-bis(2-amino-ethylether)-N,N,N',N'-tetra-acetic acid (EGTA), monodeuterated acetic acid (CH_3CO_2D), bromoacetyl bromide, guanidine hydrochloride, Trizma base, Trizma hydrochloride, sodium dodecyl sulfate (SDS), EZBlue™ gel staining reagent, methanol (HPLC grade), bovine catalase, bovine serum albumin, yeast enolase, bovine apo-transferrin, yeast alcohol dehydrogenase, rabbit muscle aldolase and equine myoglobin were purchased from Sigma (St. Louis, MO, USA). Hydrogen peroxide (30% aqueous solution), hydrochloric acid, carbon disulfide (ACS grade) and magnesium chloride were obtained from Columbus Chemical Industries (Columbus, WI, USA). Glacial acetic acid (ACS grade), formic acid (ACS grade), anhydrous aluminum

chloride and anhydrous magnesium sulfate were from Spectrum Chemicals (Gardena, CA, USA). Acetonitrile (HPLC grade) and dimethyl sulfoxide were purchased from EMD Chemicals (Gibbstown, NJ, USA). Dithiothreitol (DTT) and acrylamide (electrophoresis grade) were obtained from Boehringer Mannheim Corporation (Indianapolis, IN, USA). Ammonium bicarbonate was from J.T. Baker Chemical Company (Phillipsburg, NJ, USA). EDTA and dichloromethane (ACS grade) were purchased from Mallinckrodt (Phillipsburg, NJ, USA). Trifluroacetic acid was obtained from Pierce (Rockford, IL, USA). Phenacylbromide was from Fluka (St. Louis, MO, USA). Deuterium oxide (D_2O), deuterated methanol (CD_3OD) and $^{13}C_6$-benzene were purchased from Cambridge Isotope Laboratories (Andover, MA, USA). Tris, glycine, 4-20% tris-glycine precast gradient gels and SeeBlue Plus2® prestained molecular mass markers were obtained from Invitrogen (Carlsbad, CA, USA). Potassium chloride was from Jade Scientific (Canton, MI, USA). Sequencing grade modified trypsin was purchased from Promega (Madison, WI, USA). Sequencing grade LysC was obtained from Roche Diagnostics (Indianapolis, IN, USA). Standard tryptic protein digests of equine myoglobin, bovine serum albumin, bovine glutamate dehydrogenase, *E. coli* glycerokinase, human alpha lactalbumin, human lactotransferrin and yeast enolase were from Michrom Bioresources (Auburn, CA, USA). Wildtype calcineurin was a gift from Dr. Paul Stemmer of the Institute of Environmental Health Sciences at Wayne State University. All solutions were prepared using deionized water purified by a Barnstead nanopure diamond purification system (Dubuque, IA, USA).

3.2 Synthesis of $^{13}C_6$ Phenacylbromide

$^{13}C_6$ phenacylbromide ($BrCH_2CO^{13}C_6H_5$) used in Chapter 6 was synthesized by Ms. Suchitra Kaplinghat following the method of Finkielsztein *et al.*[199] Briefly, $AlCl_3$ (11.8 g, 89.3 mmol) was added in small portions to a stirred solution of $^{13}C_6$-benzene (500 mg, 6.0 mmol) and bromoacetyl bromide (646 μL, 7.4 mmol) in CS_2 (60 mL). The reaction was refluxed for 30 min at 45°C, cooled to room temperature and carefully poured onto ice. The product was extracted into dichloromethane (75 mL), washed with water (45 mL) and the organic layer was dried over anhydrous $MgSO_4$. The organic layer was then filtered and evaporated under reduced pressure to give the product as a light yellow solid in 56% yield (692 mg).

3.3 S-alkylation of Cysteine-containing Peptides

S-alkyl cysteine-containing peptides used in Chapters 4 and 5 were individually prepared by dissolving 1 mg of lyophilized cysteine-containing peptide in 1 mL of 500 mM Tris (pH 7.8) containing 25 mM alkylating reagent. The reaction was allowed to proceed at room temperature for 20 min (iodoacetamide), 30 min (iodomethane and iodoacetic acid), 60 min (acrylamide) or 120 min (4-vinylpyridine). The samples were then immediately de-salted (Sep-Pak Classic C_{18} cartridges; Waters, Milford, MA) and dried completely by centrifugal evaporation.

3.4 Oxidation of Synthetic Peptides

Synthetic peptides were dissolved in 30% hydrogen peroxide containing 5% acetic acid[81] and allowed to react at room temperature. Reaction times ranged from 5 to 210 min for the studies performed in Chapter 4 and 30 min for the studies performed in Chapter 5. At each time point an aliquot of the reaction was immediately desalted (Sep-Pak Classic C_{18}) prior to its introduction to the mass spectrometer for analysis.

3.5 Oxidation of Calcineurin

Purified calcineurin (2.5 μM) used in Chapter 7 was oxidized in 10 mM HEPES (pH 7.6), 100 mM KCl, 1 mM $MgCl_2$ and 0.1 mM $CaCl_2$ with 12 mM H_2O_2 at room temperature in the dark for 1, 2, 4 or 10 h. Oxidation was stopped by the addition of catalase to a final concentration of 2 μg/mL followed by incubation for 5 min at room temperature.

3.6 Reduction of Synthetic Peptides

Desalted oxidized synthetic peptides (25 μg) used in Chapter 4 were dissolved in 100 μL of 10 M hydrochloric acid containing 1 M dimethyl sulfide.[200] The reaction was allowed to proceed at room temperature for reaction times ranging from 5 to 45 min after which the samples were diluted, then immediately subjected to mass spectrometry analysis without further purification.

3.7 One-dimensional SDS-PAGE Separation of Standard Proteins

SDS-PAGE was performed on the individual standard proteins bovine serum albumin, yeast enolase, bovine apo-transferrin, yeast alcohol dehydrogenase, rabbit muscle aldolase and equine myoglobin (5 μg each) using 10 cm^2 x 1.0 mm precast polyacrylamide gels (4-20%). Electrophoresis was carried out at 125 V for 90 min at 20°C in an XCell SureLock™ Mini-cell apparatus (Invitrogen) using Tris-glycine SDS running buffer (25 mM Tris, 192 mM glycine, 0.1% w/v SDS, pH 8.3). Immediately following electrophoresis, the gel was rinsed and stained using EZBlue™ gel staining reagent (Sigma). Individual gel bands were then excised, placed in separate Eppendorf tubes and dehydrated by centrifugal evaporation prior to further processing.

3.8 In-gel Tryptic Digestion of Standard Proteins

Dehydrated gel bands were rehydrated in 200 μL of reduction buffer (10 mM DTT in 200 mM Tris, 2 mM EDTA, pH 8.4) then incubated at 40°C for 1 h. The reduction buffer was removed then 200 μL of 25 mM iodoacetamide was added followed by incubation for 1 h at room temperature. The bands were then washed with 2 x 1 mL of 0.1 M NH_4HCO_3/50% CH_3CN for 30 min each at 30°C, and dried completely by centrifugal evaporation. Protein digestion was carried out by the addition of sequencing grade modified trypsin (in 200 mM NH_4HCO_3/0.5 mM $CaCl_2$) at an enzyme:substrate ratio of 1:20 (wt/wt), followed by the addition of 200 μL of 200 mM NH_4HCO_3/0.5 mM $CaCl_2$, and incubation overnight at 37°C. The incubation buffer from each gel band was then collected in separate Eppendorf tubes. 200 μL of 1% trifluroacetic acid (TFA) was then added to each band followed by sonication for 30 min at room temperature. The

extract was collected and 200 µL of 0.1% TFA/60% CH_3CN was added to the gel bands followed by sonication for 30 min at room temperature. The extracts were collected and pooled, then concentrated by centrifugal evaporation. The resultant peptide mixtures were then analyzed by LC-MS/MS either directly, or following their reduction (45 min at room temperature with 1 M DMS/10 M HCl) and de-salting using OMIX® C18 tips (Varian, Palo Alto, CA, USA).

3.9 Solution-phase Tryptic Digestion of Standard Proteins

The standard proteins bovine serum albumin, yeast enolase, bovine apo-transferrin, yeast alcohol dehydrogenase, rabbit muscle aldolase and equine myoglobin (100 µg each) used in Chapters 4 and 5 were individually dissolved in 100 µL of 6 M guanidine/500 mM Tris (pH 7.8) and 10 mM DTT, then heated at 37°C for 1 h. Iodoacetamide was then added to a final concentration of 21 mM followed by incubation for 20 min at room temperature. The solution was then diluted with 380 µL of water and sequencing grade modified trypsin was added at an enzyme:substrate ratio of 1:20 (wt/wt). Protein digestion was performed overnight at 37°C after which the samples were immediately desalted by Sep-Pak Classic C_{18} solid-phase extraction. The resultant peptide mixtures were then analyzed by LC-MS/MS either directly, or following their oxidation for 30 min at room temperature with 30% hydrogen peroxide containing 5% acetic acid.

3.10 Solution-phase LysC Digestion of Calcineurin

Native or oxidized wildtype calcineurin (2.5 μM in 10 mM HEPES (pH 7.6), 100 mM KCl, 1 mM $MgCl_2$ and 0.1 mM $CaCl_2$) used in Chapter 7 was reduced by incubation with 4 mM DTT for 30 min at 60°C. Iodoacetamide was then added to a final concentration of 11 mM followed by incubation for 1 h at room temperature. DTT was then added to a final concentration of 4 mM followed by incubation for 30 min at room temperature to inactivate excess iodoacetamide. The pH of the reaction was then adjusted to pH 8.0 by the addition of 50 mM ammonium bicarbonate. Protein digestion was performed by the addition of sequencing grade LysC (dissolved in 10 mM EGTA) at a LysC:calcineurin ratio of 1:10 (wt/wt) followed by incubation overnight at 37°C. The resultant peptide mixtures were then analyzed directly by LC-MS/MS without further purification.

3.11 Side Chain Fixed-Charge Derivatization of Methionine-Containing Peptides

"Light" and "heavy" side chain fixed-charge sulfonium ion derivatives of the synthetic peptides MK, MR, MDR and MSK (100 μg dissolved in 100 μL of aqueous 20% HOAc containing 30% CH_3CN[169]) used in Chapter 6 were individually prepared by the addition of 10 μL of a 1 M solution of either phenacylbromide or $^{13}C_6$ phenacylbromide freshly prepared in CH_3CN. Reactions were allowed to proceed for 24 h at room temperature after which the samples were diluted and then used without further purification. The standard protein tryptic digests (1 pmol each) used in Chapter 6 were "spiked" with either 100 fmol, 500 fmol or 1 pmol of a "light" sulfonium ion containing peptide, or with mixtures of "light" and "heavy" sulfonium ion containing peptides in

amounts ranging from 100 fmol to 1 pmol and at abundance ratios ranging from 0.1 to 10 or from 10 to 0.1, prior to LC-MS/MS analysis.

Native and oxidized LysC digests of calcineurin (0.6 μM) used in Chapter 7 were individually subjected to side chain fixed-charge derivatization by incubation with a 2000-fold molar excess of phenacylbromide in aqueous 20% HOAc containing 30% CH_3CN for 24 h at room temperature. The samples were then diluted and analyzed directly by LC-MS/MS without further purification.

3.12 Mass Spectrometry of Model Peptides

Synthetic peptides used in Chapter 5 were dissolved in aqueous 50% methanol, 1% acetic acid to a final concentration of 0.04 mg/mL and were then introduced to a linear quadrupole ion trap mass spectrometer (Thermo model LTQ, San Jose, CA) by nanospray ionization (nanoESI) at 0.5 μL/min. The spray voltage was maintained at 1.8 kV. The heated capillary temperature was 200°C. Uniformly labeled hydrogen/deuterium exchanged peptides used in Chapter 5 were prepared by repeatedly drying and dissolving the sample (0.4 mg/mL) in 50% CD_3OD/50% D_2O containing 0.17 M CH_3CO_2D. Then, samples were diluted and introduced to a quadrupole ion trap mass spectrometer (Thermo model LCQ Deca, San Jose, CA) by electrospray ionization (ESI) at 4 μL/min. Typical ESI conditions were: spray voltage, 5 kV; nitrogen sheath gas, 25 psi; heated capillary temperature, 200°C. Nitrogen auxiliary gas (15, arbitrary units) was added to minimize deuterium back exchange during electrospray sample introduction. CID-MS/MS and MS^n experiments on both the LTQ and LCQ instruments were performed on monoisotopically

mass selected ions using standard isolation and excitation procedures. The spectra shown are the average of 80 scans.

3.13 Liquid Chromatography/Mass Spectrometry

3.13.1 Model Peptides and Standard Protein Digests

LC-MS/MS experiments in Chapters 4 and 5 were performed using a Paradigm MS4 capillary RP-HPLC system (Michrom Bioresources, Auburn, CA, USA) directly coupled to a linear quadrupole ion trap mass spectrometer (Thermo model LTQ, San Jose, CA, USA) equipped with a nanospray ionization (nanoESI) source. RP-HPLC conditions were as follows: 75 μm id x 150 mm fused silica column packed with Magic C18 (5 μm, 200 Å), operated at a flow rate of 0.25 μL/min using either a linear 45 min gradient from 5-50% solvent B (synthetic peptides used in Chapter 4) or a linear 80 min gradient from 5-45% solvent B (protein digests used in Chapters 4 and 5). Solvent A was 0.05% formic acid in H_2O and solvent B was 0.05% formic acid in CH_3CN. For each analysis, either 5 μL (synthetic peptides) or 3 μL (protein digests) of a 1 pmol/μL solution prepared in 97.9% H_2O/2% CH_3CN/0.1% formic acid was injected. These sample loading amounts were chosen to ensure that sufficient signal was available to accurately determine the ratio of oxidized and reduced peptides, even when one of these was present at low abundance, as well as to maximize the sequence coverage obtained by analysis of the various protein digests. The spray voltage was maintained at 1.8 kV. The heated capillary temperature was 200°C. To monitor the extent of oxidation or reduction occurring in the synthetic tryptic peptides after varying reaction times (Chapter 4), the mass spectrometer was operated in a data dependent acquisition mode where the three

most abundant precursor ions identified above a preset threshold of 1.0 x 10^4 counts were automatically isolated and subjected to CID-MS/MS following the acquisition of a full MS scan (m/z 300-2000). For LC-MS/MS analysis of individual tryptic protein digests (Chapters 4 and 5), the five most abundant precursor ions identified above a preset threshold of 1.0 x 10^4 counts were isolated and subjected to CID-MS/MS following the acquisition of a full MS scan (m/z 300-1700). Dynamic exclusion was enabled with a repeat count of 3 and the exclusion duration time set to 90 s.

3.13.2 Fixed-Charge Methionine-Containing Peptides within Standard Protein Digests

LC-MS/MS experiments in Chapter 6 were performed using a Paradigm MS4 capillary RP-HPLC system (Michrom Bioresources, Auburn, CA, USA) directly coupled to a triple quadrupole mass spectrometer (Thermo model TSQ Quantum Ultra, San Jose, CA, USA) equipped with a nanospray ionization (nESI) source. RP-HPLC conditions were as follows: 150 μm id x 150 mm fused silica column packed with Magic C18 (5 μm, 200 Å), operated at a flow rate of 1 μL/min using a linear 55 min gradient from 5 to 60% solvent B. Solvent A was 0.05% formic acid in H_2O and solvent B was 0.05% formic acid in CH_3CN. The spray voltage was maintained at 2.0 kV. The ion transfer tube of the mass spectrometer was maintained at 150°C. All MS and MS/MS spectra were acquired automatically by methods created using the Xcalibur software (Thermo, San Jose, CA). The Q1 and Q3 peak widths for the MS, neutral loss scan mode MS/MS and product ion scan mode MS/MS experiments were maintained at 1.0 m/z. The Q2 argon

collision gas pressure was set at 0.7 mtorr. MS and MS/MS scans were typically acquired using scan rates of 500 m/z second^{-1}.

3.13.2.1 Data Dependent Identification and Characterization

Following the acquisition of an optional full MS scan (m/z 300-1500) (scan event 1), a neutral loss mode MS/MS scan of 83.0 m/z to monitor for the loss of $CH_3SCH_2COC_6H_5$ (166 Da) from doubly charged ($[M^+ + H]^{2+}$) precursor ions (scan event 2) and a neutral loss MS/MS scan of 55.3 m/z to monitor for the loss of $CH_3SCH_2COC_6H_5$ from triply charged ($[M^+ + 2H]^{3+}$) precursor ions (scan event 3) were acquired using collision energies of 19 and 12 V, respectively. Then, precursor ions observed in scan events 2 and 3 that appeared above a predefined threshold abundance of 1.0×10^6 counts were automatically subjected to data dependent energy-resolved "pseudo MS^3" using collision energies of 0.05 Vz/m (scan event 4) and 0.04 Vz/m (scan event 5), respectively.

3.13.2.2 Quantitative Analysis

Following the acquisition of an optional full MS scan (m/z 300-1500) (scan event 1), neutral loss mode MS/MS scans of 83.0 m/z (scan event 2) and 86.0 m/z (scan event 3) were performed to monitor for the loss of $CH_3SCH_2COC_6H_5$ (166 Da) and $CH_3SCH_2CO^{13}C_6H_5$ (172 Da) from doubly charged precursor ions, respectively, using a collision energy of 19 V, followed by neutral loss mode MS/MS scans of 55.3 m/z (scan event 4) and 57.3 m/z (scan event 5) for the losses of $CH_3SCH_2COC_6H_5$ and

$CH_3SCH_2CO^{13}C_6H_5$ from triply charged precursor ions, respectively, using a collision energy of 12 V.

3.13.3 LysC Digests of Native and Oxidized Calcineurin Prior to and Following Side Chain Fixed-Charge Derivatization

LC-MS/MS experiments in Chapter 7 were performed using a Paradigm MS4 capillary RP-HPLC system (Michrom Bioresources, Auburn, CA, USA) directly coupled to a linear quadrupole ion trap mass spectrometer (Thermo model LTQ, San Jose, CA, USA) equipped with an Advance source (Michrom Bioresources). RP-HPLC conditions were as follows: 200 μm id x 50 mm column packed with Magic C18 (3 μm, 200 Å), operated at a flow rate of 2 μL/min using a linear 45 min gradient from 5-50% solvent B. Solvent A was 0.1% formic acid in H_2O and solvent B was 0.1% formic acid in CH_3CN. For each analysis 5 μL of a 100 fmol/μL solution prepared in 3% CH_3COOH/5% CH_3CN was injected. The spray voltage was maintained at 2.0 kV. The heated capillary temperature was 180°C. The mass spectrometer was operated in a data dependent acquisition mode where the five most abundant precursor ions identified above a preset threshold of 1.0×10^4 counts were automatically isolated and subjected to CID-MS/MS following the acquisition of a full MS scan (m/z 300-2000). Dynamic exclusion was disabled in an effort to increase the number of MS/MS spectra aquired across a chromatographic peak for a given precursor ion.

3.14 Molecular Orbital Calculations

Low energy transition state structures were initially located at the PM3 semi empirical level of theory, then subjected to further optimization at the B3LYP/6-31+G(d,p) level of theory using the GAUSSIAN 98 molecular modeling package.[201] Intrinsic reaction coordinate (IRC) searches were then performed, followed by geometry optimizations to locate the appropriate reactant and product ion structures associated with each transition state. All optimized structures were subjected to harmonic vibrational frequency analysis and visualized using the computer package GaussView 2.1 to determine the nature of the stationary points. Zero point energies were obtained from harmonic frequency calculations without scaling. Complete structural details for all optimized structures are listed in the Appendix.

3.15 Data Analysis

3.15.1 Calculation of Percent Oxidation and Reduction

To quantify the extent of oxidation or reduction which had occurred at the side chains of methionine, tryptophan, cysteine or S-carboxyamidomethyl cysteine residues contained within individual peptide sequences (Chapter 4), the percent oxidation or reduction for a given peptide was calculated by determining the ratio of the precursor ion abundances from both its oxidized and reduced forms. If a peptide was observed in multiple precursor ion charge states, the abundances of each of the precursor ions were combined. All peptide sequences were confirmed by manual inspection of the corresponding CID-MS/MS product ion spectra. The average percent oxidation observed for the standard protein tryptic digests was determined by dividing the sum of the percent

oxidation for each individual peptide by the total number of peptides observed containing the given amino acid residue of interest (i.e., peptides observed entirely in their reduced form were also included in the calculation).

3.15.2 MS/MS Database Analysis

Uninterpreted MS/MS spectra acquired for the oxidized tryptic digest of bovine serum albumin (Chapter 5) were searched against the sequence of bovine serum albumin using the SEQUEST algorithm[9] (Thermo Finnigan) with the following parameters: Enzyme type: trypsin; Number of possible missed cleavage sites: 3; Precursor mass tolerance: 1.5; Peptide mass tolerance: 2.0. All spectra were searched with dynamic mass modifications of +16.0 u (methionine sulfoxide), +57.0 u (S-carboxyamidomethyl cysteine) and +73.0 u (S-carboxyamidomethyl cysteine sulfoxide). Manual inspection of each spectrum was performed to validate all SEQUEST identifications.

3.15.3 Quantitative Analysis of Product Ion Abundances

Quantitative evaluation of non-sequence product ion abundances in the model S-alkyl cysteine sulfoxide- or methionine sulfoxide-containing peptide ions (Chapter 5) were performed by cleavage intensity ratio (CIR) calculations, essentially as described previously.[76, 81] Product ion abundances were first normalized by dividing the experimentally observed abundances by the square root of their charge states. Then, CIR calculations were performed by dividing the normalized abundance of the non-sequence product ion by the average normalized abundance of all the product ions observed from all cleavage sites within the peptide. CIR values greater than 1.0 are indicative of an

"enhanced" cleavage, while values less than 1.0 indicate a "suppressed" cleavage. The fractional abundance of product ions formed by sequential fragmentations (i.e., formation of a non-sequence product ion followed by further loss of H_2O or by further sequence ion fragmentation, or vice versa) included in the non-sequence CIR calculations were based on the relative abundances of the individual non-sequence and sequence product ions from which they were formed.

Quantitative analysis of non-sequence product ions from the oxidized tryptic digest of bovine serum albumin (Chapter 5) were performed by first filtering the spectra to remove any ions present below 50 counts (empirically determined to be a reasonable approximation of the level of chemical noise in the spectra). Then, the percent total product ion abundances were obtained by expressing the summed abundances of product ions formed by the loss of H_2NCOCH_2SOH, as well as the fractional abundance of product ions resulting from sequential losses (i.e., formation of a non-sequence product ion followed by immediate sequence ion fragmentation, or vice versa), as a fraction of the total product ion abundance.

3.15.4 Quantitative Analysis of Calcineurin Methionine Oxidation

Three different approaches were employed to quantify the extent of oxidation which had occurred at the side chain of individual methionine residues following the treatment of calcineurin with hydrogen peroxide for varying reaction times (Chapter 7). In the first approach, previously described by Carruthers *et al.*,[202] the precursor ion abundances for both the reduced and oxidized forms of the methionine-containing peptides of interest were determined following LC-MS/MS analysis of the native or

oxidized LysC digests prior to side chain fixed-charge derivatization. If a peptide was observed in multiple precursor ion charge states, the abundances of each of the precursor ions were combined. All peptide sequences were confirmed by manual inspection of the corresponding CID-MS/MS product ion spectra. The proportion of the peptide in the reduced form was then calculated as $[Met_{native}]/([Met_{native}] + [Met_{oxidized}])$.

In the second approach, the precursor ion abundances for the side chain fixed-charge derivatives of the methionine-containing peptides of interest were determined following LC-MS/MS analysis of the native and oxidized LysC digests which had been subjected to fixed-charge derivatization. If a peptide was observed in multiple precursor ion charge states, the abundances of each of the precursor ions were combined. The proportion of the peptide in the reduced form was then calculated by dividing the precursor ion abundance of the fixed-charge methionine-containing peptide from the oxidized sample by the precursor ion abundance of the fixed-charge methionine-containing peptide from the native sample.

In the third approach, the abundances of the product ions resulting from the neutral loss of $CH_3SCH_2COC_6H_5$ from the fixed-charge methionine-containing peptides of interest were determined following LC-MS/MS analysis of the native and oxidized LysC digests which had been subjected to side chain fixed-charge derivatization. If a peptide was observed in multiple precursor ion charge states, the abundances of each of the neutral loss product ions were combined. The proportion of the peptide in the reduced form was then calculated by dividing the neutral loss product ion abundance determined for the oxidized sample by the netural loss product ion abundance determined for the native sample.

CHAPTER FOUR

The Origin and Control of *Ex Vivo* Oxidative Peptide Modifications Prior to Mass Spectrometry Analysis*

4.1 Introduction

A common result of the numerous *ex vivo* sample handling steps typically employed for protein purification and sample preparation prior to mass spectrometry analysis (e.g., one- or two-dimensional gel electrophoresis, multidimensional chromatography, proteolytic digestion, etc.), is the partial oxidative modification of certain amino acids, including methionine, cysteine, S-alkyl cysteine and tryptophan.[3, 4, 122, 133, 134, 203-205] In addition, the oxidation of individual amino acid residues has also been demonstrated to occur during the electrospray ionization process.[206] The presence of these modifications can lead to a significant increase in the heterogeneity of the resultant peptide mixture, thereby compromising the sensitivity for analysis of individual peptides, as well as reduce the overall number of proteins that may be identified from its analysis. Artifactual oxidation during sample processing can also impede efforts to identify, characterize and quantify the sites of biologically significant *in vivo* oxidative modifications,[207-211] as well as limit the applicability of chemical derivatization strategies that have been developed to selectively identify and/or quantify peptides containing these amino acids.[40, 46, 48, 169, 172, 212-215]

---

* The results described in this Chapter have been published in: Froelich, J.M.; Reid, G.E. The Origin and Control of *Ex Vivo* Oxidative Peptide Modifications Prior to Mass Spectrometry Analysis. *Proteomics* **2008**, *8*, 1334-1345.

As discussed in Section 1.3.3 of Chapter 1, low-energy CID-MS/MS fragmentation of methionine sulfoxide-containing peptide ions results in the formation of dominant product ions via the neutral loss of methane sulfenic acid (CH_3SOH, 64 Da) from the modified amino acid side chain under non-mobile or partially mobile proton conditions.[4, 122, 204, 216-218] Similar losses have also been observed from the fragmentation reactions of oxidized S-alkyl cysteine-containing peptide ions.[122, 133-135] The information provided by these structurally diagnostic non-sequence ions can be used to assist the manual validation of peptide assignments from CID-MS/MS product ion spectra[219, 220] and could potentially be employed to improve the specificity of subsequent database analysis strategies by enabling searches against only a subset of the peptides contained within the sequence database (i.e., those containing methionine or cysteine). However, the formation of non-sequence ions at high abundance may result in the loss of sequence information potentially limiting the utility of database search algorithms[9, 10] or de-novo analysis strategies[7] employed for protein identification and characterization. In these cases, alternate analysis strategies involving automatically subjecting the initial neutral loss product ion to MS^3 analysis in a data dependent mode of operation can be employed to significantly increase the extent of sequence information obtained.[137, 140] Thus, it is important to determine the source(s) of these *ex vivo* sample handling related oxidative modifications and, depending on the mass spectrometry based strategy to be employed for protein identification and characterization, to develop conditions for the deliberate reduction or oxidation of peptides containing these amino acids prior to their analysis by mass spectrometry.

The reduction of organic sulfoxides to their corresponding thioethers, or the reduction of methionine sulfoxide to methionine within peptides and proteins, have previously been achieved using a variety of reagents including dithiothreitol, mercaptoacetic acid, mercaptoethanol, N-methylmercaptoacetamide, dimethylsulfide and tris(2-carboxyethyl)phosphine.[200, 221-224] However, a number of these reagents require elevated temperatures, extended reaction times, or both. Similarly, a number of reagents, including hydrogen peroxide, dimethyl sulfoxide, periodate, chloramine-T, N-chlorosuccinimide and mild brominating agents have previously been employed for the deliberate oxidation of methionine residues within peptides and proteins.[200, 224-232] Many of these reagents have also been shown to result in oxidation of other amino acid residues, including tryptophan, cysteine or histidine.[78, 224, 228-235] Modified amino acids such as S-alkyl cysteine, which are commonly formed during the sample processing steps employed prior to peptide analysis, may also be susceptible to oxidation using these reagents.

Here, the origin of *ex vivo* sample handling related oxidative peptide modifications of methionine, S-alkyl cysteine and tryptophan have been investigated by analysis of peptide mixtures obtained by tryptic digestion of a series of standard proteins, either in solution, or following their separation by one-dimensional gel electrophoresis. Conditions for controlling the oxidation state (both oxidation and reduction) of peptides containing these residues, as well as those containing cysteine, have also been determined using a series of model synthetic peptides. The utility of these conditions were then evaluated by analysis of a series of peptide mixtures obtained from standard proteins under typical solution-phase or in-gel digestion conditions.

4.2 Determining the Origin of *Ex Vivo* Sample Handling Related Oxidative Peptide Modifications under In-solution versus In-gel Proteolytic Digestion Conditions

To determine the origin of oxidative peptide modifications as a function of the sample handling steps employed prior to mass spectrometry analysis, the standard proteins bovine apo-transferrin, equine myoglobin, yeast enolase, rabbit aldolase, yeast alcohol dehydrogenase and bovine serum albumin (BSA) were each subjected to tryptic digestion, either in solution or following their initial separation by one-dimensional gel electrophoresis. For both digestion strategies, the proteins were reduced and alkylated with iodoacetamide prior to proteolytic digestion. Each of the resultant peptide mixtures were then individually analyzed by capillary LC-MS/MS. The extent of oxidation observed for methionine, tryptophan and S-carboxyamidomethyl (S-cam) cysteine containing peptides, following triplicate analysis of individual solution-phase and in-gel tryptic digests of the bovine apo-transferrin protein, are shown in Table 4.1.

Under in-gel tryptic digestion conditions, an average of 25% oxidation of methionine-containing peptides was observed, whereas the peptides obtained under in-solution tryptic digestion conditions resulted in an average of only 4% methionine oxidation. The extent of methionine oxidation observed under the in-gel digestion conditions employed here was somewhat lower than that from a previous study, where approximately 50% of methionine residues were found to be oxidized following in-gel digestion and LC-MS/MS analysis.[81] This difference is likely due to the fact that in the current study, particular emphasis was placed on minimizing the time taken between the electrophoretic separation and in-gel digestion steps, and the mass spectrometry analysis, whereas in the prior study, no particular emphasis was given toward minimizing the

expected temporal dependence on the magnitude of sample handling related oxidation. Although we have not performed additional experiments, an alternate explanation could also be that the extent of *ex vivo* sample handling related oxidation may have some dependence on the amount of protein initially loaded onto the gel (Note that in the current study, 3 pmol of each protein digest was analyzed by LC-MS/MS in order to maximize the sequence coverage obtained by analysis of the various protein digests, whereas in the previous report, the sample amounts were more typical (approx. 100 fmol-1 pmol) of that encountered in conventional proteomics based protein identification strategies). The average percent oxidation of tryptophan-containing peptides from the bovine apo-transferrin tryptic digest was also found to be greater when produced under the in-gel digestion conditions compared to that from the in-solution digestion (8% versus 3%, respectively). Similarly, the extent of oxidation of S-carboxyamidomethyl cysteine residues following in-gel digestion was found to be generally higher than those obtained under the in-solution conditions. However, both in-gel and in-solution digestion strategies resulted in average percent oxidation levels for S-cam cysteine of less than 1%. Essentially identical results, in terms of the average % oxidation of methionine, tryptophan and S-carboxyamidomethyl cysteine peptides observed under in-gel versus in-solution tryptic digestion conditions, were also obtained by analysis of the additional proteins investigated in this study (equine myoglobin, yeast enolase, rabbit aldolase, yeast alcohol dehydrogenase and bovine serum albumin). These results are summarized in Tables 4.2, 4.3 and 4.4 for methionine, tryptophan and S-carboxyamidomethyl cysteine residues, respectively.

Table 4.1 Triplicate analysis of the *ex vivo* sample handling related oxidation of methionine, tryptophan and S-cam cysteine residues of the standard protein bovine apo-transferrin following in-solution or in-gel tryptic digestion.

Peptide[a),b)]	% Oxidation[c)]					
	Methionine[d)]		Tryptophan[e)]		S-cam Cysteine[f)]	
	Solution	In-gel	Solution	In-gel	Solution	In-gel
GEADAMSLDGGYLYIAGK	0 ± 0	25 ± 11	–	–	–	–
IMKGEADAMSLDGGYLYIAGK	4 ± 1[g)]	36 ± 8[g)]	–	–	–	–
TAGWNIPMGLLYSK	3 ± 1	25 ± 1	0 ± 0	25 ± 1	–	–
C*LMEGAGDVAFVK	3 ± 0.1	13 ± 3	–	–	0 ± 0	0 ± 0
SVDDYQEC*YLAMVPSHAVVAR	6 ± 2	25 ± 5	–	–	0 ± 0	0 ± 0
KSVDDYQEC*YLAMVPSHAVVAR	5 ± 1	24 ± 5	–	–	0 ± 0	0 ± 0
TSDANINWNNLK	–	–	5 ± 1	4 ± 0	–	–
DQTVIQNTDGNNEAWAK	–	–	0 ± 0	0 ± 0	–	–
WC*TISTHEANK	–	–	4 ± 0.3	4 ± 1	0 ± 0	0 ± 0
WC*AIGHQER	–	–	6 ± 2	8 ± 6	0 ± 0	0 ± 0
C*LASIAK	–	–	–	–	0 ± 0	0 ± 0
INNC*KFDEFFSAGC*APGSPR	–	–	–	–	3 ± 0.2[h)]	10 ± 3[h)]
SVTDC*TSNFC*LFQSNSK	–	–	–	–	0 ± 0	0 ± 0
C*AC*SNHEPYFGYSGAFK	–	–	–	–	0 ± 0	0 ± 0
KENFEVLC*K	–	–	–	–	0 ± 0	0 ± 0
ILESGPFVSC*VK	–	–	–	–	0 ± 0	0 ± 0
C*LVEKGDVAFVK	–	–	–	–	0 ± 0	0 ± 0
NYELLC*GDNTR	–	–	–	–	0 ± 0	0 ± 0
C*ASFRENVLR	–	–	–	–	0 ± 0	0 ± 0
AAANFFSASC*VPCADQSSFPK	–	–	–	–	0 ± 0	0 ± 0
Average % Oxidation	4 ± 2	25 ± 7	3 ± 3	8 ± 10	< 1.0 ± 1	< 1.0 ± 3

a) Peptide sequences confirmed by CID-MS/MS.

b) C* represents S-carboxyamidomethyl (S-cam) cysteine.

c) % Oxidation reported as the average and standard deviation of three replicate experiments.

d) Single oxidation to yield methionine sulfoxide.

e) Single oxidation to yield oxindolylalanine.

f) Single oxidation to yield S-cam cysteine sulfoxide.

g) Site of oxidation at one of the methionine residues.

h) Site of oxidation at one of the S-cam cysteine residues.

Table 4.2 *Ex vivo* sample handling related oxidation and deliberate reduction of methionine residues of standard proteins following in-solution or in-gel tryptic digestion.

Protein	Peptide[a),b)]	% Oxidation		
		Methionine[c)]		
		Solution	In-gel	Reduced In-gel[d)]
Equine Myoglobin	HPGDFGADAQGAMTK	2[e)]	35[e)]	7[e)]
Yeast Enolase	SIVPSGASTGVHEALEMR	4	34[e)]	5[e)]
	AAQDSFAAGWGVMVSHR	5	44	18
	WLTGPQLADLYHSLMK	0	37	NA[f)]
Rabbit Aldolase	YSHEEIAMATVTALR	10	79	0
	IGEHTPSALAIMENANVLAR	14	32	4
Yeast Alchohol Dehydrogenase	ANGTTVLVGMPAGAK	1	26	5
	LPLVGGHEGAGVVVGMGENVK	0	0	0
	SANLMAGHWVAISGAAGGLGSLAVQYAK	2	NA[f)]	NA[f)]
Bovine Serum Albumin	TVMENFVAFVDK	1	13	8
	MPC*TEDYLSLILNR	9	24	0
	VASLRETYGDMADC*C*EK	0	0	NA[f)]
Average % Oxidation		4±5	29±22	5±6

a) Peptide sequences confirmed by CID-MS/MS.

b) C* represents S-carboxyamidomethyl (S-cam) cysteine.

c) Single oxidation to yield methionine sulfoxide.

d) Reduction performed following peptide extraction from the gel.

e) Methionine sulfone present at <1%.

f) Reduced or oxidized forms of the peptide were not observed.

Table 4.3 *Ex vivo* sample handling related oxidation and deliberate reduction of tryptophan residues of standard proteins following in-solution or in-gel tryptic digestion.

Protein	Peptide[a]	% Oxidation Tryptophan[b]		
		Solution	In-gel	Reduced In-gel[c]
Equine Myoglobin	GLSDGEWQQVLNVWGK	0	NA[d]	NA[d]
Yeast Enolase	AAQDSFAAGWGVMVSHR	3	16	11
	WLTGPQLADLYHSLMK	0	0	NA[d]
Rabbit Aldolase	AWGGKKENLK	0	NA[d]	NA[d]
Yeast Alchohol Dehydrogenase	LPLVGGHEGAGVVVGMGENVK	–	–	–
	SANLMAGHWVAISGAAGGLGSLAVQYAK	0	NA[d]	NA[d]
Bovine Serum Albumin	ALKAWSVAR	0	3	5
Average % Oxidation		1±1	6±9	8±4

a) Peptide sequences confirmed by CID-MS/MS.

b) Single oxidation to yield oxindolylalanine.

c) Reduction performed following peptide extraction from the gel.

d) Reduced or oxidized forms of the peptide were not observed.

Table 4.4 *Ex vivo* sample handling related oxidation and deliberate reduction of S-carboxyamidomethyl (S-cam) cysteine residues of standard proteins following in-solution or in-gel tryptic digestion.

Protein	Peptide[a),b)]	% Oxidation		
		S-cam Cysteine[c)]		
		Solution	In-gel	Reduced In-gel[d)]
Yeast Enolase	IGLDC*ASSEFFK	0	1	2
Rabbit Aldolase	ALANSLAC*QGK	< 1	< 1	0
Yeast Alchohol Dehydrogenase	C*C*SDVFNQVVK	0	0	0
Bovine Serum Albumin	MPC*TEDYLSLILNR	0	0	0
	VASLRETYGDMADC*C*EK	0	0	NA[e)]
	LKEC*C*DKPLLEK	0	0	0
	VHKEC*C*HGDLLEC*ADDR	0	0	NA[e)]
	YIC*DNQDTISSK	6	6	0
	GAC*LLPK	0	0	0
	EYEATLEEC*C*AK	0	0	NA[e)]
	LAKEYEATLEEC*C*AK	0	0	0
	C*C*AADDKEAC*FAVEGPK	0	0	0
	NEC*FLSHKDDSPDLPK	2	0	0
	QEPERNEC*FLSHKDDSPDLPK	1	0	NA[e)]
	YNGVFQEC*C*QAEDK	0	NA[e)]	NA[e)]
	YNGVFQEC*C*QAEDKGAC*LLPK	0	0	0
	DDPHAC*YSTVFDK	0	0	NA[e)]
	LKPDPNTLC*DEFK	0	0	0
	LKPDPNTLC*DEFKADEK	0	8	0
	RPC*FSALTPDETYVPK	0	0	0
	SLHTLFGDELC*K	1	7	10
	C*C*TESLVNR	0	0	0
Average % Oxidation		<1±1	1±3	1±3

a) Peptide sequences confirmed by CID-MS/MS.

b) C* represents S-carboxyamidomethyl (S-cam) cysteine.

c) Single oxidation to yield S-cam cysteine sulfoxide.

d) Reduction performed following peptide extraction from the gel.

e) Reduced or oxidized forms of the peptide were not observed.

Given the relative ease by which peptides containing particular amino acid residues such as methionine, tryptophan and S-alkyl cysteine can become oxidized during sample preparation, it is important to evaluate the effect of these oxidative modifications on the resultant CID-MS/MS product ion spectra. This is particularly important given the increasing application of *in silico* product ion intensity prediction algorithms for use in enhanced database search analysis strategies.[236-241] As demonstrated previously, oxidative modifications may result in the formation of dominant diagnostic non-sequence product ions by fragmentation of the modified amino acid side chain during MS/MS (e.g., the loss of CH_3SOH or RSOH (where R=alkyl) from methionine sulfoxide or S-alkyl cysteine sulfoxide residues, respectively).[81, 133] An example is provided in Figures 4.1A and 4.1B, where the mass spectra obtained following CID-MS/MS of the doubly protonated precursor ions of the reduced and singly oxidized peptide MPC(S-cam)TEDYLSLILNR derived from the in-gel tryptic digest of BSA are shown. The presence of the dominant product ion corresponding to the loss of CH_3SOH in Figure 4.1B confirms the site of oxidation at the methionine side chain. As an alternative to the formation of diagnostic non-sequence product ions, the effect of oxidation may also be to alter the identity and relative abundances of the sequence ions observed. For example, comparison of the CID-MS/MS spectra obtained from dissociation of the doubly protonated precursor ions of the reduced and singly oxidized peptide ALKAWSVAR from the in-gel tryptic digest of BSA (Figures 4.1C and 4.1D, respectively), revealed that the site of oxidation was at the tryptophan residue, and that the abundance of the sequence ions adjacent to the tryptophan residue (i.e. the y_4, y_5, b_4 and b_5 ions) had decreased upon oxidation. Although not structurally diagnostic, tryptophan oxidation

may also result in an increase in the neutral loss of water, as shown by comparison of the CID-MS/MS product ion spectra of the triply protonated precursor ions of the reduced and oxidized (at the tryptophan reside) peptide WC(S-cam)TISTHEANK from the in-gel tryptic digest of bovine apo-transferrin (Figures 4.1E and 4.1F, respectively). This is consistent with a previous study on the oxidation of model peptide derivatives containing tryptophan.[78]

Figure 4.1 CID-MS/MS product ion spectra of reduced and oxidized forms of methionine- and tryptophan-containing peptides derived from in-gel tryptic digests of bovine serum albumin (Figures 4.1A-4.1D) and bovine apo-transferrin (Figures 4.1E and 4.1F). (A) the $[M+2H]^{2+}$ precursor ion of reduced MPC(S-cam)TEDYLSLILNR, (B) the $[M+2H]^{2+}$ precursor ion of singly oxidized M(ox)PC(S-cam)TEDYLSLILNR, (C) the $[M+2H]^{2+}$ precursor ion of reduced ALKAWSVAR, (D) the $[M+2H]^{2+}$ precursor ion of singly oxidized ALKAW(ox)SVAR, (E) the $[M+3H]^{3+}$ precursor ion of reduced WCTISTHEANK and (F) the $[M+3H]^{3+}$ precursor ion of singly oxidized W(ox)CTISTHEANK.

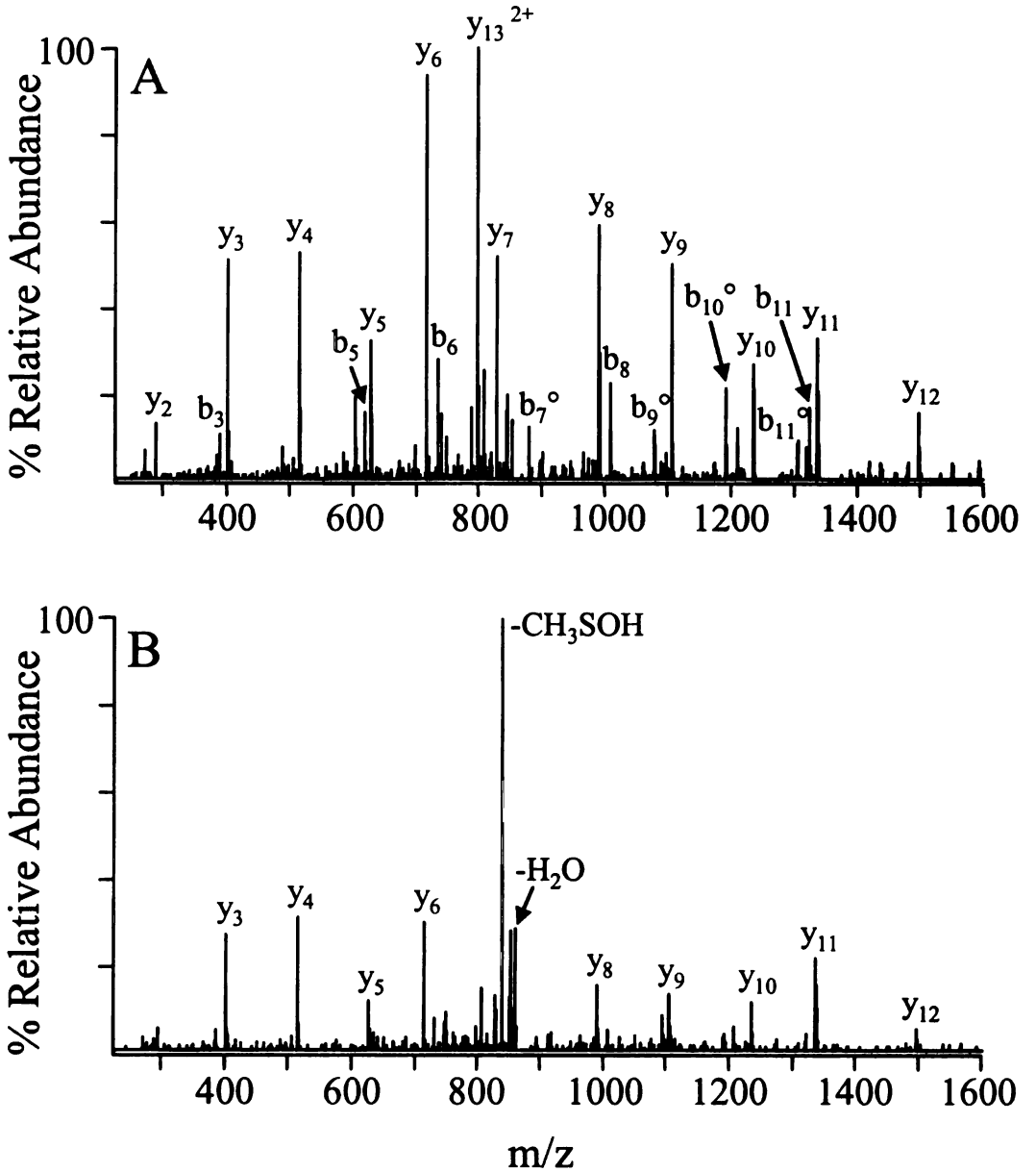
A
100
% Relative Abundance
y_{13}^{2+}
y_6
y_3
y_4
y_7
y_8
y_9
$b_{10}°$
b_{11}
y_{11}
y_5
b_5
b_6
y_{10}
b_8
y_2
b_3
$b_7°$
$b_9°$
$b_{11}°$
y_{12}
400
600
800
1000
1200
1400
1600
B
100
% Relative Abundance
-CH_3SOH
-H_2O
y_3
y_4
y_6
y_5
y_8
y_9
y_{10}
y_{11}
y_{12}
400
600
800
1000
1200
1400
1600
m/z

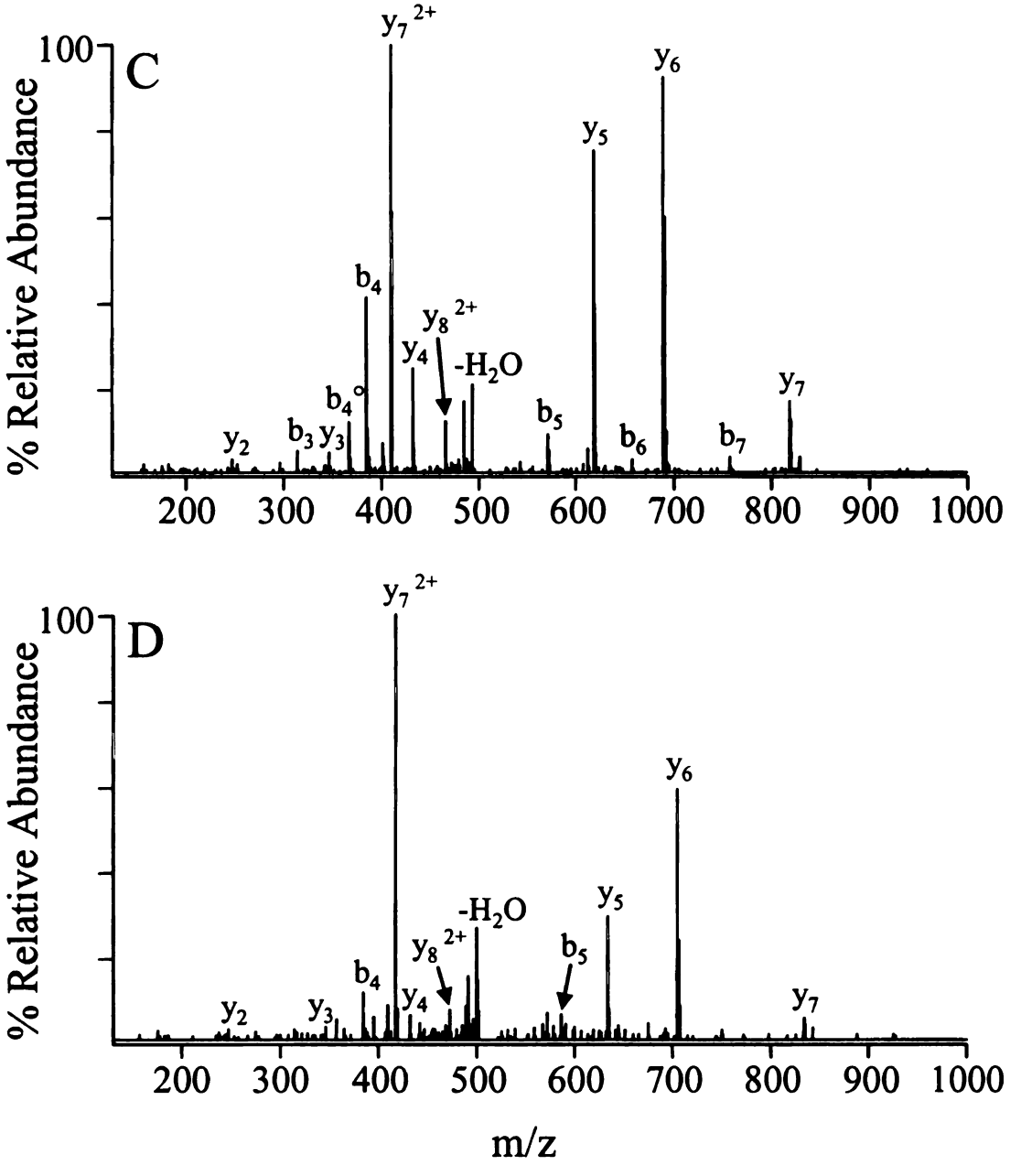

Figure 4.1 (continued)

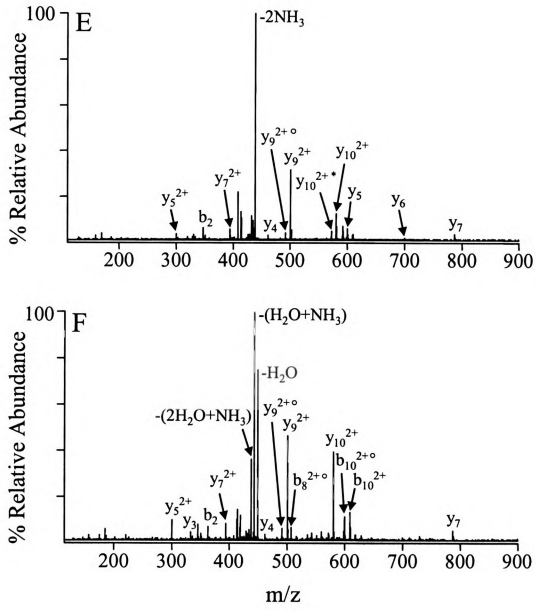

Figure 4.1 (continued)

4.3 Determining Optimized Conditions for Peptide Oxidation Prior to MS/MS Analysis

As discussed above, it may be beneficial to purposely oxidize peptides containing amino acid residues such as methionine and S-alkyl cysteine, which give rise to dominant structurally diagnostic non-sequence product ions upon CID-MS/MS, in order to assist in the selective identification and characterization of these peptides by "targeted" proteome analysis strategies. Therefore, conditions for effectively controlling the oxidation of these residues, while minimizing unwanted oxidative modifications of other amino acids, must be determined. In an initial attempt to address this issue, oxidation of the synthetic model tryptic peptide VTMAHFWNFGK (MWK) was carried out by reaction with 1 M dimethyl sulfoxide (DMSO)/4 M HCl/11 M acetic acid (CH_3COOH) for 5 minutes at room temperature, as previously described.[78, 234] MWK was chosen for this evaluation due to the presence of methionine, tryptophan and histidine residues, each of which could potentially undergo oxidation to form methionine sulfoxide, oxindolylalanine and 2-oxo-histidine, respectively.[78, 200, 231, 234, 235] Under these reaction conditions, complete oxidation of both methionine to methionine sulfoxide and tryptophan to oxindolylalanine was observed, while the histidine residue was found to be unaffected (determined by MS/MS, data not shown). Thus, given the extent of tryptophan oxidation observed, it was determined that the 1 M DMSO/4 M HCl/11 M CH_3COOH reaction conditions would not be suitable for applications where only the selective oxidation of methionine residues was desired. In contrast, Table 4.5 shows the % oxidation of individual amino acid residues following reaction of MWK, as well as several other methionine-containing peptides GAILMGAILK (MK), GAILMGAILR (MR) and VTMGHFDNFGR (MDR),

using reaction conditions of 30% hydrogen peroxide (H_2O_2)/5% CH_3COOH[81] at room temperature for time points of 5, 30 and 45 minutes. Complete conversion of all four peptides to their singly oxidized forms (+16 mass units) was observed after reaction for 5 minutes. The product ion spectra obtained by CID-MS/MS of the doubly protonated precursor ions of the reduced and singly oxidized MWK peptide are shown in Figures 4.2A and 4.2B, respectively. It can be seen from Figure 4.2B that the characteristic neutral loss of CH_3SOH from the methionine sulfoxide side chain was observed as the dominant fragmentation pathway, indicating that oxidation had occurred at the methionine residue. No evidence was observed for oxidation at the tryptophan or histidine residues, as indicated by the presence of the y_5, y_6, y_7 and y_8 product ions at identical *m/z* values to those in the reduced peptide. The exclusive oxidation of methionine to methionine sulfoxide in the MK, MR and MDR peptides was also confirmed by CID-MS/MS (data not shown). After reaction for 45 minutes, the singly oxidized M(ox)WK peptide had undergone secondary oxidation to a level of approximately 20% (Table 4.5). CID-MS/MS of the doubly protonated precursor ion of this peptide resulted in observation of the y_5, y_6, y_7 and y_8 product ions at *m/z* values +16 mass units higher than those in the reduced peptide, indicating that the secondary oxidation had occurred exclusively at the tryptophan residue to yield oxindolylalanine (Figure 4.2C). No evidence for secondary oxidation of the methionine sulfoxide residue to methionine sulfone in the M(ox)WK, M(ox)K, M(ox)R or M(ox)DR peptides was observed, except at reaction times longer than 24 hours.

Table 4.5 Oxidation of individual amino acid residues following the reaction of model tryptic peptides with 30% H_2O_2/5% CH_3COOH at room temperature.

Peptide	Modification [a] (Reduced → Oxidized)	% Oxidation		
		5 min	30 min	45 min
GAILMGAILK	Methionine → Methionine Sulfoxide	100	100	100
GAILMGAILR	Methionine → Methionine Sulfoxide	100	100	100
VTMGHFDNFGR	Methionine → Methionine Sulfoxide	100	100	100
VTMAHFWNFGK	Methionine → Methionine Sulfoxide	100	100	100
	Tryptophan → Oxindolylalanine	0	0	18
VTMGHFCNFGK	Methionine → Methionine Sulfoxide	100	100	100
	Cysteine → Cysteic Acid	100	100	100
GAILCGAILK	Cysteine → Cysteic Acid	15	58	86
GAILCGAILR	Cysteine → Cysteic Acid	100	100	100
VTMGHFC(S-cam)NFGK	Methionine → Methionine Sulfoxide	100	100	100
	S-cam Cysteine → S-cam Cysteine Sulfoxide	49	100	100
GAILC(S-cam)GAILK	S-cam Cysteine → S-cam Cysteine Sulfoxide	32	100	100
GAILC(S-cam)GAILR	S-cam Cysteine → S-cam Cysteine Sulfoxide	39	100	100

[a] S-cam = S-carboxyamidomethyl

Figure 4.2 CID-MS/MS product ion spectra of the $[M+2H]^{2+}$ precursor ions of (A) reduced VTMAHFWNFGK (MWK), (B) singly oxidized VTM(ox)AHFWNFGK (M(ox)WK) formed by reaction with 30% H_2O_2/5% CH_3COOH at room temperature for 5 minutes, (C) doubly oxidized VTM(ox)AHFW(ox)NFGK (M(ox)W(ox)K) formed by reaction with 30% H_2O_2/5% CH_3COOH at room temperature for 45 minutes and (D) singly oxidized VTMAHFW(ox)NFGK (MW(ox)K) formed by reaction with 1 M DMS/10 M HCl at room temperature for 45 minutes.

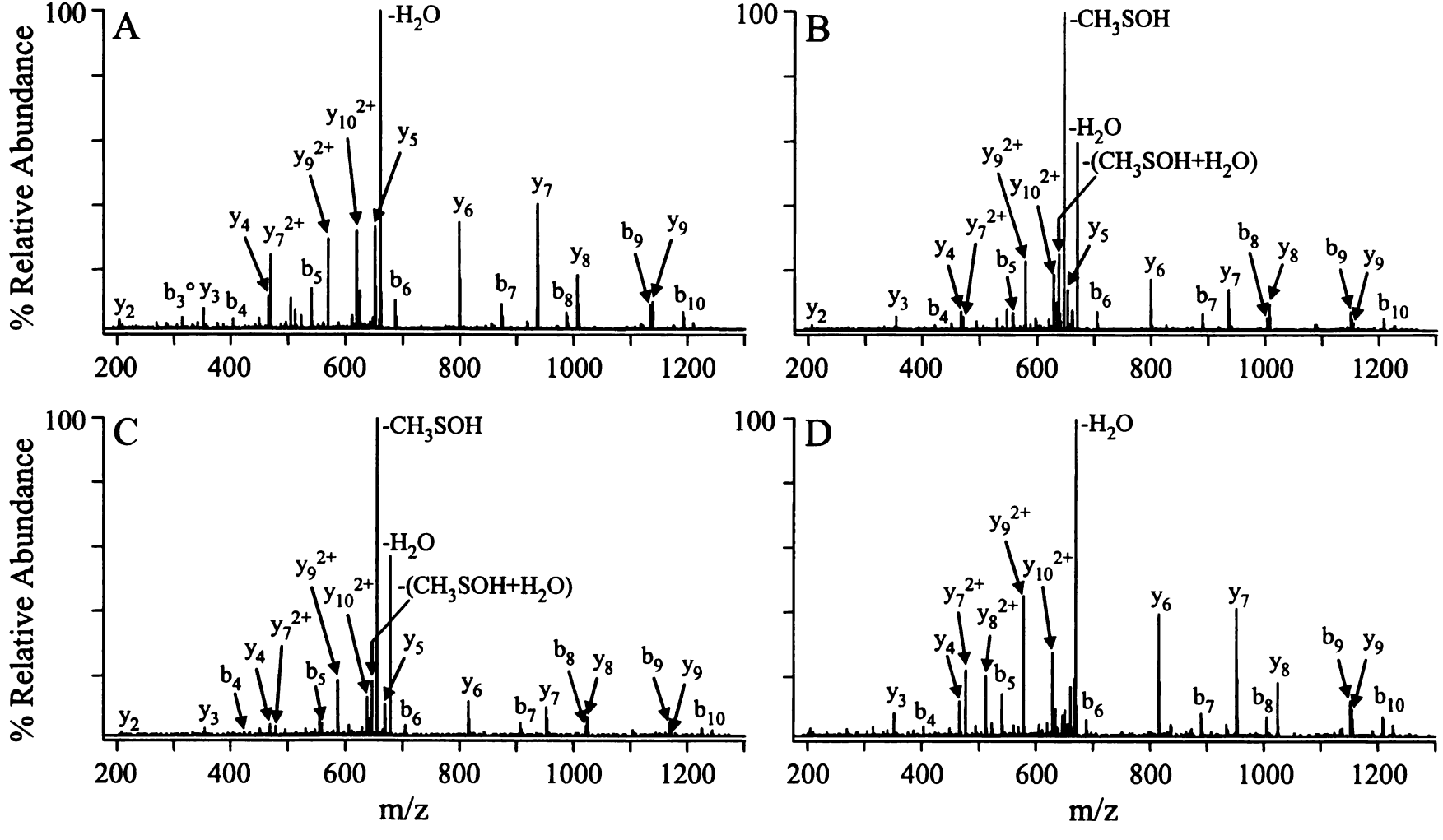
A
B
C
D
100
% Relative Abundance
m/z
200
400
600
800
1000
1200
-H2O
-CH3SOH
-(CH3SOH+H2O)
y2
y3
b3°
b4
y4
y7 2+
y9 2+
y10 2+
b5
y5
b6
y6
b7
y7
b8
y8
b9
y9
b10

It was also important to determine what effect, if any, the 30% H_2O_2/5% CH_3COOH reaction conditions would have on the oxidation of cysteine to cysteic acid.[116, 117] Furthermore, as most tandem mass spectrometry approaches typically involve the reduction and alkylation of cysteine residues prior to enzymatic digestion,[3, 242-244] it was also of interest to determine the effect of these reaction conditions on the oxidation of S-alkyl cysteine to S-alkyl cysteine sulfoxide. The reduced cysteine-containing peptides VTMGHFCNFGK (MCK), GAILCGAILK (CK) and GAILCGAILR (CR) along with their S-carboxyamidomethyl (S-cam) derivatives, prepared by reaction with 25 mM iodoacetamide under basic conditions (pH 7.8) for 20 minutes at room temperature (VTMGHFC(S-cam)NFGK (MC(S-cam)K), GAILC(S-cam)GAILK (C(S-cam)K) and GAILC(S-cam)GAILR (C(S-cam)R)), were subjected to reaction at room temperature with 30% H_2O_2/5% CH_3COOH for time periods of 5, 30 and 45 minutes. The % oxidation observed from these reactions is summarized in Table 4.5. The product ion spectra obtained by CID-MS/MS of the doubly protonated precursor ion of the reduced MCK peptide, as well as the spectrum obtained from analysis of the modified MCK peptide (corresponding to an increase of +64 mass units compared to the reduced peptide) after a reaction period of 5 minutes, are shown in Figures 4.3A and 4.3B, respectively. Interpretation of these spectra indicated that complete conversion of both methionine to methionine sulfoxide and of cysteine to cysteic acid had occurred (i.e., M(ox)C(ox_3)K). Although complete oxidation of the cysteine residue in the CR peptide was also observed after 5 minutes, only 86% of the CK peptide was oxidized, even after a 45 minute reaction period, suggesting that oxidation rates may vary depending on the

amino acid sequence. Figure 4.4A depicts the product ion spectrum obtained by CID-MS/MS of the doubly protonated precursor ion of the alkylated MC(S-cam)K peptide. Oxidation of this peptide for 5 minutes at room temperature in 30% H_2O_2/5% CH_3COOH resulted in the formation of two products, corresponding to the addition of +16 and +32 mass units. CID-MS/MS of the doubly protonated precursors of these products revealed that the addition of +16 mass units resulted from oxidation of the methionine residue (M(ox)C(S-cam)K, Figure 4.4B), while the addition of +32 mass units corresponded to the oxidation of both the methionine and S-cam cysteine residues (i.e., M(ox)C(S-cam)(ox)K, Figure 4.4C). Complete oxidation of the S-alkyl cysteine residue in the MC(S-cam)K peptide, as well as in the C(S-cam)K and C(S-cam)R peptides, was found to require a reaction time of 30 minutes (Table 4.5).

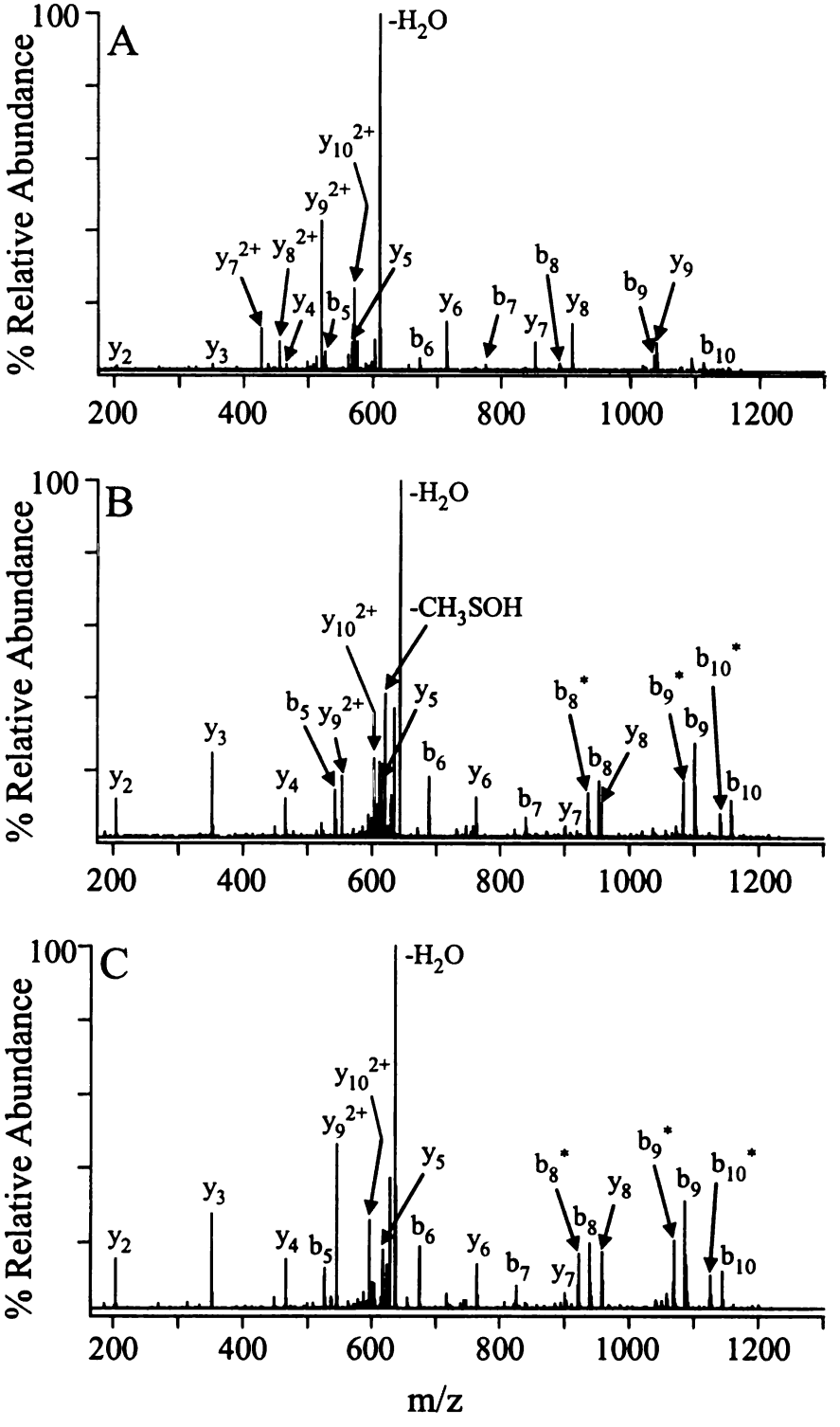

Figure 4.3 CID-MS/MS product ion spectra of the $[M+2H]^{2+}$ precursor ions of (A) reduced VTMGHFCNFGK (MCK), (B) quadruply oxidized VTM(ox)GHFC(ox_3)NFGK (M(ox)C(ox_3)K) formed by reaction with 30% H_2O_2/5% CH_3COOH at room temperature for 5 minutes and (C) triply oxidized VTMGHFC(ox_3)NFGK (MC(ox_3)K) formed by reaction with 1 M DMS/10 M HCl at room temperature for 10 minutes.

Figure 4.4 CID-MS/MS product ion spectra of the $[M+2H]^{2+}$ precursor ions of (A) reduced VTMGHFC(S-cam)NFGK (MC(S-cam)K), (B) singly oxidized VTM(ox)GHFC(S-cam)NFGK formed by reaction with 30% H_2O_2/5% CH_3COOH at room temperature for 5 minutes, (C) doubly oxidized VTM(ox)GHFC(S-cam)(ox)NFGK (M(ox)C(S-cam)(ox)K) formed by reaction with 30% H_2O_2/5% CH_3COOH at room temperature for 5 minutes and (D) singly oxidized VTMGHFC(S-cam)(ox)NFGK (MC(S-cam)(ox)K) formed by reaction with 1 M DMS/10 M HCl at room temperature for 10 minutes.

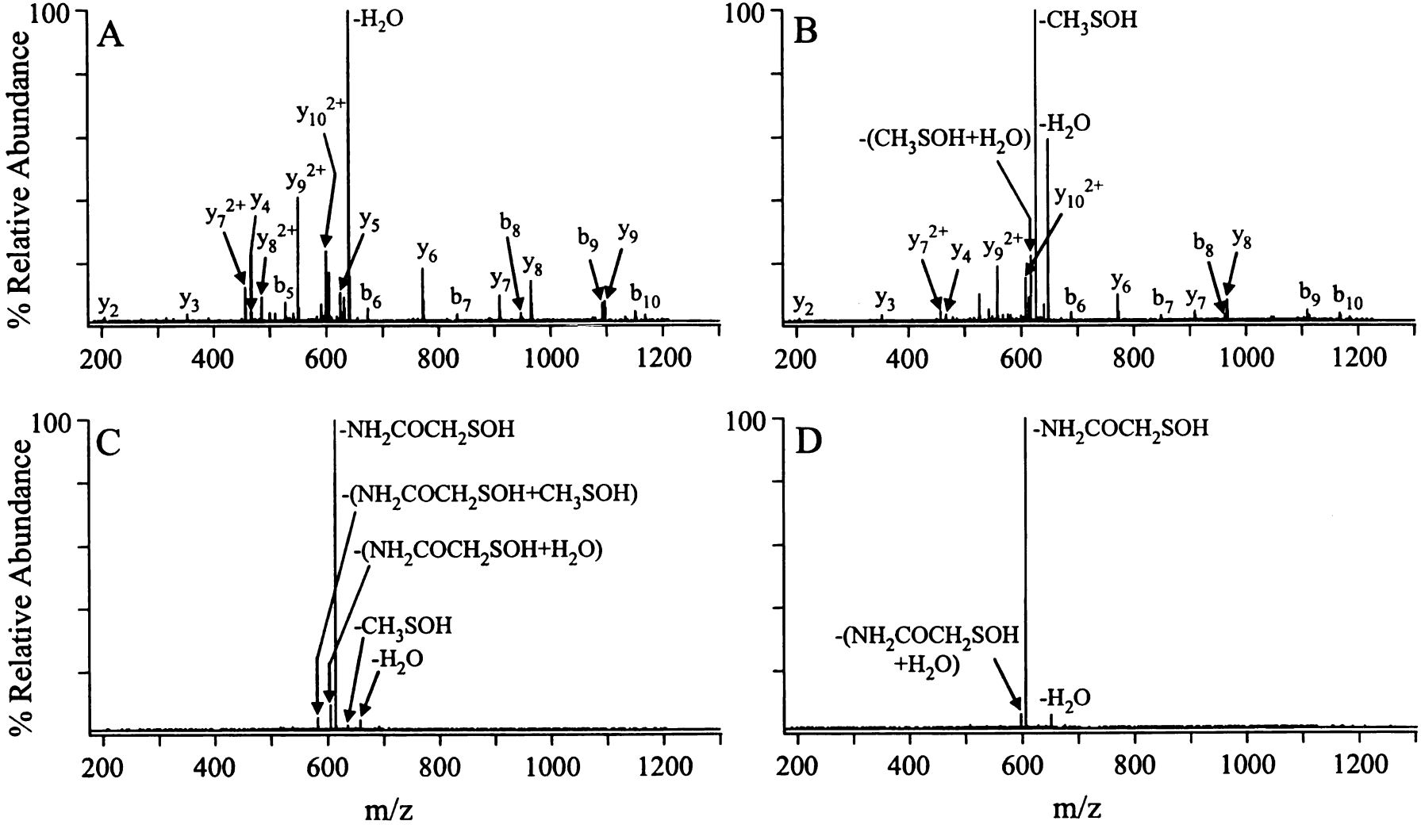
A
B
C
D
% Relative Abundance
m/z
100
200
400
600
800
1000
1200
-H2O
-CH3SOH
-(CH3SOH+H2O)
-NH2COCH2SOH
-(NH2COCH2SOH+CH3SOH)
-(NH2COCH2SOH+H2O)
y2
y3
y4
y5
y6
y7
y8
y9
y10
b5
b6
b7
b8
b9
b10

The above results indicate that optimized conditions for the oxidation of methionine to methionine sulfoxide and of S-carboxyamidomethyl cysteine to S-carboxyamidomethyl cysteine sulfoxide can be achieved by reaction with 30% H_2O_2/5% CH_3COOH at room temperature for 30 minutes. For this reaction time, the oxidation of tryptophan or histidine residues was not observed to any significant extent. In cases where cysteine residues are not alkylated prior to analysis, reaction with 30% H_2O_2/5% CH_3COOH at room temperature for at least 45 minutes is required to achieve the complete oxidation of methionine residues to methionine sulfoxide and of cysteine residues to cysteic acid. Under these conditions however, some oxidation of tryptophan to oxindolylalanine can result.

Confirmation that the oxidation conditions outlined above (30% H_2O_2/5% CH_3COOH at room temperature for 30 minutes) were generally applicable to the oxidation of more complex peptide mixtures was obtained by the observation of essentially complete oxidation of both methionine (93% average oxidation) and S-carboxyamidomethyl cysteine (95% average oxidation) residues in the S-carboxyamidomethylated in-solution tryptic digests of the standard proteins examined in Table 4.1 and Tables 4.2-4.4 (data not shown). The in-solution digests were chosen as they had initially resulted in only minimal levels of artifactual *ex vivo* sample handling related oxidation. For these reaction conditions, the average % oxidation of methionine sulfoxide residues to methionine sulfone was observed to be only 7%. Interestingly however, moderate levels of oxidation of individual tryptophan residues in these digests

(30% average oxidation) was observed, again suggesting that oxidation rates are dependant to some extent on the amino acid composition of the peptide.

4.4 Determining Optimized Conditions for Peptide Reduction Prior to MS/MS Analysis

Conditions for the effective reduction of methionine sulfoxide to methionine were initially evaluated by reaction of the oxidized M(ox)K peptide with a variety of previously proposed reducing agents, including dithiothreitol (DTT), N-methylmercaptoacetamide and tris(2-carboxy-ethyl)phosphine (TCEP)/iodine.[222, 223] Even in the presence of high concentrations of DTT (725 mM) and extended reaction times of up to 72 hours at 37°C, only minimal reduction of methionine sulfoxide was observed. Up to 85% reduction of the M(ox)K peptide could be achieved following reaction for 24 hours at 60°C in 0.1 M N-methylmercaptoacetamide prepared in 10% CH_3COOH. However, these elevated reaction temperatures could potentially result in competing losses of the peptide due to degradation by acid hydrolysis. Elevated temperatures of 80-90°C were also required to achieve reduction of the M(ox)K peptide by incubation in 10 and 5 mole equivalents of TCEP and iodine, respectively. However, the reaction was not observed to proceed to completion under these conditions due to competing oxidation of the methionine sulfoxide residue to yield methionine sulfone, presumably due to the presence of iodine in the reaction mixture. Thus, given the harsh conditions required for reduction to occur using these reagents, and the observation of incomplete reduction even at extended reaction times, it was determined that these

reagents would not be suitable for routine application when reactions under room temperature conditions or when reaction times of less than one hour were desired.

In contrast, reaction of the singly oxidized M(ox)K, M(ox)R and M(ox)DR peptides, as well as the doubly oxidized M(ox)W(ox)K and the quadruply oxidized M(ox)C(ox_3)K peptides, with 1 M dimethyl sulfide (DMS)/10 M HCl,[200] was found to be effective in achieving complete reduction of methionine sulfoxide to methionine, in a time period of only 10 minutes at room temperature (Table 4.6). In each case, the site of reduction was confirmed by CID-MS/MS of the doubly protonated precursor ions (data not shown). Using these conditions, the oxindolylalanine residue in the doubly oxidized M(ox)W(ox)K peptide was retained in its oxidized form, as was the cysteic acid residue in the M(ox)C(ox_3)K peptide, even after reaction for 45 minutes (Table 4.6). The CID-MS/MS product ion spectrum of the doubly protonated precursor ion of the MW(ox)K peptide is shown in Figure 4.2D, while that for the MC(ox_3)K peptide is shown in Figure 4.3C. Similarly, no reduction of the cysteic acid residues in the C(ox_3)K and C(ox_3)R peptides were observed, even at the extended 45 minute reaction time (Table 4.6). Reaction of the doubly oxidized M(ox)C(S-cam)(ox)K peptide in 1 M DMS/10 M HCl for 10 minutes at room temperature also resulted in complete reduction of the methionine sulfoxide residue to methionine. However, only 54% reduction of the oxidized S-cam cysteine residue was obtained under these conditions (Table 4.6). The CID-MS/MS product ion spectrum of the doubly charged precursor ion of the MC(S-cam)(ox)K peptide is shown in Figure 4.4D. Complete reduction of the S-cam cysteine sulfoxide residue in this peptide, as well those in the C(S-cam)(ox)K and C(S-cam)(ox)R peptides, was achieved however, after a reaction period of 45 minutes (Table 4.6).

Table 4.6 Reduction of individual amino acid residues following the reaction of oxidized model tryptic peptides with 1 M DMS/10 M HCl at room temperature.

Peptide	Modification [a] (Oxidized → Reduced)	% Reduction	
		10 min	45 min
GAILM(ox)GAILK	Methionine Sulfoxide → Methionine	100	100
GAILM(ox)GAILR	Methionine Sulfoxide → Methionine	100	100
VTM(ox)GHFDNFGR	Methionine Sulfoxide → Methionine	100	100
VTM(ox)AHFW(ox)NFGK	Methionine Sulfoxide → Methionine	100	100
	Oxindolylalanine → Tryptophan	0	0
VTM(ox)GHFC(ox_3)NFGK	Methionine Sulfoxide → Methionine	100	100
	Cysteic Acid → Cysteine	0	0
GAILC(ox_3)GAILK	Cysteic Acid → Cysteine	0	0
GAILC(ox_3)GAILR	Cysteic Acid → Cysteine	0	0
VTM(ox)GHFC(S-cam)(ox)NFGK	Methionine Sulfoxide → Methionine	100	100
	S-cam Cysteine Sulfoxide → S-cam Cysteine	54	100
GAILC(S-cam)(ox)GAILK	S-cam Cysteine Sulfoxide → S-cam Cysteine	61	100
GAILC(S-cam)(ox)GAILR	S-cam Cysteine Sulfoxide → S-cam Cysteine	52	100

[a] S-cam = S-carboxyamidomethyl

These data indicate that optimized conditions for the reduction of methionine sulfoxide residues to methionine may be readily achieved by reaction with 1 M DMS/10 M HCl at room temperature for 10 minutes. In cases where S-carboxyamidomethyl cysteine sulfoxide residues may also be present, a reaction time of 45 minutes is required. None of the reduction conditions evaluated were found to result in reduction of oxindolylalanine, cysteic acid or methionine sulfone.

Given that increased levels of methionine oxidation were found to be associated with the gel electrophoresis and/or in-gel tryptic digestion strategy compared to that from in-solution digestion conditions (Table 4.1 and Table 4.2), further evaluation of the conditions outlined above (1 M DMS/10 M HCl at room temperature for 45 minutes) was performed by reduction of the S-carboxyamidomethylated in-gel tryptic digests from the standard proteins examined in Tables 4.2-4.4. Initially, reduction was performed at the intact protein level, directly following electrophoretic separation. However, levels of oxidation similar to those seen in the absence of the reduction step were still observed following proteolytic digestion, peptide extraction and mass spectrometry analysis (data not shown), suggesting that either efficient reduction had not occurred in the gel matrix, or that oxidation had occurred during the sample handling (i.e., in-gel digestion and/or peptide extraction) steps prior to MS/MS analysis. In contrast, reduction of the extracted peptide mixtures immediately prior to mass spectrometry analysis was found to result in oxidation levels that were essentially the same as those observed from the in-solution digestion conditions. Note however, that incomplete reduction was observed for several individual peptides containing methionine sulfoxide or S-carboxyamidomethyl cysteine sulfoxide (Table 4.2 and Table 4.4), suggesting that particular residues are either

refractory to reduction or exhibit slower rates of reduction as a result of their amino acid compositions. It is also possible that individual residues may have undergone some re-oxidization during the sample clean-up steps employed after peptide reduction, but prior to MS/MS analysis. As expected, essentially equivalent values for the % oxidation of tryptophan residues were observed both prior to and following reduction, as oxindolylalanine residues were not able to be reduced under these conditions.

4.5 Conclusions

The results presented here confirm that increased levels of *ex vivo* sample handling related oxidative peptide modifications, particularly those involving methionine, result from the extended sample handling steps associated with electrophoretic separation and/or in-gel proteolytic digestion of proteins prior to their analysis by mass spectrometry. MS/MS of protonated peptides containing oxidative modifications of methionine and S-alkyl cysteine may result in the loss of sequence information due to the formation of dominant non-sequence product ions, potentially limiting the utility of current database search algorithms employed for protein identification and characterization. Thus, in cases where solution-phase digestion approaches are not appropriate, the deliberate reduction of in-gel peptide digests prior to MS/MS analysis, using 1 M DMS/10 M HCl for 45 minutes at room temperature, is recommended. Alternatively, if observation of these neutral loss products is desired for use in "targeted" proteome analysis strategies, optimized conditions for the selective oxidation of methionine and S-alkyl cysteine containing peptides may be achieved by reaction with 30% H_2O_2/5% CH_3COOH at room temperature for 30 minutes.

CHAPTER FIVE

Mechanisms for the Proton Mobility Dependent Gas-Phase Fragmentation Reactions of S-alkyl Cysteine Sulfoxide-Containing Peptide Ions*

5.1 Introduction

Conventional approaches for mass spectrometry based protein identification and characterization typically involve the reduction and alkylation of cysteine residues prior to enzymatic digestion.[3, 242-244] Numerous reports in the literature have demonstrated that the resulting thio-ether bonds are susceptible to oxidation, either during the enzymatic digestion process or subsequent sample handling steps, prior to mass spectrometry analysis.[122, 133-135] These reports have also demonstrated that fragmentation of the resultant S-alkyl cysteine sulfoxide-containing peptides under low-energy CID-MS/MS conditions can result in the formation of abundant product ions via cleavages occurring within the modified cysteine side chains.[122, 133-135] While these non-sequence ions are indicative of the presence of the modified amino acid residue within the peptide, their formation at high abundance may "suppress" the formation of desired sequence ion information, thereby limiting the utility of de-novo analysis strategies[7] or current database search algorithms[9, 10] employed for the identification and characterization of these modified peptide ions. Thus, it is important to determine the conditions, such as

---

* The results described in this Chapter have been published in: Froelich, J.M.; Reid, G.E. Mechanisms for the Proton Mobility-Dependent Gas-Phase Fragmentation Reactions of S-alkyl Cysteine Sulfoxide-Containing Peptide Ions. *J. Am. Soc. Mass Spectrom.* **2007**, *18*, 1690-1705.

charge state and peptide composition (i.e., proton mobility), under which these non-sequence fragmentation pathways are observed as dominant processes. Furthermore, given that MS^3 dissociation of abundant non-sequence product ions may often be employed to obtain additional sequence information to facilitate further structural characterization[137, 140] it is also important to determine the mechanisms responsible for their formation, and the structures of the resultant product ions.

Anecdotal evidence from the literature suggests that the loss of XSOH from S-alkyl cysteine sulfoxide-containing peptides (Scheme 5.1, pathway A) occurs as a dominant fragmentation process primarily from singly protonated peptide ions.[122, 133] Consistent with these observations, the mechanism responsible for the loss of XSOH from S-alkyl cysteine sulfoxide-containing peptides formed by reaction with iodoacetamide, where X= CH_2CONH_2, has been proposed to occur via a charge-remote *cis*-1,2 elimination reaction involving transfer of the α-hydrogen atom to yield an acyclic dehydroalanine containing product ion **(1)** (Scheme 5.1, pathway A).[133, 134] A similar *cis*-1,2 elimination mechanism, yielding a cysteine sulfenic acid containing product ion **(2)** (Scheme 5.1, pathway B), has also been proposed for the loss of CH_2CHX' from S-alkyl cysteine sulfoxide-containing peptides formed by reaction with acrylamide (X'= $CONH_2$)[122] or vinylpyridine (X'= C_5H_4N),[135] as well as for the loss of $C_6H_7NO_2$ from S-alkyl cysteine sulfoxide-containing peptides formed by reaction with N-ethylmaleimide.[135] These mechanistic proposals are also consistent with those previously determined for the fragmentation of methionine sulfoxide-containing peptide ions, where the dominant side chain loss of CH_3SOH occurs via a charge-remote *cis*-1,2 elimination

reaction under conditions of low proton mobility.[76, 81] Note however, that alternative charge-directed mechanisms for the loss of XSOH from S-alkyl cysteine sulfoxide-containing peptides should also be considered, involving the formation of a protonated dehydroalanine product ion **(3)** (Scheme 5.1, pathway C) via an E2 elimination reaction (this ion would have the same primary structure, but different site of protonation to the dehydroalanine product ion formed via pathway A), or the formation of a five-membered protonated oxazoline product ion **(4)** via an S_N2 neighboring group participation reaction (Scheme 5.1, pathway D).

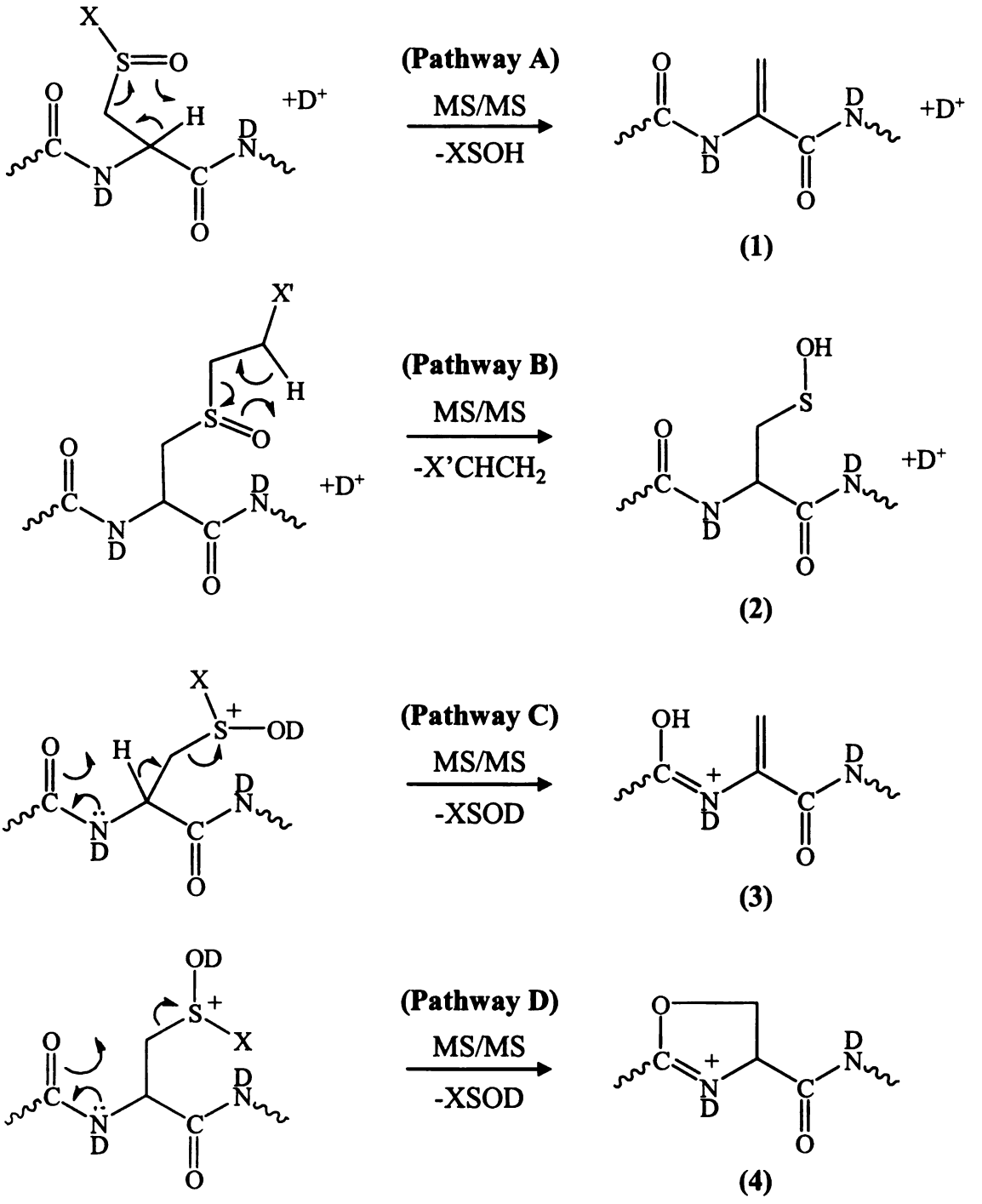

Scheme 5.1 Potential mechanisms for the loss of XSOH or CH_2CHX' from the side chains of S-alkyl cysteine sulfoxide-containing peptide ions.

To date, however, detailed experimental studies to determine the mechanisms and the proton mobility dependence to these fragmentation reactions, as well as to determine the mechanisms responsible for the subsequent fragmentation reactions of the initial product ions, have not been carried out. Here, the proton mobility dependence and mechanisms responsible for the loss of XSOH and CH_2CHX' from singly and multiply protonated S-alkyl cysteine sulfoxide-containing peptide ions prepared by reaction with the commonly employed alkylating reagents iodomethane, iodoacetamide, iodoacetic acid, acrylamide and 4-vinylpyridine have been examined using a combination of multistage tandem mass spectrometry (MS/MS, MS^3 and MS^4), hydrogen/deuterium exchange reactions and molecular orbital calculations (at the B3LYP/6-31+G(d,p) level of theory).

5.2 Multistage Tandem Mass Spectrometry and H/D Exchange Reactions for the Fragmentation of S-Methyl and S-Carboxyamidomethyl Cysteine Sulfoxide-Containing Peptide Ions

The product ion spectra obtained by CID-MS/MS of the singly and doubly protonated precursor ions of the cysteine sulfoxide-containing peptide GAILCGAILK (C(S-me)(ox)K), (where me=CH_3), prepared by reaction with iodomethane followed by oxidation with hydrogen peroxide, are shown in Figures 5.1A and 5.1B, respectively. In both cases, product ions corresponding to the neutral loss of CH_3SOH (64 Da) from the S-alkyl cysteine sulfoxide side chain were observed as the most abundant fragmentation processes. Differentiation of the charge-remote versus charge-directed mechanisms proposed in Scheme 5.1 for the loss of CH_3SOH from these ions was readily achieved by

CID-MS/MS of their uniformly deuterated precursor ions. Fragmentation via the charge-remote *cis*-1,2 elimination reaction (Scheme 5.1, pathway A) would result in the loss of CH_3SOH, while fragmentation via either of the charge-directed pathways (Scheme 5.1, pathways C and D) would result in the loss of CH_3SOD. The insets to Figures 5.1A and 5.1B show expanded regions of the product ion spectra obtained by CID-MS/MS of the uniformly deuterated $[M+D]^+$ and $[M+2D]^{2+}$ precursor ions of C(S-me)(ox)K. The loss of CH_3SOH (64 Da) was observed for both precursor ions, confirming that fragmentation had occurred via the charge-remote *cis*-1,2 elimination mechanism.

***Figure* 5.1** Multistage tandem mass spectrometry of the S-methyl cysteine sulfoxide-containing peptide GAILCGAILK (C(S-me)(ox)K). (A) CID-MS/MS product ion spectrum of the $[M+H]^+$ ion. (B) CID-MS/MS product ion spectrum of the $[M+2H]^{2+}$ ion. (C) CID MS^3 product ion spectrum of the $[M+H-CH_3SOH]^+$ neutral loss product ion from panel A. (D) CID MS^3 product ion spectrum of the $[M+2H-CH_3SOH]^{2+}$ neutral loss product ion from panel B. The insets to panels A and B, showing expanded regions of the product ion spectra obtained by CID-MS/MS of the uniformly deuterated $[M+D]^+$ and $[M+2D]^{2+}$ precursor ions, confirm that the loss of CH_3SOH occurs via the charge-remote *cis*-1,2 elimination pathway. Key: Δ = $-CH_3SOH$; ○ = $-H_2O$; * = $-NH_3$.

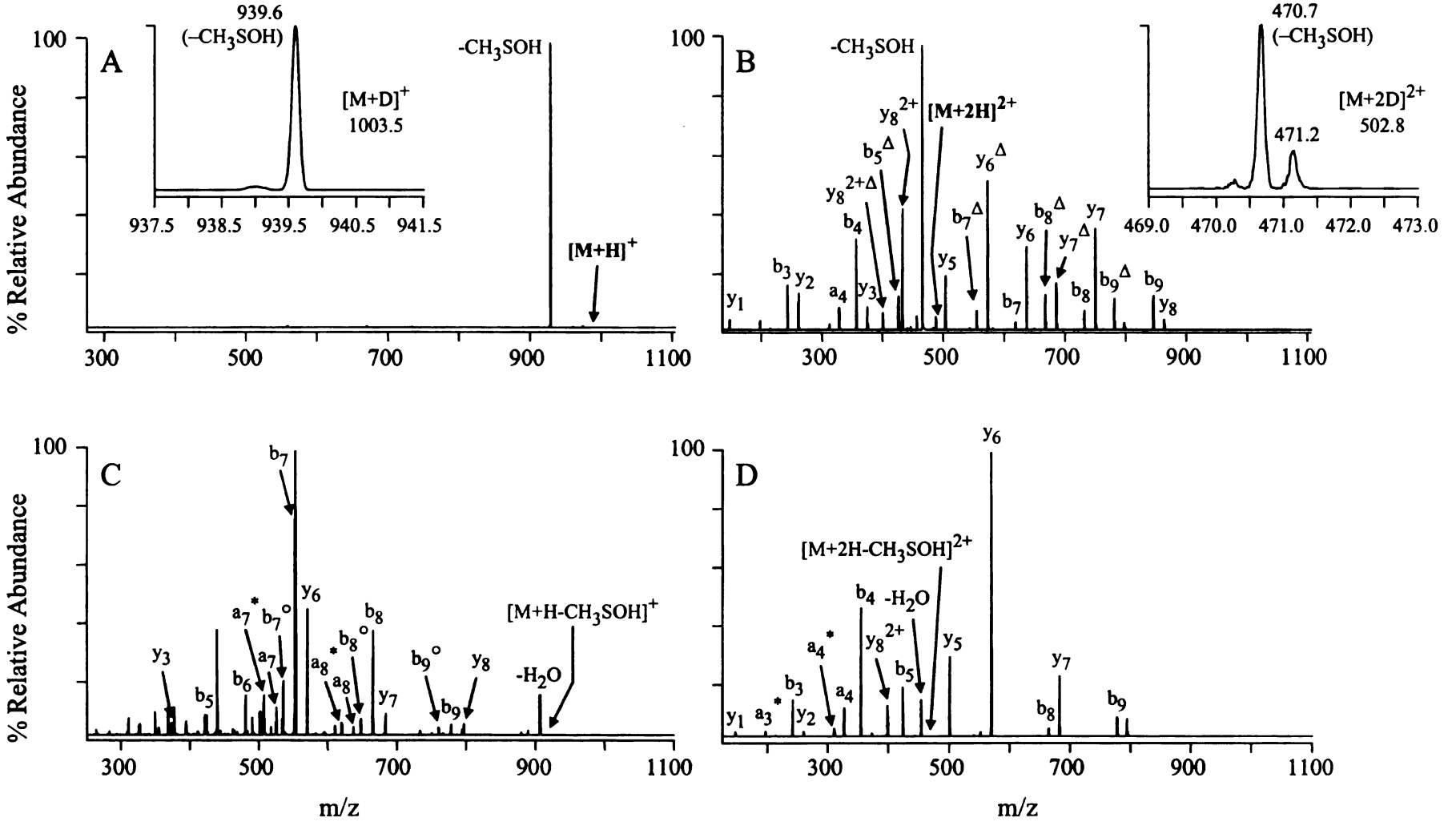
A
939.6
(–CH3SOH)
[M+D]+
1003.5
937.5 938.5 939.5 940.5 941.5
-CH3SOH
[M+H]+
100
% Relative Abundance
300 500 700 900 1100
B
-CH3SOH
[M+2H]2+
y8 2+
b5 Δ
y6 Δ
y8 2+Δ
b4
b7 Δ
b8 Δ
y7
y7 Δ
y6
b9 Δ
b9
y8
b3 y2
a4
y3
y5
b7
b8
y1
470.7
(–CH3SOH)
[M+2D]2+
502.8
471.2
469.0 470.0 471.0 472.0 473.0
C
b7
y6
a7 * b7 °
b8
b8 °
a7
a8 *
a8
y3
b6
b5
y7
b9 °
y8
b9
[M+H-CH3SOH]+
-H2O
m/z
D
y6
[M+2H-CH3SOH]2+
b4 -H2O
a4 *
y8 2+
y5
b3
b5
y7
a4
y1
a3 *
y2
b8
b9
m/z

Given that the neutral loss of CH_3SOH was observed as the exclusive fragmentation process following MS/MS of the singly protonated precursor ion (Figure 5.1A), and as the most abundant fragmentation process following MS/MS of the doubly protonated precursor ion (Figure 5.1B), MS^3 dissociation of the $[M+H-CH_3SOH]^+$ and $[M+2H-CH_3SOH]^{2+}$ product ions from these spectra was employed to obtain additional sequence ions for further structural characterization and to further confirm the mechanism responsible for the neutral losses (Figures 5.1C and 5.1D, respectively). The b_5 and y_6 ions observed in the MS^3 product ion spectrum of the $[M+H-CH_3SOH]^+$ ion, and the b_4, b_5, y_5 and y_6 product ions observed in the MS^3 product ion spectrum of the $[M+2H-CH_3SOH]^{2+}$ ion, all corresponding to fragmentation on either side of the dehydroalanine containing product, provided further evidence for the *cis*-1,2 elimination mechanism. Notably, it can also be seen by comparison of Figures 5.1D and 5.1B, that MS^3 of the $[M+2H-CH_3SOH]^{2+}$ ion resulted in a product ion spectrum with equivalent sequence information, but reduced spectral complexity compared to that obtained by MS/MS of the $[M+2H]^{2+}$ ion, where abundant product ions corresponding to sequential fragmentations of both non-sequence side chain and sequence peptide backbone cleavage sites were observed.

The proton mobility dependence to the abundances of the non-sequence side chain cleavage product ions from the singly and doubly protonated C(S-me)(ox)K precursor ions, as well as from the singly and doubly protonated precursor ions of the S-methyl cysteine sulfoxide-containing peptide GAILCGAILR (C(S-me)(ox)R) and the singly, doubly and triply protonated precursor ions of the methionine sulfoxide- and S-

methyl cysteine sulfoxide-containing peptide VTMGHFCNFGK (M(ox)C(S-me)(ox)K), was quantitatively evaluated by cleavage intensity ratio (CIR) calculations performed on each of the non-sequence product ions[76, 81] (Table 5.1). These data clearly indicate that loss of the side chain is a more dominant process under "non-mobile" and "partially mobile" proton conditions, i.e., where the number of ionizing protons is $\leq$ the combined number of basic residues (Arg, Lys or His), compared to that observed under "mobile" proton conditions, where the number of ionizing protons is > the combined number of basic residues (Arg, Lys or His).[76]

For the methionine sulfoxide- and S-methyl cysteine sulfoxide-containing peptide M(ox)C(S-me)(ox)K, the neutral loss of CH_3SOH could result from side chain cleavage of the S-methyl cysteine sulfoxide or methionine sulfoxide residues, or both. However, given the minimal loss of CH_3SOH observed during MS/MS of the methionine sulfoxide- and S-carboxyamidomethyl cysteine sulfoxide-containing peptide M(ox)C(S-cam)(ox)K (where cam= CH_2CONH_2), and the similar fragmentation behaviors of the S-methyl and S-carboxyamidomethyl cysteine sulfoxide-containing peptides C(S-me)(ox)K and C(S-cam)(ox)K (see below), it is expected that loss from the S-methyl cysteine sulfoxide residue was the dominant process.

Essentially identical spectra to those discussed above for dissociation of the S-methyl cysteine sulfoxide-containing peptide ions were also obtained following CID-MS/MS of the singly, doubly or triply protonated precursor ions of the S-carboxyamidomethyl cysteine sulfoxide-containing peptides C(S-cam)(ox)K, C(S-cam)(ox)R and M(ox)C(S-cam)(ox)K formed by reaction with iodoacetamide and oxidation with hydrogen peroxide (Table 5.1). Hydrogen/deuterium exchange followed

by MS/MS, as well as MS^3 of the resultant $[M+nH-H_2NCOCH_2SOH]^{nH+}$ product ions, confirmed that the side chain neutral loss of H_2NCOCH_2SOH (107 Da) from these peptides also occurred exclusively via the charge-remote *cis*-1,2 elimination reaction mechanism shown in pathway A of Scheme 5.1. As expected, the spectra obtained by MS^3 dissociation of the $[M+nH-H_2NCOCH_2SOH]^{nH+}$ product ions were identical to those from the S-methyl cysteine sulfoxide-containing peptides (data not shown).

Notably, the CIR values calculated for the losses of CH_3SOH or H_2NCOCH_2SOH from the doubly protonated (i.e., mobile proton) S-methyl and S-carboxyamidomethyl cysteine sulfoxide-containing derivatives of GAILCGAILK (CIR values of 3.9 and 2.5, respectively) and GAILCGAILR (CIR values of 4.0 and 3.1, respectively), were significantly higher than the CIR values calculated for the loss of CH_3SOH from the doubly protonated precursor ions of the equivalent methionine sulfoxide-containing peptides GAILM(ox)GAILK (CIR 0.1) and GAILM(ox)GAILR (CIR 0.2) (Table 5.1). Furthermore, while the mechanism for the side chain fragmentation from the doubly protonated methionine sulfoxide derivative was previously demonstrated to occur via a charge-directed mechanism,[81] the side chain losses from the S-alkyl cysteine sulfoxide-containing peptides were observed to occur via the charge-remote mechanism. These observations can be rationalized as being due to the increased acidity of the α-hydrogen atom of the S-alkyl cysteine sulfoxide side chain compared to the β-hydrogen atoms of the methionine sulfoxide side chain.

Table 5.1 Cleavage intensity ratio (CIR) values for the "non-sequence" side chain fragmentation reactions of S-alkyl cysteine sulfoxide- and methionine sulfoxide-containing peptide ions.

a) "Non-mobile" proton [76, 81].

b) "Partially mobile" proton [76, 81].

c) "Mobile" proton [76, 81].

d) Contributions from sequential losses are included in the CIR calculation.

e) Corresponds to side chain cleavage from Cys(X)(ox) and/or Met(ox).

f) Observed exclusively as a charged loss.

g) Observed as both charged and neutral losses.

Peptide	X=	Precursor ion charge state	Calculated CIR value			
			-XSOH[d]	-(X-H)[d]	$-CO_2$[d]	$-CH_3SOH$ from Met(ox)
GAILC(X)(ox)GAILK (C(X)(ox)K)	CH_3	+1[b]	11.0	0	–	–
		+2[c]	3.9	0	–	–
	CH_2CONH_2	+1[b]	10.8	0	–	–
		+2[c]	2.5	0	–	–
	CH_2CO_2H	+1[b]	6.5	0	5.4	–
		+2[c]	2.4	0	0	–
	$CH_2CH_2CONH_2$	+1[b]	5.4	6.6	–	–
		+2[c]	3.9	2.6	–	–
	$CH_2CH_2C_5H_4N$	+1[b]	10.0	2.0	–	–
		+2[c]	0	12.0[f]	–	–
		+3[c]	0	10.9[f]	–	–
GAILC(X)(ox)GAILR (C(X)(ox)R)	CH_3	+1[a]	11.0	0	–	–
		+2[c]	4.0	0	–	–
	CH_2CONH_2	+1[a]	10.9	0	–	–
		+2[c]	3.1	0	–	–
	CH_2CO_2H	+1[a]	5.3	0	6.6	–
		+2[c]	3.5	0	0	–
	$CH_2CH_2CONH_2$	+1[a]	4.9	6.9	–	–
		+2[c]	4.0	2.2	–	–
	$CH_2CH_2C_5H_4N$	+1[a]	10.8	1.2	–	–
		+2[c]	0	12.0[f]	–	–
		+3[c]	0	11.7[f]	–	–

Table 5.1 (continued)

Peptide	X=	Precursor ion charge state	Calculated CIR value			
			-XSOH[d]	-(X-H)[d]	$-CO_2$[d]	$-CH_3SOH$ from Met(ox)
VTM(ox)GHFC(X)(ox)NFGK (M(ox)C(X)(ox)K)	CH_3	+1[b]	12.9[e]	0	–	–
		+2[b]	12.6[e]	0	–	–
		+3[c]	5.7[e]	0	–	–
	CH_2CONH_2	+1[b]	12.2	0	–	0.2
		+2[b]	12.2	0	–	0.1
		+3[c]	5.1	0	–	0.1
	CH_2CO_2H	+1[b]	7.0	0	6.9	0
		+2[b]	9.0	0	4.7	0
		+3[c]	4.0	0	6.3	0
	$CH_2CH_2CONH_2$	+1[b]	7.3	6.5	–	0.1
		+2[b]	9.3	4.6	–	0
		+3[c]	3.7	8.0	–	0
	$CH_2CH_2C_5H_4N$	+1[b]	11.2	2.5	–	0.1
		+2[b]	1.5	12.5[g]	–	0
		+3[c]	0	14.0[f]	–	0
GAILM(ox)GAILK (M(ox)K)		+1[b]	–	–	–	9.3
		+2[c]	–	–	–	0.1
GAILM(ox)GAILR (M(ox)R)		+1[a]	–	–	–	10.9
		+2[c]	–	–	–	0.2

Further examples of the proton mobility dependence to the preferential side chain fragmentation behavior of S-carboxyamidomethyl cysteine sulfoxide residues are shown in Figure 5.2 and in Table 5.2. Figures 5.2A and 5.2B show selected mass spectra obtained by capillary HPLC-mass spectrometry analysis of an S-carboxyamidomethylated and oxidized tryptic digest of bovine serum albumin, prepared by reduction and alkylation with iodoacetamide, followed by oxidation with hydrogen peroxide. The CID-MS/MS product ion spectra obtained by dissociation of the doubly (m/z 797.5) and triply (m/z 532.3) protonated precursor ions in Figure 5.2A are shown in Figures 5.2C and 5.2D, respectively. SEQUEST analysis of these spectra, followed by manual verification of the search results, enabled the peptide to be identified as the singly oxidized LKPDPNTLC(S-cam(ox))DEFK. It can be seen that the non-sequence loss of H_2NCOCH_2SOH dominated the product ion spectrum (82.4% total product ion abundance) for the doubly protonated precursor ion (i.e., partially mobile proton conditions). In contrast, the same loss (including the sequential loss of H_2O) was only observed at 20.5% total product ion abundance from dissociation of the triply protonated precursor ion (i.e., mobile proton conditions), with numerous abundant sequence product ions also being observed. The remaining doubly, triply and quadruply protonated ions in Figure 5.2A were found to correspond to the singly oxidized peptide LKPDPNTLC(S-cam(ox))DEFKADEK (Table 5.2).

Interestingly, dissociation of the doubly protonated precursor ion at m/z 989.1 in Figure 5.2B resulted in the sequential loss of up to three H_2NCOCH_2SOH neutral molecules, with a combined total product ion abundance of 89.4% (see Figure 5.2E). This peptide was subsequently identified by SEQUEST analysis and manual verification of the

search results as the triply oxidized peptide C(S-cam(ox))C(S-cam(ox))AADDKEAC(S-cam(ox))FAVEGPK. Similar to that seen in Figures 5.2C and 5.2D however, dissociation of this peptide (Figure 5.2F) under mobile proton conditions (i.e., the triply protonated precursor ion at m/z 660.2 in Figure 5.2B) resulted in substantially less abundant non-sequence ions (combined total product ion abundance of 15.1%) and the formation of extensive sequence information.

These data, as well as those obtained from the oxidized peptides in Table 5.2, indicate that the formation of abundant product ions corresponding to the loss of H_2NCOCH_2SOH under conditions of low proton mobility allows both the presence and number of S-carboxyamidomethyl cysteine sulfoxide residues within a given peptide to be readily determined. This information can be particularly useful to assist in identification of the peptide when sequence ions are present at low abundance. For example, automated SEQUEST analysis of the spectra obtained by CID-MS/MS of the triply protonated precursor ion of the peptide LKEC(S-cam(ox))C(S-cam(ox))DKPLLEK (Table 5.2) resulted in this peptide being included as only the second ranked candidate. However, manual interrogation of the spectrum enabled the observation of product ions corresponding to the loss of up to two H_2NCOCH_2SOH neutral molecules with a combined total product ion abundance of 92.8%, indicating that the peptide contained two S-carboxyamidomethyl cysteine sulfoxide residues. Given that the higher ranked candidate sequence corresponded to a peptide with only one oxidized cysteine residue, it could be immediately discounted, thereby bringing the correct sequence to the top of the candidate list. This is an approach that is directly analogous to those recently described

for identification of phosphoserine or phosphothreonine containing peptide ion product ion spectra that give rise to the dominant loss of H_3PO_4 upon CID-MS/MS.[219, 220]

Figure 5.2 Capillary HPLC-mass spectrometry analysis of S-carboxyamidomethyl cysteine sulfoxide- (S-cam(ox)) containing peptides from an oxidized tryptic digest of bovine serum albumin. Mass spectra obtained from region 1 (28.2-29.2 minutes) and region 2 (22.5-23.5 minutes) of the LC-MS chromatogram (shown in the inset to panel A) are shown in panels A and B, respectively. The CID-MS/MS product ion spectra obtained from dissociation of the doubly (m/z 797.5) and triply (m/z 532.3) protonated precursor ions of the singly oxidized peptide LKPDPNTLC(S-cam(ox))DEFK in panel A are shown in panels C and D, respectively. The CID-MS/MS product ion spectra obtained from dissociation of the doubly (m/z 989.1) and triply (m/z 660.2) protonated precursor ions of the triply oxidized peptide C(S-cam(ox))C(S-cam(ox))AADDKEAC(S-cam(ox))FAVEGPK in panel B are shown in panels E and F, respectively.
Key: Δ = $-H_2NCOCH_2SOH$; $\circ$ = $-H_2O$; * = $-NH_3$.

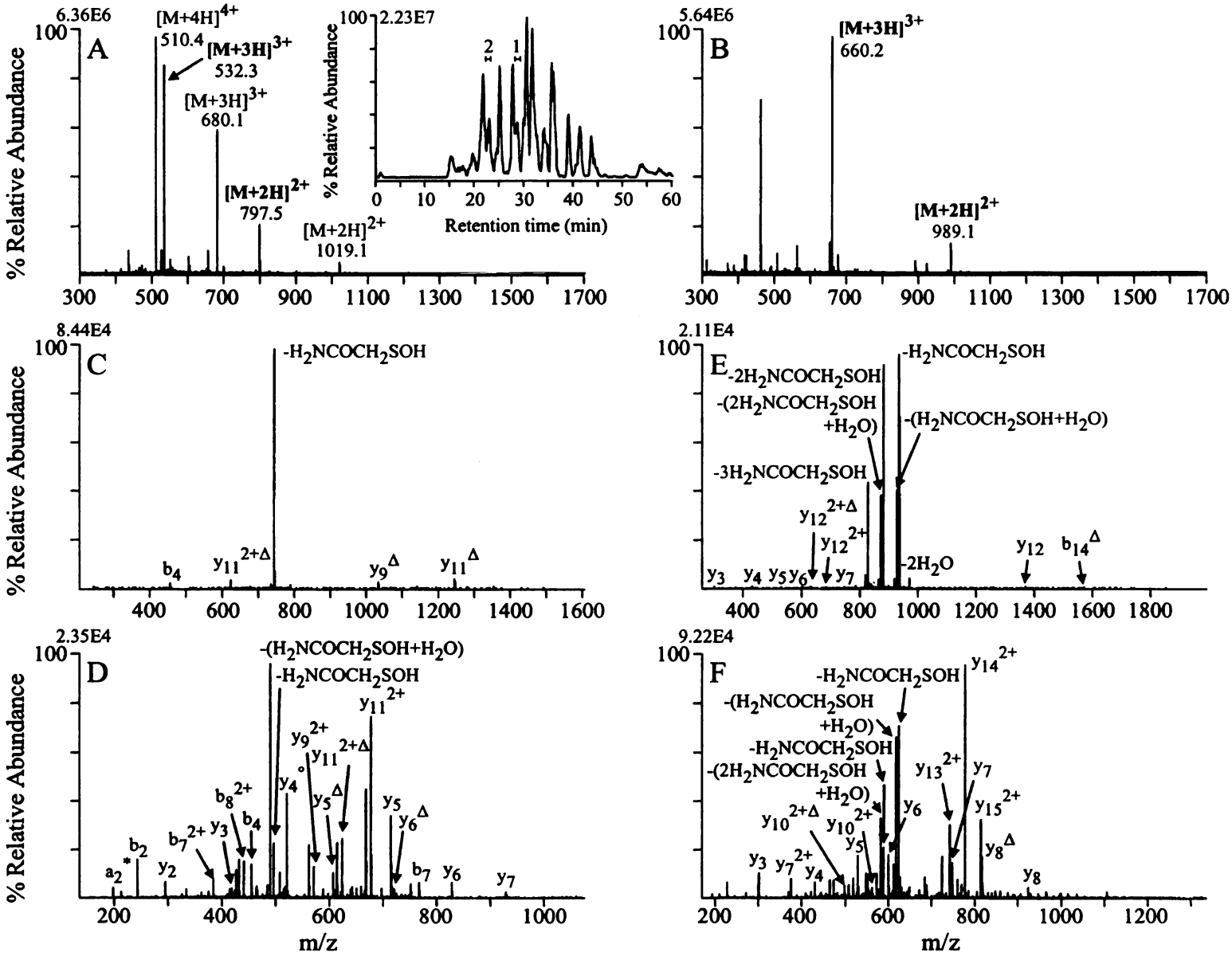
A
6.36E6
[M+4H]4+
510.4
[M+3H]3+
532.3
[M+3H]3+
680.1
[M+2H]2+
797.5
[M+2H]2+
1019.1
% Relative Abundance
2.23E7
Retention time (min)
B
5.64E6
[M+3H]3+
660.2
[M+2H]2+
989.1
C
8.44E4
-H2NCOCH2SOH
D
2.35E4
-(H2NCOCH2SOH+H2O)
-H2NCOCH2SOH
E
2.11E4
-2H2NCOCH2SOH
-(2H2NCOCH2SOH +H2O)
-(H2NCOCH2SOH+H2O)
-3H2NCOCH2SOH
-2H2O
F
9.22E4
m/z

Table 5.2 Percent total product ion abundances for the "non-sequence" side chain neutral loss of H_2NCOCH_2SOH from S-carboxyamidomethyl (S-cam) cysteine sulfoxide-containing peptide ions of an oxidized tryptic digest of bovine serum albumin.

	% Total product ion abundance [a]				
	Precursor ion charge state				
Peptide sequence	+1	+2	+3	+4	+5
GAC(S-cam(ox))LLPK	57.9 [d]	14.5 [e]	–	–	–
SLHTLFGDELC(S-cam(ox))K	73.7 [d]	49.9 [d]	22.4 [e]	–	–
YIC(S-cam(ox))DNQDTISSK	–	44.9 [e]	–	–	–
C(S-cam(ox))C(S-cam)TESLVNR [b]	–	48.3 [e]	–	–	–
EYEATLEEC(S-cam(ox))C(S-cam(ox))AK	–	29.3 [e]	–	–	–
DDPHAC(S-cam(ox))YSTVFDK	–	51.9 [d]	25.9 [e]	–	–
RPC(S-cam(ox))FSALTPDETYVPK	–	81.3 [d]	21.8 [e]	–	–
LFTFHADIC(S-cam(ox))TLPDTEK	–	55.8 [d]	30.9 [e]	–	–
M(ox)PC(S-cam(ox))TEDYLSLILNR	–	30.5 [e]	0.5 [e]	–	–
LAKEYEATLEEC(S-cam(ox))C(S-cam(ox))AK	–	84.1 [d]	44.9 [e]	–	–
C(S-cam(ox))C(S-cam)AADDKEAC(S-cam(ox))FAVEGPK [c]	–	86.2 [d]	21.7 [e]	–	–
C(S-cam(ox))C(S-cam(ox))AADDKEAC(S-cam(ox))FAVEGPK	–	89.4 [d]	15.1 [e]	–	–
VASLRETYGDM(ox)ADC(S-cam(ox))C(S-cam(ox))EK	–	–	53.2 [e]	–	–
YNGVFQEC(S-cam(ox))C(S-cam(ox))QAEDK	–	69.1 [d]	20.9 [e]	–	–
YNGVFQEC(S-cam(ox))C(S-cam(ox))QAEDKGAC(S-cam(ox))LLPK	–	–	75.1 [e]	–	–
LKEC(S-cam(ox))C(S-cam(ox))DKPLLEK	–	–	92.8 [d]	74.0 [d]	–
VHKEC(S-cam(ox))C(S-cam(ox))HGDLLEC(S-cam(ox))ADDR	–	–	87.8 [d]	36.1 [d]	–
LKPDPNTLC(S-cam(ox))DEFK	–	82.4 [d]	20.5 [e]	–	–
LKPDPNTLC(S-cam(ox))DEFKADEK	–	76.0 [d]	61.7 [d]	9.7 [e]	–
NEC(S-cam(ox))FLSHKDDSPDLPK	–	76.0 [d]	59.6 [d]	23.9 [e]	–
QEPERNEC(S-cam(ox))FLSHKDDSPDLPK	–	–	80.3 [d]	60.3 [d]	34.0 [e]

[a] Contributions from sequential losses are included in the calculation.

[b] Site of oxidation could be at either of the cysteine residues.

[c] Site of oxidation could be at either of the two N-terminal cysteine residues.

[d] "Partially mobile" proton [76, 81].

[e] "Mobile" proton [76, 81].

5.3 Multistage Tandem Mass Spectrometry and H/D Exchange Reactions for the Fragmentation of S-Carboxymethyl Cysteine Sulfoxide-Containing Peptide Ions

Similar to that previously reported by Steen *et al.*,[133] CID-MS/MS of the singly and multiply protonated precursor ions of the S-carboxymethyl cysteine sulfoxide-containing peptides GAILCGAILK (C(S-cm)(ox)K) (where cm=CH_2CO_2H), GAILCGAILR (C(S-cm)(ox)R) and VTMGHFCNFGK (M(ox)C(S-cm)(ox)K), formed by reaction with iodoacetic acid and hydrogen peroxide, resulted in the side chain neutral loss of carboxymethyl sulfenic acid (HO_2CCH_2SOH, 108 Da). Figures 5.3A and 5.3B show the product ion spectra obtained following CID-MS/MS of the singly and doubly protonated precursor ions of C(S-cm)(ox)K. The CIR values calculated for these ions, as well as those for the C(S-cm)(ox)R and M(ox)C(S-cm)(ox)K peptides are given in Table 5.1. Hydrogen/deuterium exchange experiments performed on the singly and doubly protonated precursor ions of the C(S-cm)(ox)K peptide confirmed that the side chain neutral loss of HO_2CCH_2SOH occurred via the charge-remote *cis*-1,2 elimination reaction mechanism shown in pathway A of Scheme 5.2. Furthermore, MS^3 dissociation of the $[M+nH-HO_2CCH_2SOH]^{nH+}$ product ions were identical to those from the S-methyl cysteine sulfoxide containing-peptides (data not shown).

Figure 5.3 Multistage tandem mass spectrometry of the S-carboxymethyl cysteine sulfoxide-containing peptide GAILCGAILK (C(S-cm)(ox)K). (A) CID-MS/MS product ion spectrum of the $[M+H]^+$ ion. (B) CID-MS/MS product ion spectrum of the $[M+2H]^{2+}$ ion. (C) CID MS^3 product ion spectrum of the $[M+H-CO_2]^+$ neutral loss product ion from panel A. (D) CID MS^4 product ion spectrum of the $[M+H-CH_2O]^+$ neutral loss product ion from panel C. Key: Δ = $-HO_2CCH_2SOH$; $\square$ = $-CO_2$; ‡ = $-(CO_2+CH_2O)$; $\diamond$ = $-CH_2O$; $\circ$ = $-H_2O$; * = $-NH_3$.

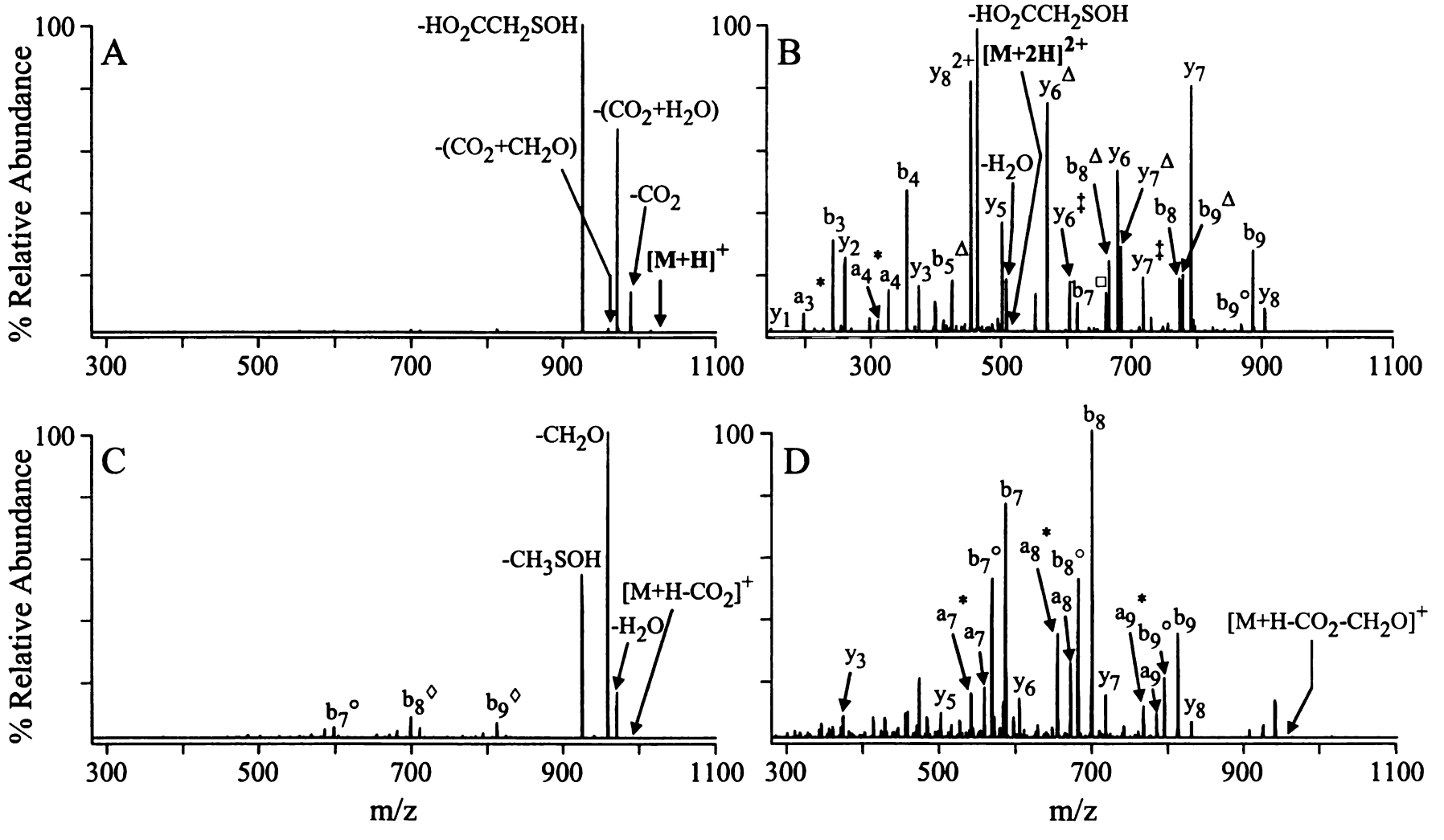
A
B
C
D
% Relative Abundance
m/z
100
300
500
700
900
1100
-HO2CCH2SOH
-(CO2+H2O)
-(CO2+CH2O)
-CO2
[M+H]+
[M+2H]2+
-H2O
-CH2O
-CH3SOH
[M+H-CO2]+
[M+H-CO2-CH2O]+

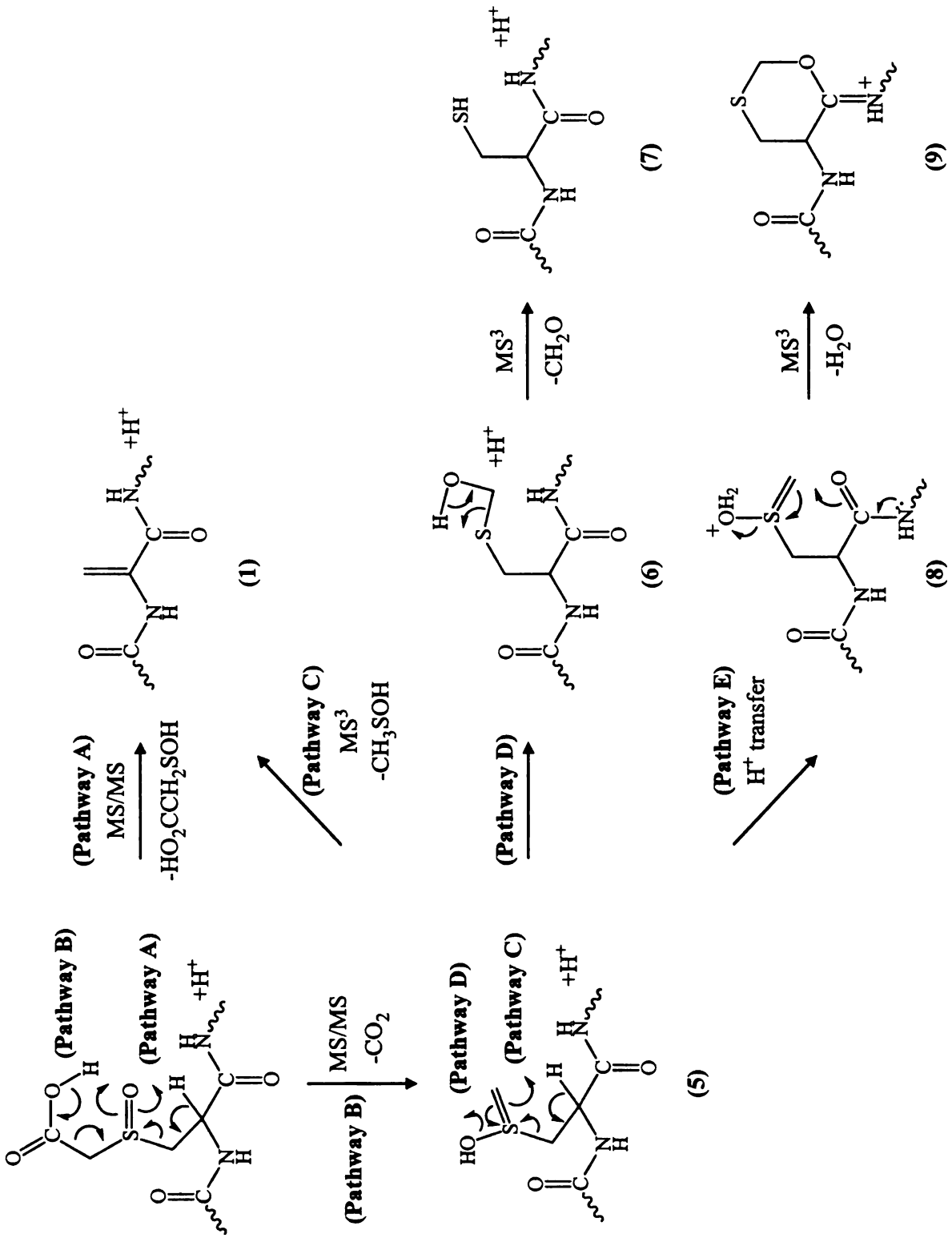

Scheme 5.2 Proposed mechanisms for the side chain fragmentation reactions of S-carboxymethyl (S-cm) cysteine sulfoxide-containing peptide ions.

In addition to the loss of HO_2CCH_2SOH, losses of CO_2 (44 Da), CO_2+H_2O (62 Da) and CO_2+CH_2O (74 Da) were also observed following CID-MS/MS of the singly protonated precursor ion of C(S-cm)(ox)K (Figure 5.3A). A dissociation pathway that would account for the neutral loss of CO_2 is shown in pathway B of Scheme 5.2, resulting in the formation of the enol form of S-methyl cysteine sulfoxide **(5)**. MS^3 dissociation of the $[M+H-CO_2]^+$ neutral loss product ion from Figure 5.3A resulted in the dominant side chain neutral losses of CH_3SOH, CH_2O and H_2O (Figure 5.3C). The neutral loss of CH_3SOH likely occurs via a charge-remote *cis*-1,2 elimination reaction (pathway C of Scheme 5.2) to yield the acyclic dehydroalanine product ion **(1)**. MS^4 of the $[M+H-CO_2-CH_3SOH]^+$ ion resulted in an identical product ion spectrum to that shown in Figure 5.1C, thereby providing evidence for the proposed mechanism (data not shown). Rearrangement of the $[M+H-CO_2]^+$ product ion via a hydroxymethylthio-containing intermediate **(6)** (pathway D of Scheme 5.2) would readily enable the neutral loss of CH_2O to yield the cysteine containing product ion **(7)**. Experimental evidence for this mechanism was obtained by comparison of the MS^4 product ion spectrum obtained by dissociation of the $[M+H-CO_2-CH_2O]^+$ product ion (Figure 5.3D) against the CID-MS/MS product ion spectrum of the singly protonated precursor ion of the peptide GAILCGAILK (CK) (data not shown). The spectra were essentially identical with regard to the observed b- and y- type product ion abundances, clearly indicating that the cysteine side chain had been formed. The neutral loss of H_2O from the $[M+H-CO_2]^+$ product ion likely occurs via intramolecular proton transfer from the peptide to the hydroxyl group of

(5) to yield **(8)** (pathway E of Scheme 5.2), followed by nucleophilic attack from either the carbonyl group of the C-terminal amide bond to yield the cyclic six-membered 1,3-oxathiane product ion **(9)** or the carbonyl oxygen of the N-terminal amide bond to yield a cyclic seven-membered 1,3,6-oxathiazepine product ion (structure not shown). Support for the proposed H^+ transfer mechanism was provided by observation of the loss of D_2O from the uniformly deuterated $[M+D-CO_2]^+$ product ion (data not shown).

5.4 Multistage Tandem Mass Spectrometry, H/D Exchange Reactions, and Molecular Orbital Calculations for the Fragmentation of S-Amidoethyl and S-Pyridylethyl Cysteine Sulfoxide-Containing Peptide Ions

Consistent with a previous report by Swiderek *et al.*,[122] CID-MS/MS of protonated precursor ions of S-amidoethyl cysteine sulfoxide-containing peptides, formed by reaction with acrylamide and hydrogen peroxide, resulted in dominant side chain neutral losses of carboxyamidoethyl sulfenic acid ($H_2NCOCH_2CH_2SOH$, 121 Da), acrylamide ($CH_2CHCONH_2$, 71 Da) and $CH_2CHCONH_2+H_2O$ (89 Da). Figures 5.4A and 5.4B show the product ion spectra obtained from dissociation of the singly and doubly protonated precursor ions of the S-amidoethyl cysteine sulfoxide-containing peptide GAILCGAILK (C(S-ae)(ox)K) (where ae=$CH_2CH_2CONH_2$). The CIR values calculated from these spectra, as well as those calculated from dissociation of the singly and multiply protonated S-amidoethyl cysteine sulfoxide-containing peptides GAILCGAILR (C(S-ae)(ox)R) and VTMGHFCNFGK (M(ox)C(S-ae)(ox)K), that demonstrate the proton mobility dependence to these losses, are shown in Table 5.1.

Figure 5.4 Multistage tandem mass spectrometry of the S-amidoethyl cysteine sulfoxide-containing peptide GAILCGAILK (C(S-ae)(ox)K). (A) CID-MS/MS product ion spectrum of the $[M+H]^+$ ion. (B) CID-MS/MS product ion spectrum of the $[M+2H]^{2+}$ ion. (C) CID MS^3 product ion spectrum of the $[M+H-CH_2CHCONH_2]^+$ neutral loss product ion from panel A. (D) CID MS^4 product ion spectrum of the $[M+H-H_2O]^+$ neutral loss product ion from panel C. Key: Δ = $-H_2NCOCH_2CH_2SOH$; † = $-(CH_2CHCONH_2+H_2O)$; ○ = $-H_2O$; * = $-NH_3$.

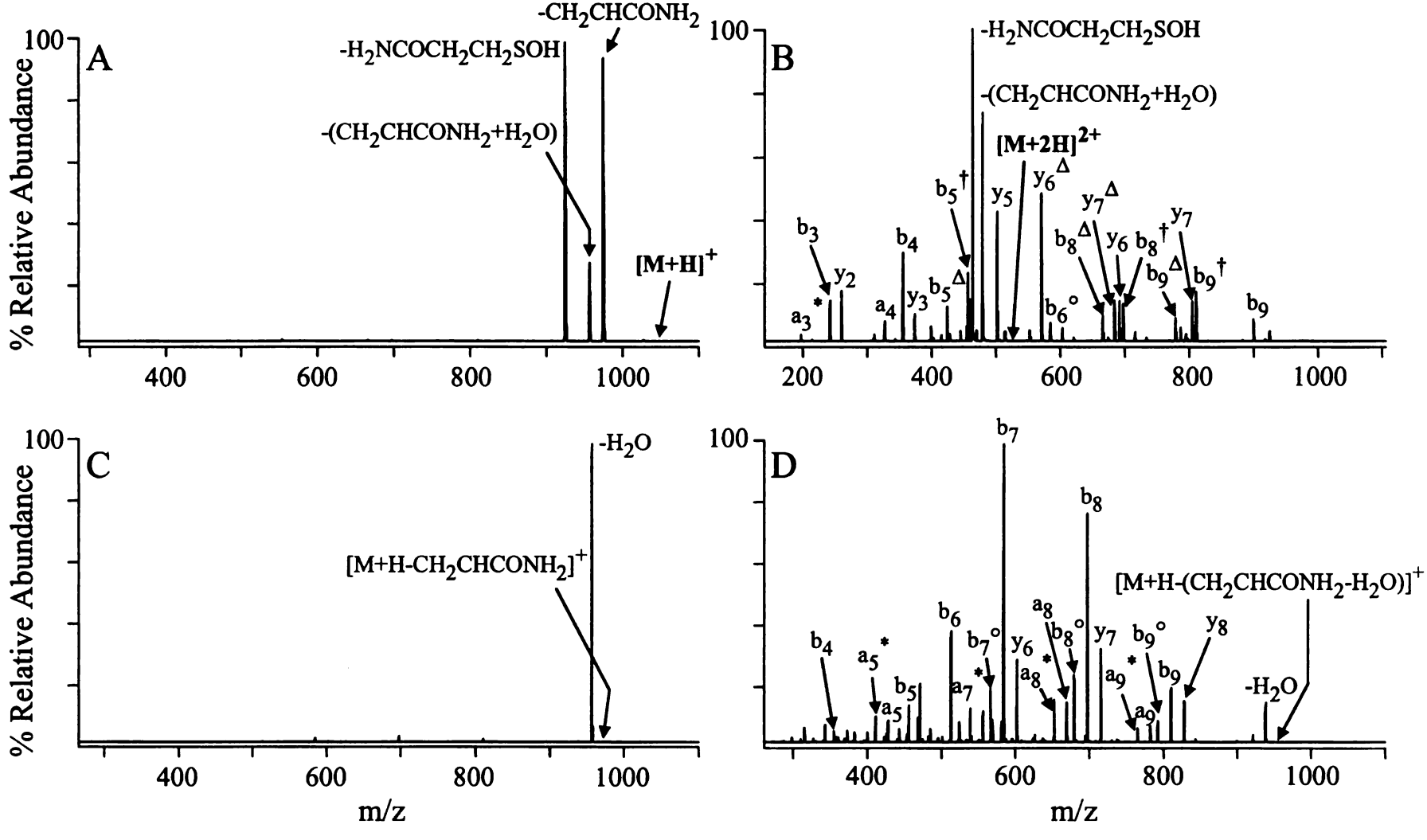
A
B
C
D
% Relative Abundance
m/z
100
400
600
800
1000
200
-CH2CHCONH2
-H2NCOCH2CH2SOH
-(CH2CHCONH2+H2O)
[M+H]+
[M+2H]2+
-H2O
[M+H-CH2CHCONH2]+
[M+H-(CH2CHCONH2-H2O)]+

CID-MS/MS of the uniformly deuterium exchanged C(S-ae)(ox)K peptide again confirmed that the loss of $H_2NCOCH_2CH_2SOH$ (XSOH) from the singly and doubly protonated precursor ions occurred via the *cis*-1,2 elimination reaction mechanism shown in pathway A of Scheme 5.1 (data not shown). H/D exchange experiments also confirmed that the neutral loss of $CH_2CHCONH_2$ (CH_2CHX', where $X'=CONH_2$) from these peptide ions occurred via a charge-remote *cis*-1,2 elimination reaction to yield the cysteine sulfenic acid containing product ion **(2)**, as shown in pathway B of Scheme 5.1. This is consistent with the mechanism recently proposed by Chowdhury *et al.* for the neutral loss of 4-vinylpyridine from S-pyridylethyl cysteine sulfoxide-containing peptides.[135]

To obtain further insights into the relative abundances of the product ions formed via the side chain losses of XSOH and CH_2CHX' from these peptides, a series of molecular orbital calculations were performed to determine the transition state barriers associated with each reaction pathway, using the simple neutral model systems $CH_3CONHCH(CH_2S(O)CH_3)CONHCH_3$ and $H_2NCOCH_2CH_2S(O)CH_3$. Potential transition state structures for each fragmentation pathway were initially examined at the PM3 semi empirical level of theory, followed by re-optimization of low energy conformers at the B3LYP/6-31+G(d,p) density functional level of theory. Vibrational frequency analysis was performed to confirm the nature of the optimized stationary point structure. Then, intrinsic reaction coordinate searches were performed, followed by geometry optimization at the same level of theory to locate the appropriate precursor and product ion structures associated with both transition states. The structures obtained from these calculations are shown in Figure 5.5.

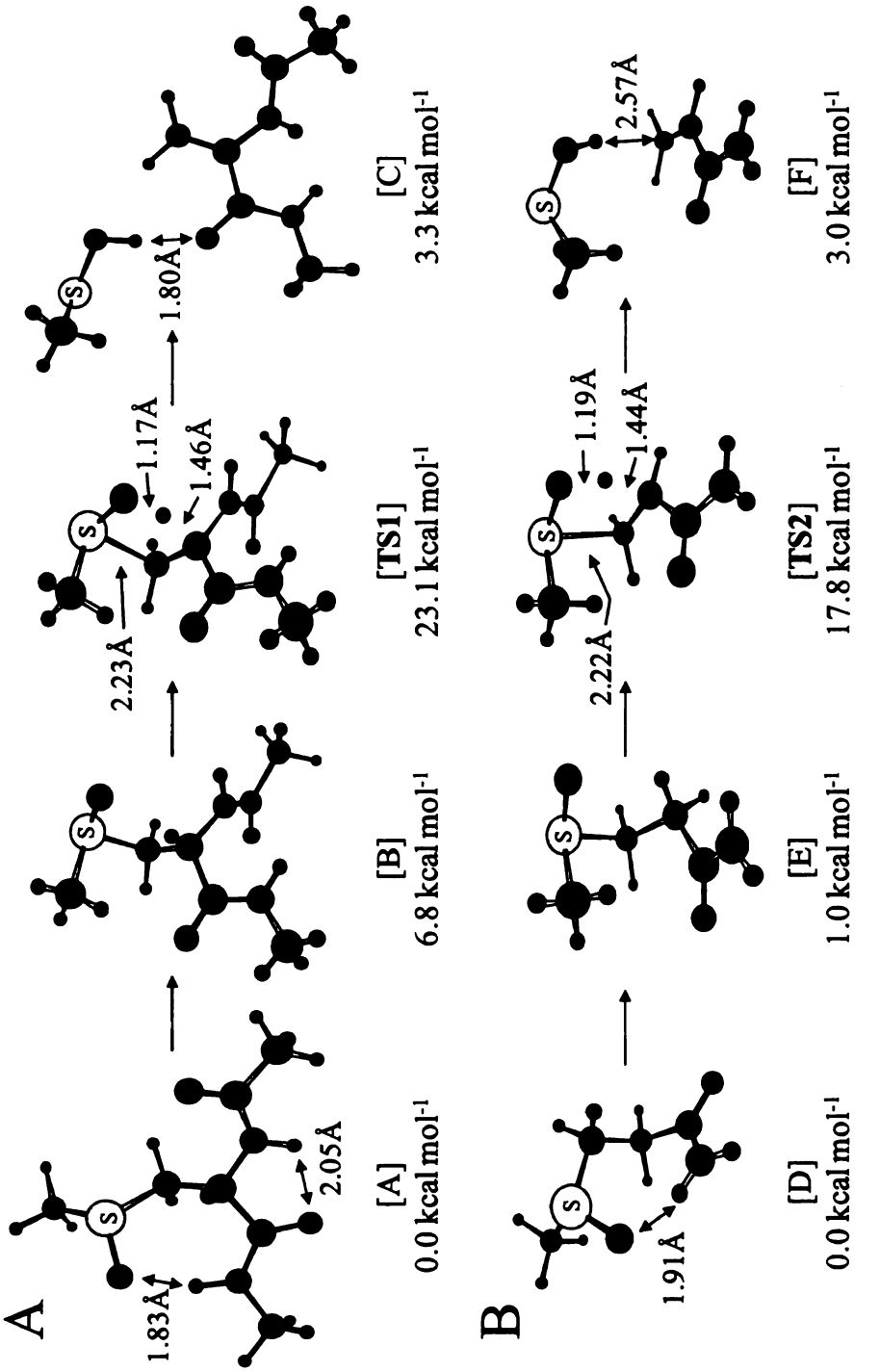

Figure 5.5 Optimized precursor, transition state and product ion structures (at the B3LYP/6-31+G(d,p) + ZPVE level of theory) for (A) the loss of CH_3SOH from the neutral model system $CH_3CONHCH(CH_2S(O)CH_3)CONHCH_3$ (equivalent to the loss of XSOH from the S-methyl cysteine sulfoxide-containing peptides) and (B) the loss of $CH_2CHCONH_2$ from the neutral model system $H_2NCOCH_2CH_2S(O)CH_3$ (equivalent to the loss of CH_2CHX' from the S-amidoethyl cysteine sulfoxide-containing peptides), via 5-membered *cis*-1,2 elimination pathways.

Structure [TS1] in Figure 5.5A shows the predicted low energy transition state structure found for the loss of CH_3SOH (equivalent to the loss of XSOH from the S-alkyl cysteine sulfoxide-containing peptides) from the model system $CH_3CONHCH(CH_2S(O)CH_3)CONHCH_3$ via a 5-membered *cis*-1,2 elimination pathway. IRC calculations, followed by geometry optimizations, were performed to locate the precursor ion [B] and the intermediate product ion [C] associated with this reaction coordinate. A further lower energy precursor ion [A] was also located. The relative energy of the transition state (+23.1 kcal mol^{-1}) was then calculated with respect to the energy of this precursor ion. Structure [TS2] in Figure 5.5B represents the low energy transition state structure found for the neutral loss of $CH_2CHCONH_2$ (equivalent to the loss of CH_2CHX' from the S-amidoethyl cysteine sulfoxide-containing peptides) from the model system $H_2NCOCH_2CH_2S(O)CH_3$. After IRC calculations were performed, the associated precursor ion [E], the intermediate product ion [F], and a lower energy precursor ion [D] were located. The energy of the transition state [TS2] with respect to that of the low energy precursor ion was found to be +17.8 kcal mol^{-1}. The total energies, zero point vibrational energies (ZPVE) and relative energies obtained for all the optimized transition structures are given in Table 5.3. The similar predicted activation barriers for the two fragmentation reactions (i.e., -XSOH and $-CH_2CHX'$) are therefore consistent with the experimentally observed product ion abundances.

Table 5.3 Total energies (E_{total}), zero point vibrational energies (ZPVE) and relative energies (E_{rel}) computed for the precursor ions, transition states and product ion structures associated with each reaction pathway at the B3LYP/6-31 + G (d,p) level of theory.

Structure	E_{total} (Hartree)	ZPVE (kcal mol^{-1})	E_{rel} (kcal mol^{-1})[a]
A	-1008.5887922	137.44180	0.0
B	-1008.5777340	137.34926	+6.8[b]
TS1	-1008.5459784	133.67822	+23.1[b]
C	-1008.5807054	135.69649	+3.3[b]
D	-761.2438197	85.48194	0.0
E	-761.2414516	85.01374	+1.06[c]
TS2	-761.2090719	81.44402	+17.8[c]
F	-761.2348465	82.84947	+3.0[c]
G	-839.6268943	111.59516	0.0
TS3	-839.5874485	107.78148	+20.9[d]
H	-839.6238461	109.49210	-0.2[d]
I	-840.0063802	120.51150	0.0
TS4	-839.9849623	117.08063	+10.0[e]
J	-840.0105422	118.44960	-4.7[e]

[a] E_{rel} = total energy + (ZPVE).

[b] Energy relative to Structure A.

[c] Energy relative to Structure D.

[d] Energy relative to Structure G.

[e] Energy relative to Structure I.

MS^3 dissociation of the neutral loss $[M+H-CH_2CHCONH_2]^+$ product ion from Figure 5.4A resulted in the exclusive loss of H_2O (Figure 5.4C). As shown in Scheme 5.3, the neutral loss of H_2O may potentially occur via a charge-remote *cis*-1,2 elimination reaction (Scheme 5.3, pathway A) to yield an amino thiopropanoic acid containing

product ion **(10)**. Alternatively, following intramolecular proton transfer from the peptide backbone to yield the protonated sulfenic acid intermediate **(11)**, the loss of H_2O could also potentially occur via a charge-directed E2 elimination reaction to yield **(12)** (Scheme 5.3, pathway B), or via S_N2 neighboring group participation reactions involving the N- or C-terminal amide carbonyl groups adjacent to the side chain to yield a cyclic five-membered 1,2 oxathiolane product **(13)** (Scheme 5.3, pathway C) or a six-membered 1,3,5 oxathiazine product (structure not shown), respectively. Hydrogen/deuterium exchange can readily be used to differentiate between the charge-remote and charge-directed fragmentation pathways proposed in Scheme 5.3, which would result in the loss of H_2O and HOD, respectively. MS^3 dissociation of the $[M+D-CH_2CHCOND_2]^+$ product ion formed by dissociation of the uniformly deuterated $[M+D]^+$ precursor ion of the C(S-ae)(ox)K peptide resulted primarily in the neutral loss of D_2O (100% relative abundance), with only minor loss of HOD observed (approx. 10% relative abundance) (data not shown). This suggested that the hydroxyl hydrogen in the sulfenic acid side chain (structure **(4)**) of the $[M+D-CH_2CHCOND_2]^+$ MS/MS product ion underwent exchange ("scrambling") with a deuterium on the peptide backbone prior to its dissociation by MS^3. Under these conditions, the charge-remote mechanism would primarily result in the neutral loss of HOD, while the charge-directed mechanisms would primarily result in the loss of D_2O. Therefore, we propose that the loss of H_2O from the $[M+H-CH_2CHCONH_2]^+$ ion occurs via a charge-directed process. The MS^4 spectrum obtained by dissociation of the $[M+H-CH_2CHCONH_2-H_2O]^+$ product ion is shown in Figure 5.4D. Observation of the b_4, b_5 and y_6 ions in this spectrum, corresponding to

cleavage of the amide bonds adjacent to the site of the cysteine side chain, suggests that the E2 elimination reaction had occurred. However, based on our recent study on the mechanisms responsible for the side chain fragmentation reactions of methionine fixed charge sulfonium ion-containing peptides, where formation of a mixture of cyclic five- and six-membered product ions were found to be favored,[170] the S_N2 neighboring group participation reactions cannot be ruled out.

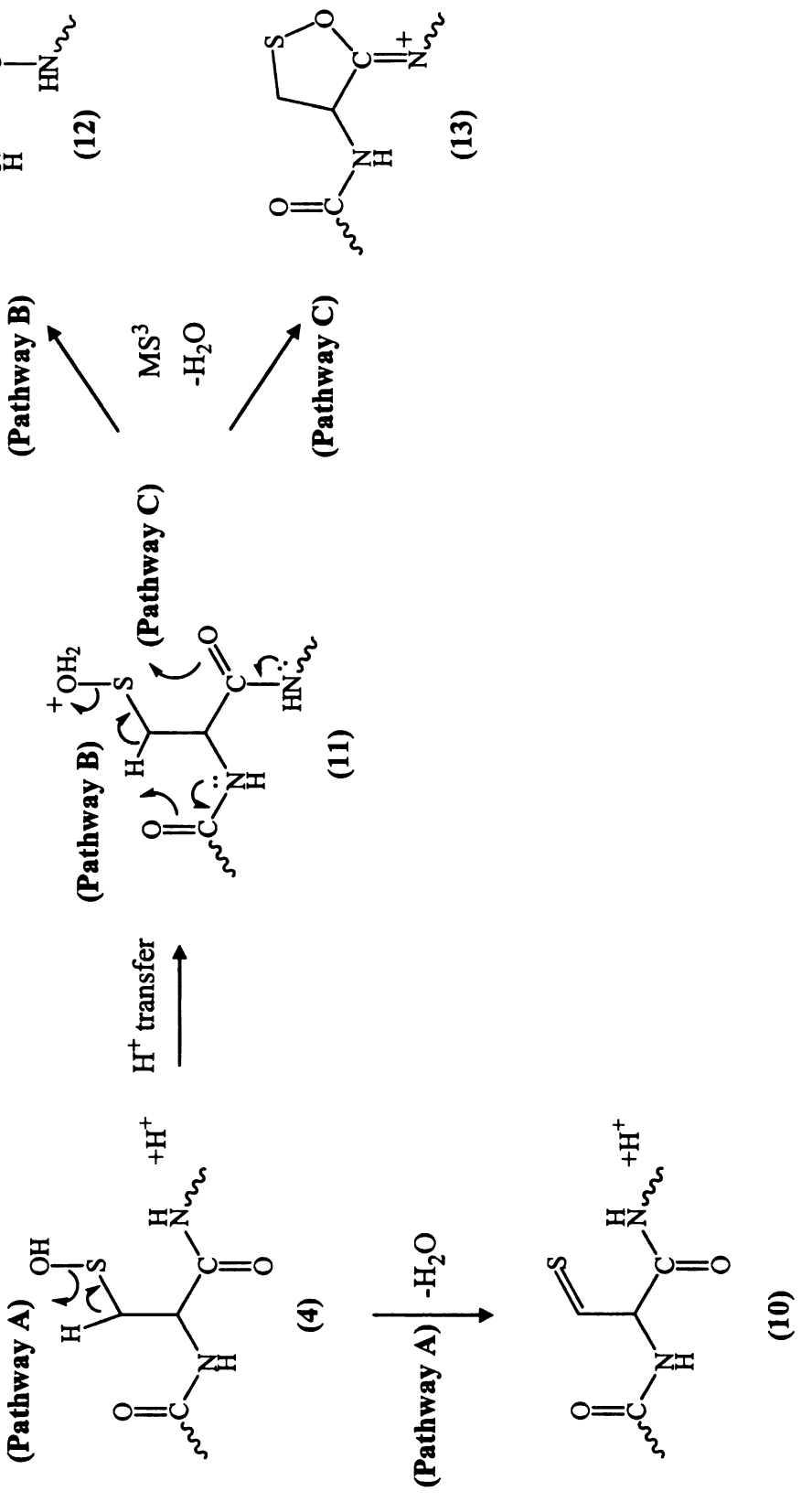

Scheme 5.3 Proposed mechanisms for the loss of H_2O from cysteine sulfenic acid-containing peptide ions.

In contrast to the data shown in Figures 5.4A and 5.4B, and in Table 5.1, where the product ions formed via the losses of $H_2NCOCH_2CH_2SOH$ and $CH_2CHCONH_2$ (and/or $CH_2CHCONH_2+H_2O$) from the S-amidoethyl cysteine sulfoxide-containing peptides were observed at similar abundances for all the precursor ion charge states examined (i.e., independently of the proton mobility of the peptide ions), the product ion abundances of the side chain losses from S-pyridylethyl cysteine sulfoxide-containing peptides were observed to vary significantly depending on the proton mobility of the precursor ion. For example, Figure 5.6 shows the product ion spectra obtained by CID-MS/MS of the singly, doubly and triply protonated precursor ions of the S-pyridylethyl cysteine sulfoxide-containing peptide VTMGHFCNFGK (M(ox)C(S-pe)(ox)K) (where pe= $CH_2CH_2C_5H_4N$) (Figures 5.6A, 5.6B and 5.6C, respectively). The CIR values calculated for the loss of pyridylethyl sulfenic acid (-XSOH, 155 Da, where X= $CH_2CH_2C_5H_4N$) and vinylpyridine (-CH_2CHX', 105 Da, where X'=C_5H_4N) from these ions, as well as those from the singly and doubly protonated S-pyridylethyl cysteine sulfoxide-containing peptides GAILCGAILK (C(S-pe)(ox)K) and GAILCGAILR (C(S-pe)(ox)R) are shown in Table 5.1. Note that the CIR values shown in Table 5.1 for the loss of CH_2CHX' also take into account the abundance of product ions formed via the combined losses of $CH_2CHC_5H_4N$ and H_2O ($CH_2CHX'+H_2O$, 123 Da). It can be seen from Figure 5.6A that CID-MS/MS of the singly protonated precursor ion of M(ox)C(S-pe)(ox)K resulted primarily in the loss of $NC_5H_4CH_2CH_2SOH$ (XSOH), with the losses of $CH_2CHC_5H_4N$ (CH_2CHX') or $CH_2CHC_5H_4N+H_2O$ ($CH_2CHX'+H_2O$) observed at somewhat lower abundances. In contrast, the losses of $CH_2CHC_5H_4N$ (CH_2CHX') and

$CH_2CHC_5H_4N+H_2O$ ($CH_2CHX'+H_2O$) from the doubly and triply protonated precursors (Figures 5.6B and 5.6C, respectively), were observed as the most abundant products. Furthermore, the observation of these losses as charged (protonated) species was observed to increase with increasing charge state (proton mobility). Similar trends were also observed from dissociation of the C(S-pe)(ox)K and C(S-pe)(ox)R peptide ions (Table 5.1).

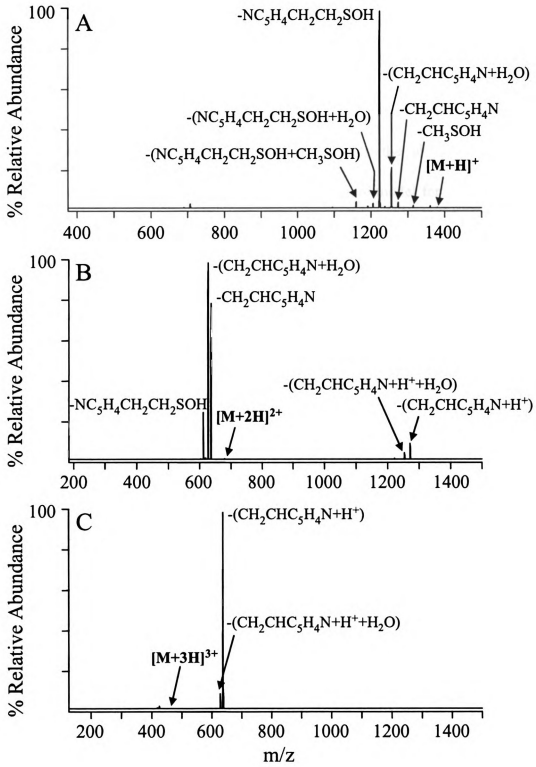

Figure 5.6 CID-MS/MS product ion spectra of the methionine sulfoxide- and S-pyridylethyl cysteine sulfoxide-containing peptide VTMGHFCNFGK (M(ox)C(S-pe)(ox)K). (A) $[M+H]^+$ ion. (B) $[M+2H]^{2+}$ ion. (C) $[M+3H]^{3+}$ ion.

The differences in fragmentation behavior observed between the S-pyridylethyl and S-amidoethyl cysteine sulfoxide-containing peptides can be rationalized by taking into consideration the expected sites of protonation in the singly and multiply protonated precursor ions of each of the peptides, and the effect of the site of protonation on the transition state barriers for the loss of CH_2CHX' via the charge remote *cis*-1,2 elimination pathway. The proton affinity of an appropriate model for the S-pyridylethyl cysteine sulfoxide side chain is 4-ethylpyridine (227.3 kcal mol^{-1}).[245] Although this is lower than the proton affinities of arginine (251.2 kcal mol^{-1}) and lysine (238 kcal mol^{-1}), it is significantly higher than that of appropriate models for the S-amidoethyl cysteine sulfoxide side chain, i.e., propionamide (209.4 kcal mol^{-1}), and the amide backbone (i.e., N-methyl acetamide (212.4 kcal mol^{-1}).[245] Therefore, the site of protonation for all the singly charged precursor ions examined here is expected to be at either the terminal lysine or arginine residues of the peptide sequence. In contrast, while the addition of a second ionizing proton would be expected to result in protonation along the amide backbone for the S-amidoethyl cysteine sulfoxide-containing peptides, thereby allowing backbone fragmentation processes to be observed (for example, see Figure 5.4B), a second ionizing proton added to the S-pyridylethyl cysteine sulfoxide-containing peptides would be expected to localize on the side chain pyridylethyl moiety. The effect of this localized proton on the predicted barriers for loss of the side chain CH_2CHX' is shown in Figure 5.7. Similar to that shown in Figure 5.5B for the neutral loss of $CH_2CHC_5H_4N$, the barrier for this loss from the model system $NC_5H_4CH_2CH_2S(O)CH_3$ (equivalent to the loss of CH_2CHX' from the S-pyridylethyl cysteine sulfoxide-containing peptides)

was predicted to be 20.9 kcal mol^{-1} (structure [TS3] in Figure 5.7A). In contrast, protonation of the pyridylethyl side chain resulted in a predicted transition state activation barrier of only 10.0 kcal mol^{-1} (structure [TS4] in Figure 5.7B), resulting in the loss of $CH_2CHC_5H_4NH^+$. These data are therefore entirely consistent with the experimentally observed product ion abundances shown in Figure 5.6 and in Table 5.1.

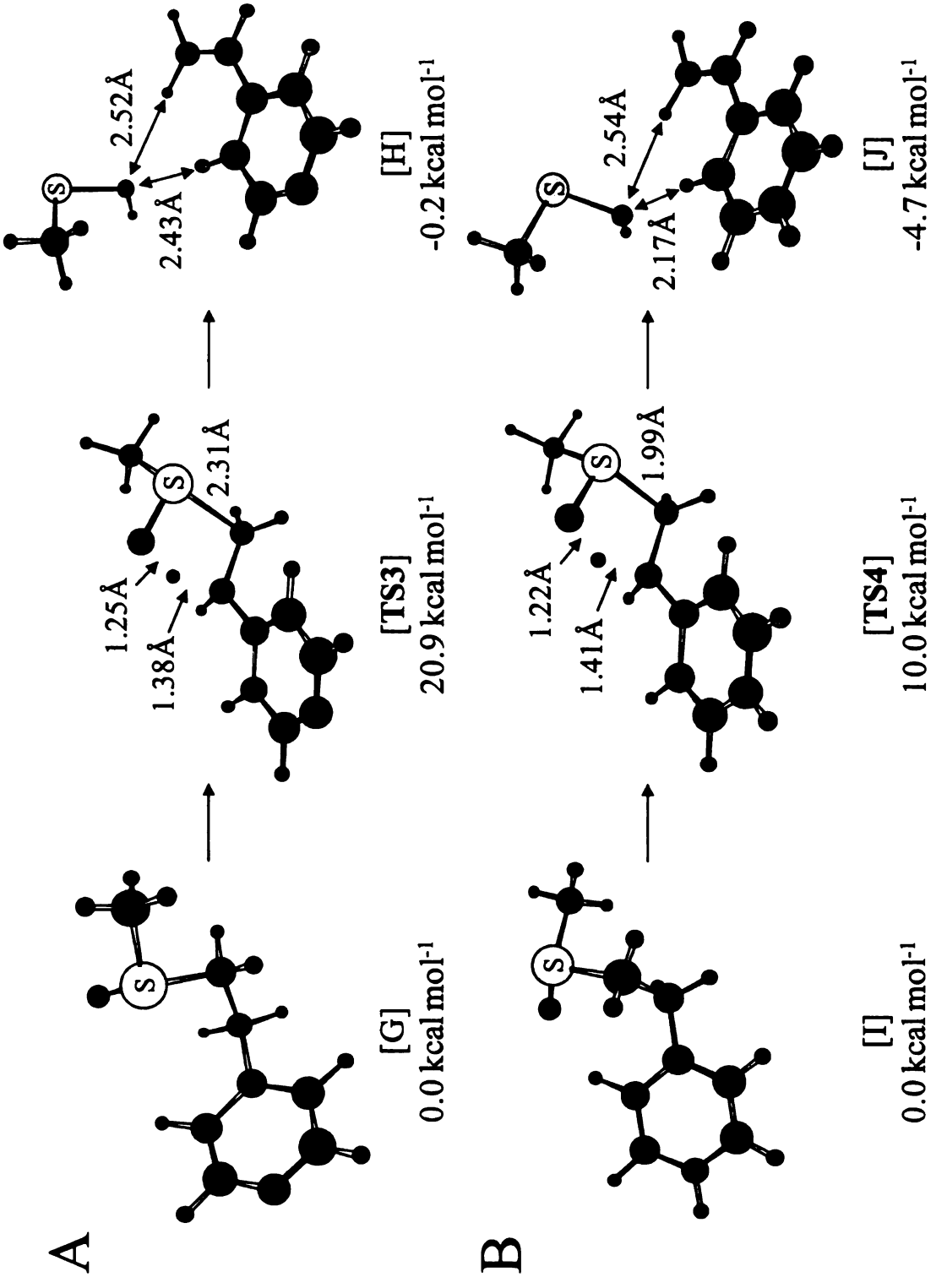

Figure 5.7 Optimized precursor, transition state and product ion structures (at the B3LYP/6-31+G(d,p) + ZPVE level of theory) for (A) the loss of $CH_2CHC_5H_4N$ from the neutral model system $NC_5H_4CH_2CH_2S(O)CH_3$ and (B) the loss of $CH_2CHC_5H_4NH^+$ from the protonated model system $HNC_5H_4CH_2CH_2S(O)CH_3^+$ (equivalent to the loss of CH_2CHX' from the S-pyridylethyl cysteine sulfoxide-containing peptides).

Loss of CH_2CHX' from the side chain of the doubly and triply protonated precursor ions of the M(ox)C(S-pe)(ox)K peptide (Figures 5.6B and 5.6C) as predominantly a neutral versus protonated species, respectively, can be readily rationalized by the expected differences in proton affinity between the singly and doubly protonated peptide product ions and the neutral 4-vinylpyridine side chain cleavage product (i.e., the order of proton affinities is expected to be $[M+H-CH_2CHC_5H_4N]^+$ > $CH_2CHC_5H_4N$ > $[M+2H-CH_2CHC_5H_4N]^{2+}$). Thus, for dissociation of the doubly protonated precursor ion, the proton affinity of the peptide product ion is higher than that of $CH_2CHC_5H_4N$, such that proton transfer within the initially formed ion-ion complex results in loss of the side chain 4-vinylpyridine product as a neutral species (Scheme 5.4, pathway A), while for dissociation of the triply protonated precursor ion, the proton affinity of the peptide product ion is lower than that of $CH_2CHC_5H_4N$, such that loss of the 4-vinylpyridine product is observed as the protonated species (Scheme 5.4, pathway B).

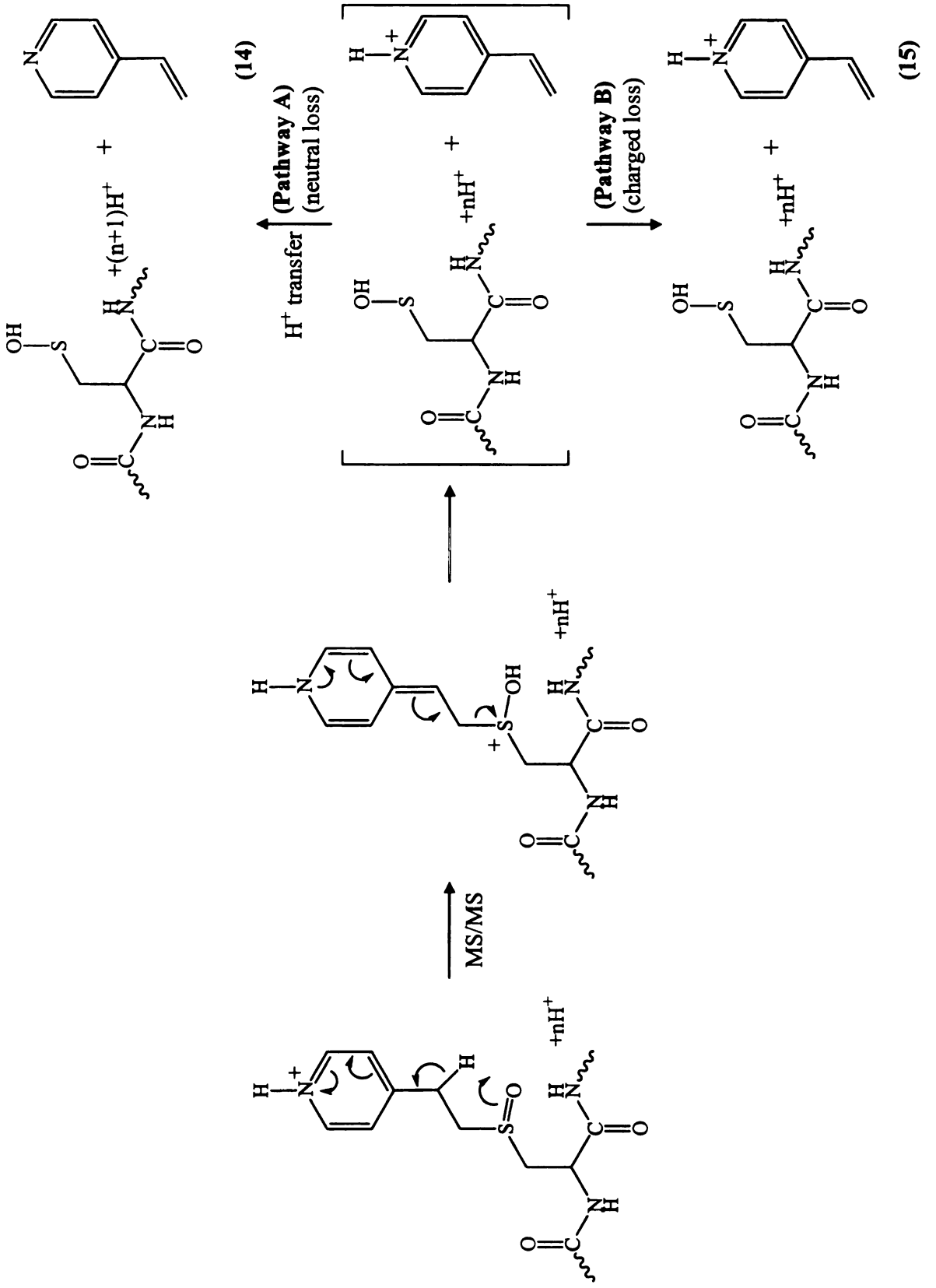

Scheme 5.4 Proposed mechanism for the loss of vinylpyridine from the protonated side chain of S-pyridylethyl (S-pe) cysteine sulfoxide-containing peptide ions.

5.5 Conclusions

The results presented here confirm that the loss of XSOH from the side chains of oxidized S-alkyl cysteine-containing peptides formed by reaction with iodomethane, iodoacetamide, iodoacetic acid, acrylamide and 4-vinylpyridine occurs via a charge-remote five-centered *cis*-1,2 elimination reaction to yield a dehydroalanine containing product ion. The mechanisms and proton mobility dependence to the losses of CO_2, CO_2+H_2O and CO_2+CH_2O from S-carboxymethyl cysteine sulfoxide-containing peptides, the loss of $CH_2CHC_5H_4N$ from S-amidoethyl cysteine sulfoxide-containing peptides, and the losses of $CH_2CHC_5H_4N$ and $CH_2CHC_5H_4NH^+$ from S-pyridylethyl cysteine sulfoxide-containing peptides following CID-MS/MS have also been examined. Clearly, both the nature of the S-alkyl substituent and the proton mobility of the peptide precursor ion have a significant influence on the appearance of the product ion spectra obtained via the gas-phase dissociation of protonated S-alkyl cysteine sulfoxide-containing peptide ions. It is expected that incorporation of the non-sequence ion fragmentation behaviors observed here into the suite of "rules" employed by automated database search algorithms for protein identification should enable the development of more comprehensive tools for the identification and characterization of modified proteins.

CHAPTER SIX

Automated Neutral Loss and Data Dependent Energy Resolved "Pseudo MS^3" for the Targeted Identification, Characterization and Quantitative Analysis of Methionine-containing Peptides*

6.1 Introduction

Recently, our laboratory has described the development of a novel MS/MS based "fixed-charge" sulfonium ion chemical derivatization strategy that enables the targeted gas-phase identification and quantitative analysis of methionine- (Scheme 1.3A) or cysteine- (Scheme 1.3B) containing peptides.[169-172] Under low-energy CID-MS/MS conditions, the dissociation of these sulfonium ion containing peptides are exclusively directed toward the site of the fixed-charge, resulting in the formation of a single characteristic product ion. Importantly, these reactions have been shown to occur independent of the proton mobility of the precursor ion. Furthermore, as all the precursor ion abundance is transferred to a single product ion, the maximum possible sensitivity for their detection is obtained. Thus, the selective identification of these derivatized peptides may be achieved by low-energy neutral loss scan mode MS/MS experiments in triple quadrupole mass spectrometers,[169] or by CID-MS/MS in a quadrupole ion trap mass spectrometer.[170-172] Further structural information regarding the amino acid sequence of

---

* The results described in this Chapter have been published in: Froelich, J.M.; Kaplinghat, S.; Reid, G.E. Automated Neutral Loss and Data Dependent Energy Resolved "Psuedo MS^3" for the Targeted Identification, Characerization and Quantitative Analysis of Methionine-containing Peptides. *Eur. J. Mass Spectrom.* **2008**, *14*, 219-229.

the identified peptides is then readily obtained by subjecting the initial neutral loss product ion to further dissociation by either MS^3 in the quadrupole ion trap, or by energy resolved "pseudo MS^3" under higher energy CID conditions in the triple quadrupole.[169, 172] In an initial report, the use of this strategy for the differential quantitative analysis of methionine-containing peptides was also demonstrated, via measurement of the abundances of the characteristic neutral loss product ions formed from "light" and "heavy" isotopically encoded forms of the fixed-charge derivatives produced by reaction with $^1H_5$- and $^2H_5$ phenacylbromide ($BrCH_2COC_6H_5$ / $BrCH_2COC_6D_5$), respectively.[169]

In this initial report however, the capability of this promising approach for targeted gas-phase peptide identification was only demonstrated for the analysis of methionine-containing peptides obtained from 10 pmol of a relatively simple protein digest of bovine serum albumin introduced to the mass spectrometer by capillary HPLC, while its capability for quantitative analysis was only demonstrated at a ratio of 1:1 for a sample consisting of 1 pmol each of a single "light" and "heavy" labeled methionine-containing peptide. Also, some chromatographic separation[246] of the $^1H_5$- and $^2H_5$ phenacylbromide labeled forms of the fixed charge sulfonium ion derivatives was observed, potentially limiting the ability of this strategy to obtain accurate quantitative measurements.

Here, to further evaluate the utility of this approach for the selective gas-phase identification and characterization of individual low abundance methionine-containing peptides contained within complex protein digests, the development of an automated ESI-HPLC, neutral loss MS/MS and data dependent "pseudo MS^3" analysis method in a triple

quadrupole mass spectrometer is described. Also, to improve the capabilities of this fixed charge derivatization strategy for the quantitative analysis of low abundance methionine-containing peptides across a range of abundance ratios, the synthesis and initial application of a ^{13}C labeled version of the phenacylbromide ($BrCH_2CO^{13}C_6H_5$) alkylation reagent is also described.

6.2 Optimization of "Low" and "High" Collision Energies Employed for Neutral Loss MS/MS and "Pseudo MS^3" Analysis

In order to develop an automated neutral loss MS/MS and data dependent energy resolved "pseudo MS^3" acquisition method for the targeted identification and characterization of phenacylsulfonium ion derivatized methionine-containing peptides in a triple quadrupole mass spectrometer, the optimal collision energies required for initial fragmentation of the sulfonium ion derivative, and for subsequent fragmentation along the amide backbone, were first determined using product ion scan mode MS/MS for a range of precursor ion charge states using the sulfonium ion derivatized synthetic model "tryptic" peptides GAILMGAILK (MK), GAILMGAILR (MR), VTMGHFDNFGR (MDR) and VTMSHFWNFGK (MSK). For doubly charged precursor ions ($[M^+ + H]^{2+}$) it was determined that an average collision energy of 19 V at an argon collision gas pressure of 0.7 mtorr was required in order for essentially exclusive fragmentation of the sulfonium ion derivative at the methionine side chain to be observed. At this "low" collision energy, approximately 80% of the precursor ion population had undergone fragmentation to exclusively yield the $[M^+ + nH - CH_3SCH_2COC_6H_5]^{(n+1)+}$ ($[M^+ + nH - CH_3SAP]^{(n+1)+}$) neutral loss product ion, thereby allowing their selective identification.

Notably, product ions formed by fragmentation along the peptide backbone were essentially non-existent, while further fragmentation of the initial product ion was minimized. At "high" average collision energy values (determined to correspond to 34 V), sequential fragmentation of the precursor ion and the initial neutral loss product yielded a series of b- and/or y-type product ions from which the sequence of the methionine containing peptide could be determined. For triply charged precursor ions ($[M^{+}+2H]^{3+}$), selective fragmentation of the sulfonium ion derivative at the methionine side chain, and subsequent fragmentations along the amide backbone, were found to require average collision energies of 12 V and 17 V, respectively. The ability to observe the initial neutral loss product ions at low collision energies is particularly beneficial for experiments aimed at quantitative analysis, because non-labeled peptide ions that may potentially overlap at the same m/z value will largely not fragment at such low collision energies.

6.3 Selective Identification and Characterization of Fixed-charge Methionine-containing Peptides by Neutral Loss MS/MS and Data Dependent Energy Resolved "Pseudo MS^3"

To demonstrate the ability to automatically and selectively identify and characterize fixed-charge methionine-containing peptides from within a complex protein digest by using a triple quadrupole mass spectrometer, the synthetic peptide MK was alkylated with phenacylbromide then spiked at a level of either 100 fmol, 500 fmol or 1 pmol into a complex mixture compromised of 1 pmol each of a seven protein tryptic digest mixture derived from equine myoglobin, bovine serum albumin, bovine glutamate

dehydrogenase, *E. coli* glycerokinase, human alpha lactalbumin, human lactotransferrin, and yeast enolase. The peptide mixture was then analyzed by on-line capillary RP-HPLC nano-ESI-MS using the approach outlined in Scheme 6.1. Following the acquisition of a full MS scan (scan event 1), sequential neutral loss MS/MS scans for 83 m/z (doubly charged precursors) (scan event 2) and 55.3 m/z (triply charged precursors) (scan event 3) were acquired using the optimized collision energy conditions described in Section 6.2 in order to "extract" and identify the presence of the fixed-charged containing peptide from the non-labeled peptides within the mixture. Then, precursor ions identified from the neutral loss MS/MS scans above a pre-defined threshold were automatically subjected to data dependent energy resolved product ion scan mode "pseudo MS^3" (scan events 4 and 5) to obtain further structural information required to identify and characterize the peptide sequence of the methionine-containing peptide.

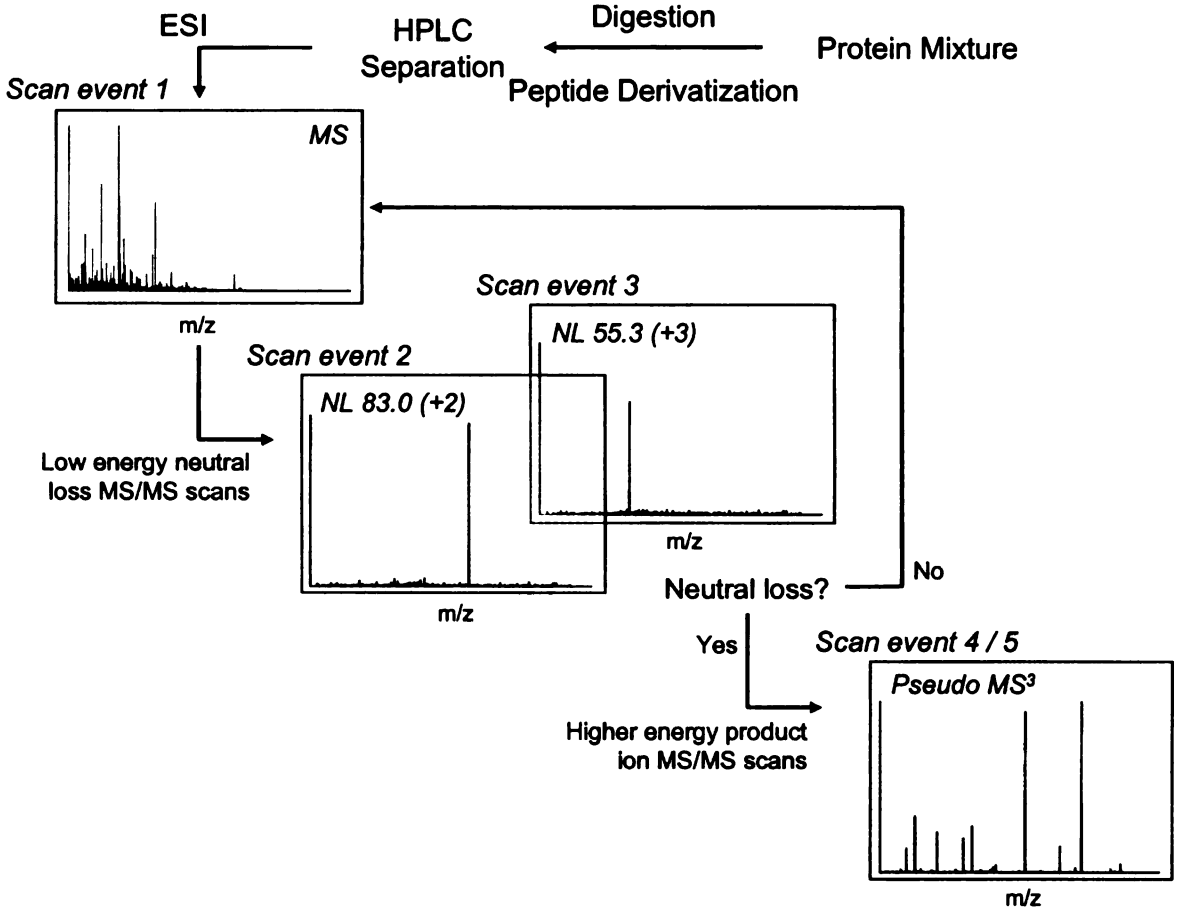

Scheme 6.1 Automated neutral loss MS/MS and data dependent energy resolved "pseudo MS^3" for the targeted identification and characterization of phenacylsulfonium ion derivatives of methionine-containing peptides in a triple quadrupole mass spectrometer.

The total ion current trace obtained by LC-MS analysis of the seven protein tryptic digest mixture (1 pmol each) containing 500 fmol of the phenacylsulfonium ion derivative of MK is depicted in Figure 6.1A. The mass spectrum obtained for the region from 19.5 - 20.5 minutes of this analysis, containing the fixed-charge phenacylsulfonium ion derivative of MK (m/z 553.0 corresponds to the doubly charged precursor ion), is shown in the inset. Note that while an MS scan was acquired here, it is important to emphasize that the MS scan does not trigger the acquisition of a neutral loss MS/MS scan, and was included here only to allow for comparative analysis of the results obtained

by MS and MS/MS. These data clearly indicate the complexity of the peptide mixture. In contrast, the total ion current traces obtained from the neutral loss MS/MS scan mode experiments to monitor for the doubly charged sulfonium ion containing precursor ions (neutral loss of 83 m/z) (Figure 6.1B), as well as the summed neutral loss MS/MS spectrum for the region from 19.5 - 20.5 minutes (Figure 6.1C) are dramatically simplified. Indeed, only a single ion corresponding to the fixed-charge phenacylsulfonium ion derivative of MK is observed in Figure 6.1C. Thus, by employing the neutral loss MS/MS scan, this peptide is selectively "extracted" from the complex peptide mixture. Similar data was obtained from the neutral loss scan mode analysis of the triply charged sulfonium ion containing precursor ions (neutral loss of 55.3 m/z) (data not shown). Following the acquisition of these neutral loss scans, and when the abundance of the neutral loss appeared above a threshold value of 1.0×10^6 counts, product ion scan mode MS/MS scans were then automatically acquired to obtain data dependent energy resolved pseudo MS^3 spectra from which the sequence of the phenacylsulfonium ion containing peptides were confirmed. Figure 6.1D shows the energy resolved pseudo MS^3 spectra obtained from the doubly charged precursor ion from Figure 6.1C.

Figure 6.1 Neutral loss MS/MS and data dependent energy resolved MS^3 for the selective identification and characterization of a single methionine-containing phenacylsulfonium ion derivative of GAILMGAILK (500 fmol) spiked into a complex tryptic digest mixture of seven proteins (1 pmol each). (A) Total ion current trace obtained by capillary HPLC-mass spectrometry analysis. The inset to panel A shows the mass spectrum obtained from the region of the chromatogram spanning 19.5-20.5 min. (B) Total ion current trace obtained by neutral loss scan mode MS/MS analysis (neutral loss of 83.0 m/z). (C) Summed neutral loss scan mode CID-MS/MS spectrum from the 19.5-20.5 min region indicated in panel B. (D) Date dependent energy resolved "pseudo" MS^3 product ion spectrum of the doubly charged precursor ion at m/z 553.1 identified from the neutral loss scan in panel C.

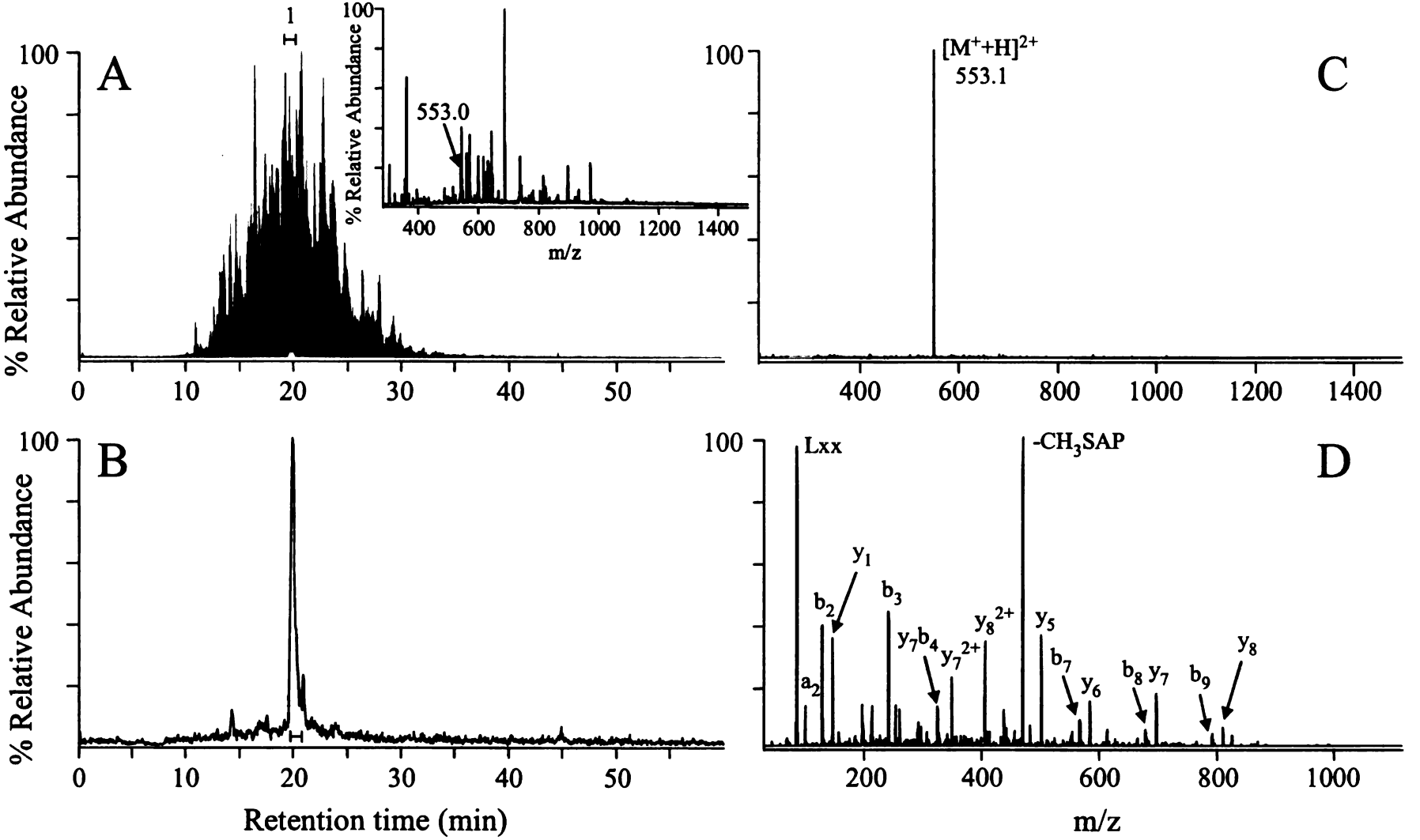
A
B
C
D
100
% Relative Abundance
1
553.0
m/z
[M+H]2+
553.1
Retention time (min)
Lxx
-CH3SAP
y1
b2
b3
y7b4
y7 2+
y8 2+
y5
b7
y6
b8 y7
b9
y8
a2

In addition to the major chromatographic peak corresponding to the phenacylsulfonium ion derivative of MK observed in the doubly charged neutral loss scan mode spectrum in Figure 6.1B, a number of other peaks were also observed at low abundance. These chromatographic peaks most likely arise due to the presence of non-labeled peptide ions within the mixture, that fortuitously give rise to a product ion at a m/z value 83 m/z lower than that of their precursor ion upon fragmentation.[247] Note that these ions are likely to correspond to highly charged (e.g., $[M+3H]^{3+}$ or higher) protonated precursor ions, as we have observed that doubly protonated ($[M+2H]^{2+}$) ions do not undergo effective fragmentation at the "low" collision energies employed for dissociation of the doubly charged ($[M^{+}+H]^{2+}$) sulfonium ion containing peptides. As the mixture complexity increases, the number of these non-labeled peptide ions which fortuitously give rise to these "contaminant" ions are likely to increase. The absolute abundance of these non-labeled peptide ion signals from the 1 pmol protein digest mixture examined here were observed to remain relatively constant. However, as the amount of the fixed-charge methionine-containing peptide decreased, for example, when a 100 fmol sample was spiked into the 1 pmol protein digest mixture (data not shown), the relative abundance of these non-labeled ions compared to the labeled peptide ion were observed to increase, thereby complicating the data acquisition and analysis procedure. In order to overcome this potential limitation for the analysis of low abundance sulfonium ion derivatized methionine-containing peptides, it may be necessary to reduce the sample mixture complexity prior to analysis. Due to the presence of the fixed-charge sulfonium ion, this can be readily achieved by the use of off- or on-

line strong cation exchange chromatography to enrich the methionine-containing peptides prior to their MS analysis.[38, 213]

Another potential limitation of the approach described here is the fact that a "true" MS^3 experiment is not being performed, i.e., the initial neutral loss product ion produced under "low" collision energy conditions is not mass selected prior to its further dissociation at "higher" collision energies. Thus, if a non-labeled peptide has the same retention time and m/z value as a labeled peptide, both will fragment simultaneously when performing "pseudo" MS^3 under higher energy conditions, yielding a mixture of sequence ions for both the labeled and unlabeled precursors. However, this problem would also be alleviated by the use of off- or on-line strong cation exchange chromatography prior to MS analysis, as described above. An alternate strategy would be to perform neutral loss MS/MS scans in the triple quadrupole mass spectrometer to identify the fixed-charge methionine-containing peptides, and to generate an "inclusion list"[3] of peptide retention times and m/z values, that could then be employed to perform "targeted" MS/MS and MS^3 analysis of a replicate sample using a quadrupole ion trap mass spectrometer.

6.4 Differential Quantitative Analysis of Fixed-charge Methionine-containing Peptides by Neutral Loss MS/MS

To demonstrate the improved capabilities of the sulfonium ion derivatization approach for the selective identification and differential quantitative analysis of methionine-containing peptides from within complex peptide mixtures, the model synthetic peptide MK was alkylated with either phenacylbromide or $^{13}C_6$-

phenacylbromide. These "light" and "heavy" labeled MK peptides were then combined in amounts ranging from 100 fmol to 1 pmol and abundance ratios ranging from 0.1 to 10, and "spiked" into the seven protein tryptic digest mixture (1 pmol each). As shown in Scheme 6.2, a series of automated experiments involving the acquisition of a full MS scan (scan event 1), followed by sequential neutral loss mode MS/MS scans of 83 m/z (scan event 2) and 86 m/z (scan event 3) for the $^{12}C_6$ and $^{13}C_6$ containing doubly charged precursor ions and 55.3 m/z (scan event 4) and 57.3 m/z (scan event 5) for the $^{12}C_6$ and $^{13}C_6$ containing triply charged precursor ions were then acquired using collision energies of 19 and 12 V, respectively. Similar to that described above, the MS scan was not required but was included in this study to allow for comparison of the quantitative analysis results obtained by MS and MS/MS.

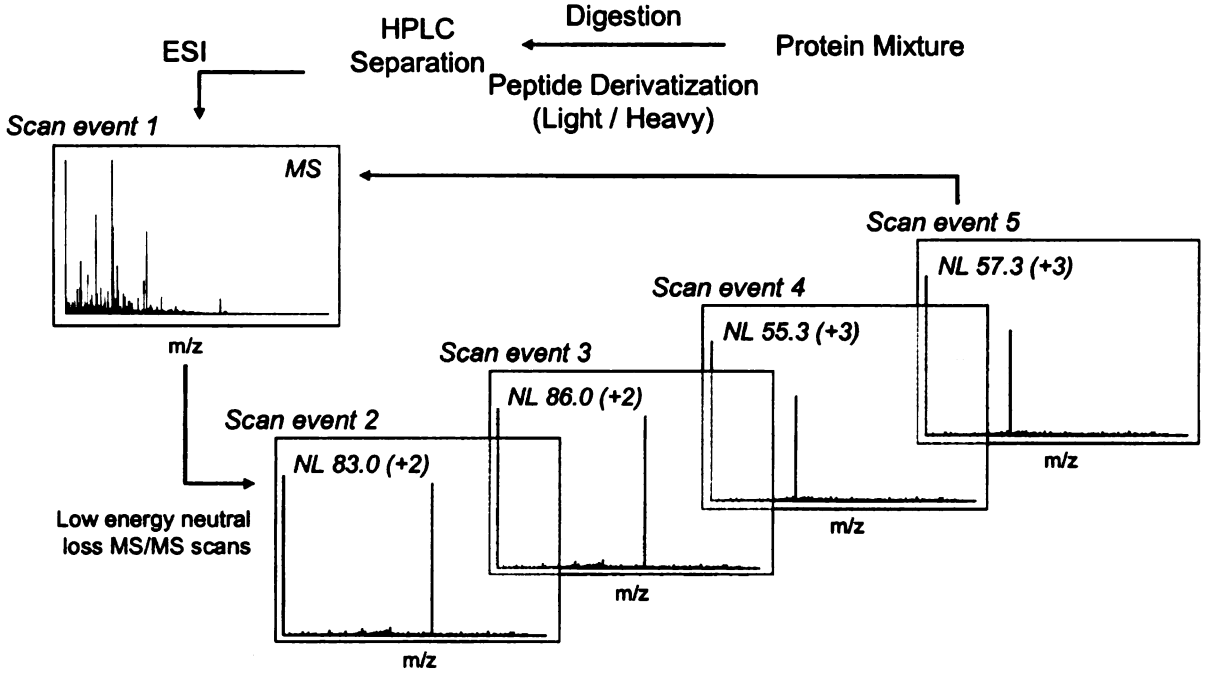

Scheme 6.2 Automated neutral loss MS/MS for the quantitative analysis of phenacylsulfonium ion derivatives of methionine-containing peptides in a triple quadrupole mass spectrometer.

The total ion current trace obtained from the LC-MS analysis of a 1:1 mixture of 100 fmol each of the "light" and "heavy" labeled MK peptides spiked into the seven protein tryptic digest mixture (1 pmol each) is shown in Figure 6.2A, with the mass spectrum for the region from 19.5 - 20.5 minutes shown in the inset. The abundance ratios for the "light" and "heavy" labeled doubly (m/z 553.0 and 556.0) and triply (m/z 369.0 and 371.0) charged precursor ions were first determined from the full scan MS spectrum. For the triply charged precursor ions, an abundance ratio of 0.91 was determined from the full scan MS spectrum, which was in good agreement with the expected ratio (Figure 6.2B). In contrast, the observed abundance ratio of 0.13 for the doubly charged ions differed substantially from the expected ratio (Figure 6.2C). By examination of the mass spectrum, it was determined that a "contaminating" non-labeled peptide ion was present at the same retention time and the same m/z as the "heavy" labeled doubly charged precursor ion, therefore precluding differential quantitative analysis by MS. In contrast, abundance ratios consistent with the expected values were successfully obtained from the successive neutral loss scan mode MS/MS experiments for the triply (Figures 6.2D and 6.2E) and doubly (Figures 6.2F and 6.2G) charged precursor ions (0.85 and 1.05, respectively). Indeed, for abundance ratios ranging from 0.1 to 10, an excellent linearity of response was observed between the expected and experimentally determined abundance ratios using the neutral loss scan mode MS/MS experiments (Figure 6.3). It is also important to note that the level of chemical noise in the spectra obtained from the neutral loss MS/MS experiments was greatly reduced in comparison to the spectra acquired by full scan MS, indicating the potential of this strategy for achieving significantly increased specificity, sensitivity and dynamic range

compared to MS based quantitative analysis approaches. Furthermore, this MS/MS based approach is very attractive for use in the identification and differential quantitative analysis of peptides which may be significantly over- or under-expressed, as both "light" and "heavy" labeled peptides are not required to be observed in order for one of the pairs, and its origin, to be determined.

Figure 6.2 Selective identification and differential quantitative analysis of a 1:1 mixture of methionine-containing phenacylsulfonium and $^{13}C_6$ phenacylsulfonium ion derivatives of GAILMGAILK (100 fmol each) spiked into a complex tryptic digest mixture of seven proteins (1 pmol each). (A) Total ion current trace following capillary HPLC-mass spectrometry analysis. The inset to panel A show the mass spectrum obtained from the region of the chromatogram spanning 19.5-20.5 min. (B) Expanded region of the mass spectrum containing the triply charged "light" (m/z 369.0) and "heavy" (m/z 371.0) labeled peptide ions. (C) Expanded region of the mass spectrum containing the doubly charged "light" (m/z 552.9) and "heavy" (m/z 555.9) labeled peptide ions. (D) Neutral loss scan mode MS/MS spectrum for the neutral loss of 55.3 m/z from $^{12}C_6$ containing triply charged ions. (E) Neutral loss scan mode MS/MS spectrum for the neutral loss of 57.3 m/z from $^{13}C_6$ containing triply charged ions. (F) Neutral loss scan mode MS/MS spectrum for the neutral loss of 83 m/z from $^{12}C_6$ containing doubly charged ions. (G) Neutral loss scan mode MS/MS spectrum for the neutral loss of 86 m/z from $^{13}C_6$ containing doubly charged ions.

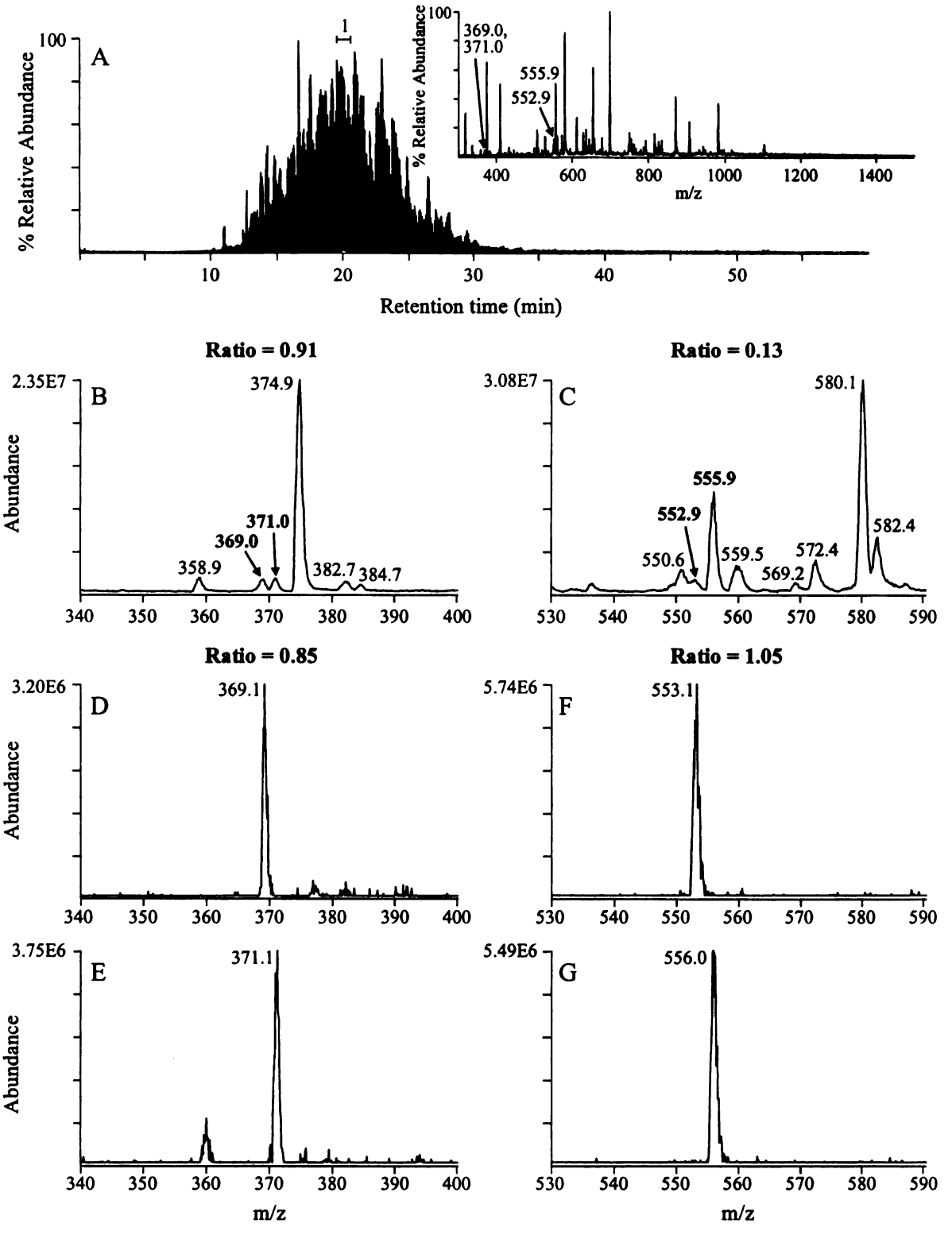
A
100
% Relative Abundance
I
10
20
30
40
50
Retention time (min)
% Relative Abundance
100
369.0,
371.0
555.9
552.9
400
600
800
1000
1200
1400
m/z
Ratio = 0.91
2.35E7
B
374.9
371.0
369.0
358.9
382.7
384.7
Abundance
340
350
360
370
380
390
400
Ratio = 0.13
3.08E7
C
580.1
555.9
552.9
582.4
550.6
559.5
572.4
569.2
530
540
550
560
570
580
590
Ratio = 0.85
3.20E6
D
369.1
Abundance
Ratio = 1.05
5.74E6
F
553.1
3.75E6
E
371.1
Abundance
5.49E6
G
556.0
m/z
m/z

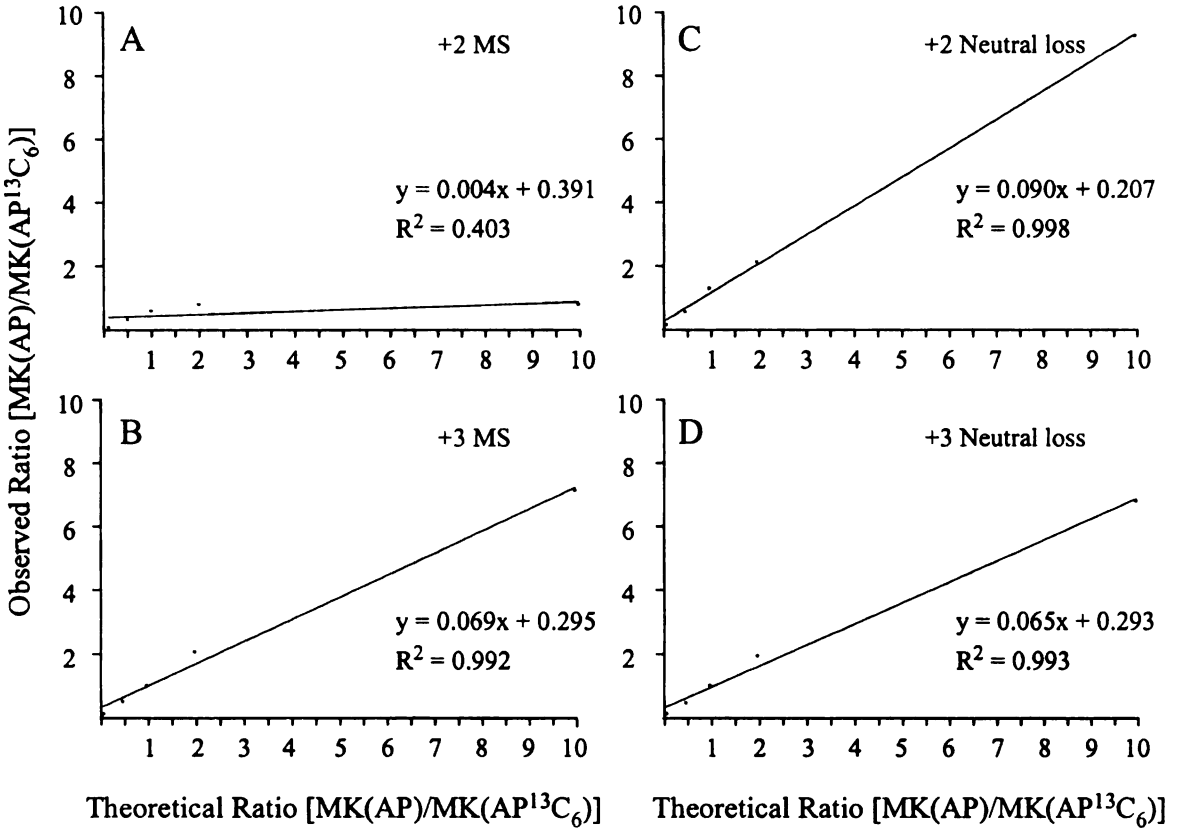

Figure 6.3 Observed versus theoretical abundance ratios for 0.1:1, 0.5:1, 1:1, 1:0.5 and 1:0.1 pmol mixtures of phenacylsulfonium and $^{13}C_6$ phenacylsulfonium ion derivatives of GAILMGAILK in a tryptic digest mixture of seven proteins (1 pmol each) obtained by MS analysis of the doubly and triply charged precursor ions (panels A and B, respectively) and by neutral loss scan mode MS/MS analysis (83.0 and 86.0 m/z for doubly charged ions and 55.3 and 57.3 m/z for triply charged ions) (panels C and D, respectively).

6.5 Conclusions

The results presented here demonstrate the utility of an automated approach for the selective gas-phase identification, characterization and differential quantitative analysis of fixed-charge methionine-containing peptides, based on neutral loss MS/MS and data dependent "pseudo MS^3" scans in a triple quadrupole mass spectrometer. Using this approach, a synthetic fixed-charge methionine-containing peptide was successfully 'extracted' in the gas-phase, and selectively identified and characterized from within a

complex seven protein tryptic digest mixture. By incorporating ^{13}C isotopic labels into the alkylating reagent employed for fixed-charge derivatization, differential quantitative analysis was achieved for a low abundance fixed-charge methionine containing peptides spiked into a complex seven protein tryptic digest mixture, by measurement of the abundances of the characteristic product ions formed by neutral loss scan mode MS/MS. In contrast to MS-based quantitative analysis strategies, the neutral loss scan mode MS/MS method employed here was able to achieve accurate quantitation for amounts ranging from 100 fmol to 1 pmol and abundance ratios ranging from 0.1 to 10. It is expected that use of the gas-phase methionine-containing peptide "enrichment" approach described here would improve the specificity of current database search analysis strategies, by enabling searches against only a subset of the peptides contained within a protein sequence database (i.e., those containing methionine).

CHAPTER SEVEN

Quantitative Analysis of Calcineurin Methionine Oxidation via Fixed-Charge Chemical Derivatization and Tandem Mass Spectrometry

7.1 Introduction

Calcineurin (protein phosphatase 2B, PP2B) is a Ca^{2+}/calmodulin-activated serine/threonine phosphatase which is found in all mammalian tissues, but is particularly abundant in the brain.[248] Calcineurin consists of two subunits, A and B, the amino acid sequences of which are depicted in Schemes 7.1 and 7.2, respectively. Calcineurin-A contains a regulatory region (amino acid residues 381-521) depicted by the underlined amino acid residues in Scheme 7.1, as well as a catalytic region. The regulatory region of calcineurin-A contains the calmodulin binding domain which is shown in Scheme 7.1 by the double underlined amino acid residues.

Calmodulin, an acidic protein with 148 amino acid residues, consists of an N-terminal and C-terminal domain, each of which can bind up to two calcium ions.[249] Binding to calcium induces a conformational change within calmodulin which subsequently exposes a hydrophobic surface. The resultant hydrophobic surface enables calmodulin to bind calcineurin, therefore resulting in an activated calcineurin-calmodulin complex. This activated calcineurin-calmodulin complex has been shown to contribute to hypertrophy in cardiac muscle cells,[250] to memory formation in neurons,[251] and to aid in the growth and differentiation of T-cells involved in immune response.[252]

MSEPKAIDPKLSTTDRVVKAVPFPPSHRLTAKEVFDNDGKPRVDILKAHLMKEGRLEESVALRIITEGASIL
RQEKNLLDIDAPVTVCGDIHGQFFDLM_{99}KLFEVGGSPANTRYLFLGDYVDRGYFSIECVLYLWALKILYPK
TLFLLRGNHECRHLTEYFTFKQECKIKYSERVYDACMDAFDCLPLAALMNQQFLCVHGGLSPEINTLDDIR
KLDRFKEPPAYGP**M$_{227}$**CDILWSDPLEDFGNEKTQEHFTHNTVRGCSYFYSYPAVCEFLQHNNLLSILRAH
EAQDAGYMYRKSQTTGFPSLITIFSAPNYLDVYNNKAAVLKYENNVMNIRQFNCSPHPYWLPNFMDVFT
WSLPFVGEKVTE**M$_{364}$**LVNVLNICSDDELGSEEDGFDGATAAARKEVIRNKIRAIGK**M$_{406}$**ARVFSVLREESE
SVLTLKGLTPTG**M$_{431}$**LPSGVLSGGKQTLQSATVEAIEADEAIKGFSPQHKITSFEEAKGLDRINERM_{483}PPR
RDAM_{490}PSDANLNSINKALTSETNGTDSNGSNSSNIQ

Scheme 7.1 Amino acid sequence of the calcineurin A subunit. The amino acid residues comprising the regulatory region are underlined. The predicted calmodulin binding domain is indicated by the double underline. Methionine residues identified both in this study and the study by Carruthers *et al.* are in bold, while the methionine residues identified exclusively in the study by Carruthers *et al.* are in italics.

MGNEASYPLEM_{11}CSHFDADEIKRLGKRFKKLDLDNSGSLSVEEFM_{44}SLPELQQNPLVQRVIDIFDTDGN
GEVDFKEFIEGVSQFSVKGDKEQKLRFAFRIYD**M$_{101}$**DKDGYISNGELFQVLKMMVGNNLKDTQLQQIVDK
TIINADKDGDGRISFEEFCAVVGGLDIHKKMVVDV

Scheme 7.2 Amino acid sequence of the calcineurin B subunit. Methionine residues identified both in this study and the study by Carruthers *et al.* are in bold, while the methionine residues identified exclusively in the study by Carruthers *et al.* are in italics.

It has been previously demonstrated that Met_{406}, the only methionine residue residing in the calmodulin binding domain of calcineurin-A, is involved in stabilizing the calcineurin-calmodulin complex.[253] Thus, it has been predicted that Met_{406} is highly solvent accessible and, as a result, potentially susceptible to oxidation by various reactive oxygen or nitrogen species. A recent study by Carruthers *et al.* showed that Met_{406} is in fact highly susceptible to oxidation following treatment of purified calcineurin with low millimolar concentrations of hydrogen peroxide *in vitro*.[202] More importantly, it was demonstrated that Met_{406} oxidation results in a decreased affinity of calcineurin for calmodulin and therefore disrupts calcineurin activation. In addition to Met_{406}, several

other methionine residues located within subunits A and B of calcineurin were found to be susceptible to oxidation, albeit to varying extents.

The results from this initial investigation by Carruthers *et al.* have suggested that a decrease in the affinity of calcineurin for calmodulin in response to oxidation may play a role in modulating calmodulin-dependent signaling as well as enable calmodulin to bind to and activate other calmodulin-dependent enzymes. Thus, the ability to accurately identify and quantify calcineurin methionine oxidation is of importance. In the study by Carruthers *et al.*, a mass spectrometry-based analysis strategy was employed to quantify calcineurin methionine oxidation. In this approach, native calcineurin, and calcineurin treated with 12 mM hydrogen peroxide for varying reaction times, was subjected to enzymatic digestion and the resultant peptide mixtures were then individually analyzed by LC-MS and MS/MS. The extent of methionine oxidation was then determined using a peptide mapping procedure whereby the extracted ion chromatographic peak areas of reduced and oxidized forms of methionine-containing peptides of interest were calculated. Using this approach, 10 of the 19 methionine residues located within subunits A and B of calcineurin were identified (Schemes 7.1 and 7.2). However, the extent of methionine oxidation could only be quantified unambiguously for five of the methionine residues due to interference from co-eluting peptides.

Despite the initial success of the peptide mapping procedure in quantifying calcineurin methionine oxidation, there are a number of limitations associated with this experimental strategy. For example, in an effort to achieve accurate quantitation, highly reproducible LC-MS analysis is required to minimize shifts in retention time and limit fluctuations in MS signal intensity. Protein quantitation may also be precluded when

peptides are present at low abundance or the MS signals of peptide ions with identical m/z values elute at the same retention time. Furthermore, the reduced and oxidized forms of a methionine-containing peptide may exhibit different ionization efficiencies and may experience differences in ionization suppression because they elute at different chromatographic retention times.

Here, as an extension of the initial study by Carruthers *et al.*, and in an effort to address the limitations associated with the peptide mapping procedure described above, a fixed-charge chemical derivatization and tandem mass spectrometry-based analysis strategy, similar to that described in Chapter 6 for the identification, characterization and quantification of methionine-containing peptides, was applied to the identification and quantification of calcineurin methionine oxidation. Using this approach, the extent of methionine oxidation was determined indirectly by measuring the decrease in phenacylbromide labeling that occurred when oxidizable or partially oxidizable methionine residues of purified calcineurin were exposed to hydrogen peroxide under non-denaturing conditions. The results obtained using the fixed-charge chemical derivatization approach were then compared to those obtained using the peptide mapping procedure described in Carruthers *et al.*

7.2 Results Obtained for the Quantitative Analysis of Calcineurin Methionine Oxidation Using Different Measurement Strategies

In an initial effort to demonstrate the utility of the fixed-charge chemical derivatization and tandem mass spectrometry-based approach for the quantitative analysis of calcineurin methionine oxidation, purified wildtype calcineurin was subjected to

oxidation in triplicate with 12 mM hydrogen peroxide (H_2O_2) at room temperature for 0, 1, 2, 4 or 10 hours under non-denaturing conditions, followed by proteolytic digestion using LysC. LysC was chosen in this study as opposed to trypsin due to the abundance of arginine and lysine residues in the calmodulin-binding domain of calcineurin-A. The resultant peptide mixtures were then individually alkylated with phenacylbromide then analyzed in triplicate by on-line capillary RP-HPLC nano-ESI-MS using a linear quadrupole ion trap mass spectrometer. The oxidation of individual methionine residues was then indirectly calculated by measuring the extent to which methionine alkylation with phenacylbromide had occurred in native versus oxidized samples. This approach is based on the fact that as the degree of methionine oxidation increases for an individual methionine residue, the extent of methionine alkylation decreases. To measure the decrease in methionine alkylation, and therefore calculate the proportion of each methionine containing peptide remaining in the reduced form, both an MS- and MS/MS-based approach were employed. In the MS-based approach, extracted ion chromatograms were used to determine the precursor ion abundance of individual fixed-charge methionine-containing peptides. In the MS/MS-based approach, the abundances of the characteristic $[M^+ + nH\text{-}CH_3SCH_2COC_6H_5]^{(n+1)+}$ neutral loss product ions resulting from selective fragmentation of the sulfonium ion derivative at the methionine side chain following CID-MS/MS analysis were determined from the resultant product ion spectra. For comparison, the native and oxidized calcineurin peptide mixtures were also subjected to LC-MS and MS/MS analysis prior to alkylation with phenacylbromide and the extent of methionine oxidation was calculated using the peptide mapping procedure described in

Carruthers *et al.* For a more detailed description of the experimental procedure employed in this study please refer to Chapter 3.

A representative example of the fixed-charge chemical derivatization MS-based quantitative analysis strategy is shown in Figure 7.1 for the methionine-containing peptide M_{406}ARVFSVLREESESVLTLK (Met_{406}) derived from subunit A of calcineurin. This peptide contains the Met_{406} residue located in the calmodulin binding domain. Extracted ion chromatograms for the $[M^{+}+3H]^{4+}$ precursor ion (m/z 579.2) of the methionine-containing phenacylsulfonium ion derivative of the Met_{406} peptide are shown in Figures 7.1A, 7.1B and 7.1C following treatment of calcineurin with 12 mM H_2O_2 for 0, 1 and 4 hours, respectively. Mass spectra obtained from the 27.0-27.3 minute region of the extracted ion chromatograms shown in Figures 7.1A, 7.1B and 7.1C are depicted in Figures 7.1D, 7.1E and 7.1F, respectively. Using this approach, the proportion of the Met_{406} peptide remaining in the reduced form was calculated as 0.58 and 0.34 following treatment of calcineurin with 12 mM H_2O_2 for 1 and 4 hours. Figures 7.2A, 7.2B and 7.2C depict the CID-MS/MS product ion spectra of the $[M^{+}+3H]^{4+}$ precursor ion (m/z 579.2) of the methionine-containing phenacylsulfonium ion derivative of the Met_{406} peptide following treatment of calcineurin with 12 mM H_2O_2 for 0, 1 and 4 hours, respectively. Using the fixed-charge chemical derivatization MS/MS-based quantitative analysis strategy, the proportion of the Met_{406} peptide remaining in the reduced form was calculated as 0.71 and 0.50 following treatment of calcineurin with 12 mM H_2O_2 for 1 and 4 hours. Using the peptide mapping procedure described in Carruthers *et al.*, the

proportion of the Met_{406} peptide remaining in the reduced form was calculated as 0.66 and 0.39 following treatment of calcineurin with 12 mM H_2O_2 for 1 and 4 hours, respectively. A plot of the proportion of the Met_{406} peptide in the reduced form as a function of the time of exposure to H_2O_2 is depicted in Figure 7.3. The data shown are the average of three replicate experiments each analyzed in triplicate where the error bars represent the standard deviation of the experimental replicates.

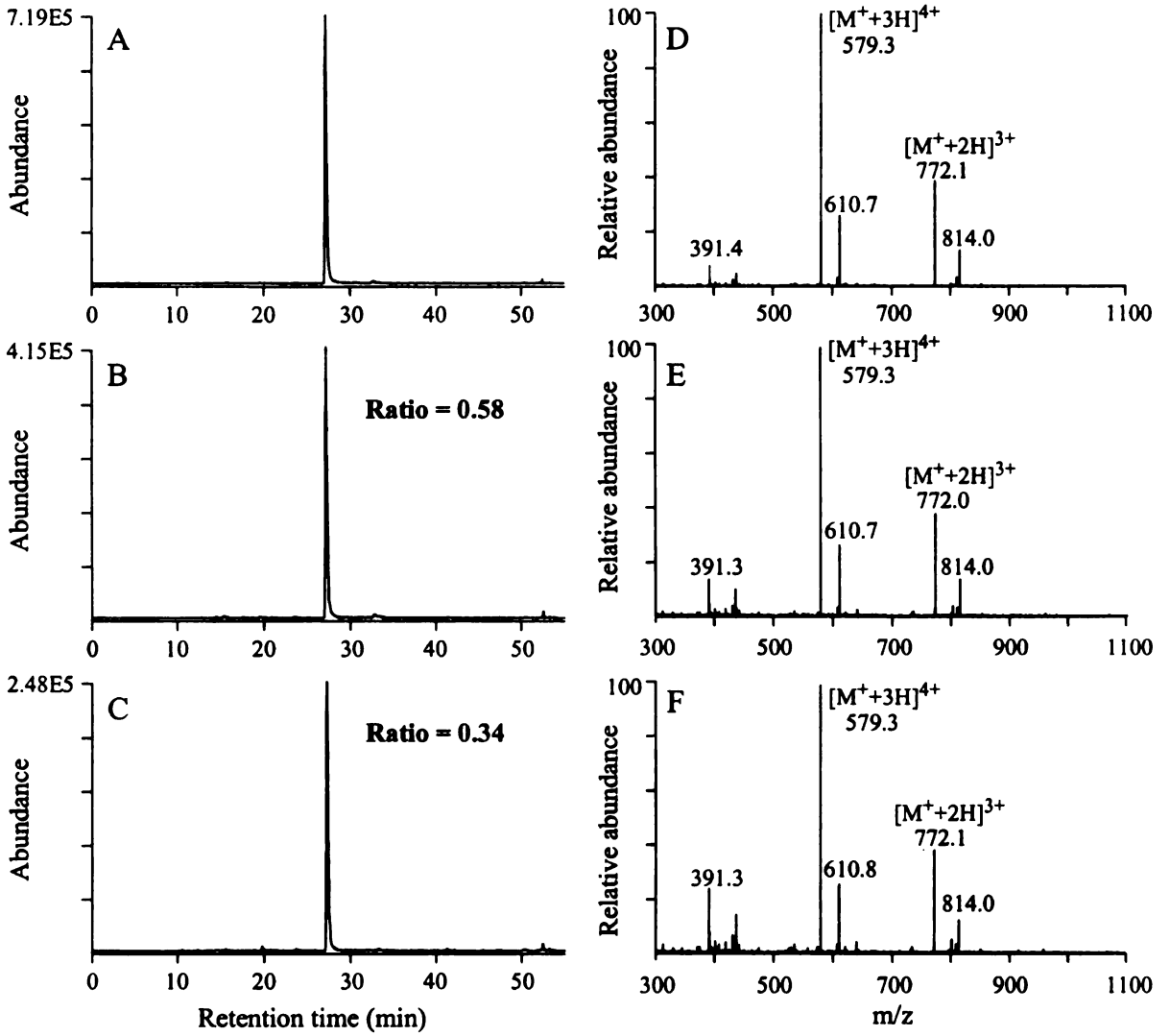

Figure 7.1 Extracted ion chromatograms of the quadruply charged ($[M^+ + 3H]^{4+}$) precursor ion (m/z 579.2) of the fixed-charge methionine-containing peptide M_{406}ARVFSVLREESESVLTLK (Met_{406}) following treatment of calcineurin with 12 mM H_2O_2 for 0 (panel A), 1 (panel B) or 4 (panel C) h, respectively. Mass spectra obtained from the 27.0-27.3 minute region of the extracted ion chromatograms in panels A-C are shown in panels D-F.

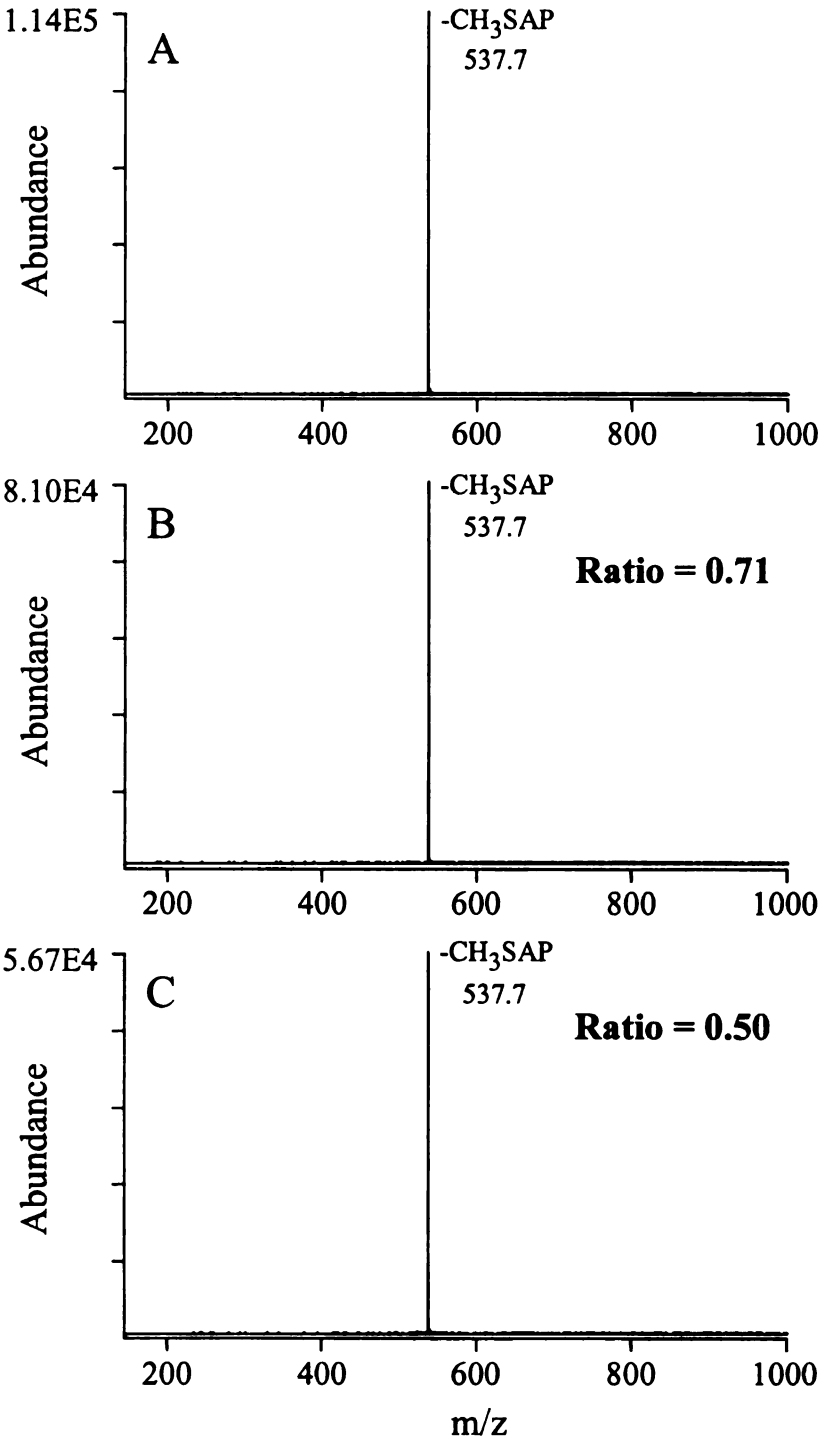

Figure 7.2 CID-MS/MS product ion spectra of the $[M^{+}+3H]^{4+}$ precursor ion of the fixed-charge methionine-containing peptide M_{406}ARVFSVLREESESVLTLK (Met_{406}) following treatment of calcineurin with 12 mM H_2O_2 for 0 (panel A), 1 (panel B) or 4 (panel C) h.

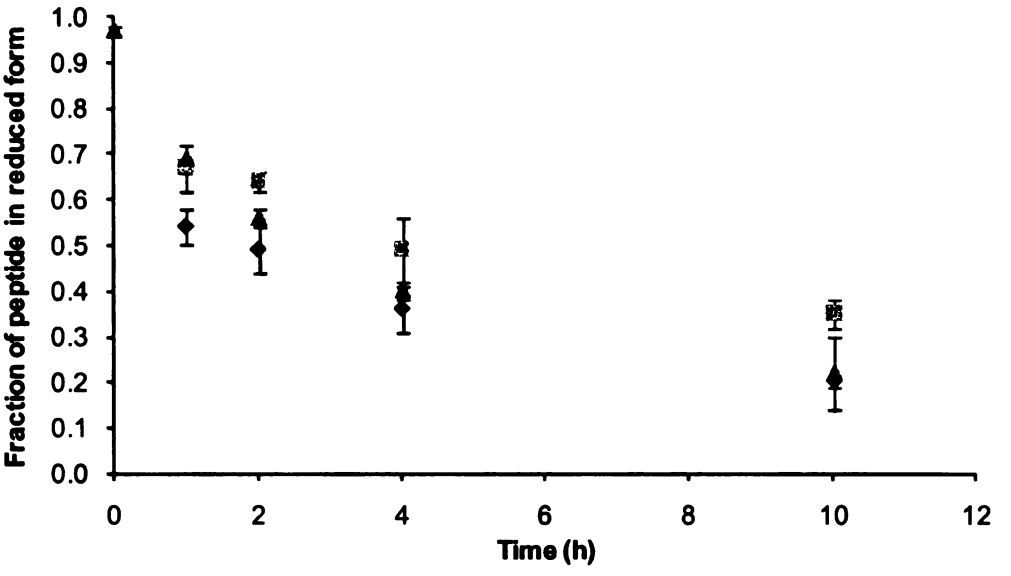

Figure 7.3 Fraction of the calcineurin-A peptide M_{406}ARVFSVLREESESVLTLK remaining in the reduced form following treatment of calcineurin with 12 mM H_2O_2 for 0, 1, 2, 4 or 10 h calculated using either the peptide mapping procedure described in Carruthers *et al.* (▲), the fixed-charge chemical derivatization-MS (♦) or the fixed-charge chemical derivatization-MS/MS (■) approach. All data are the mean of three experiments each analyzed in triplicate. Error bars are ± the standard deviation.

In addition to the Met_{406} peptide, the extent of methionine oxidation occurring within the calcineurin-A peptides GLTPTGMLPSGVLSGGK (Met_{431}), EPPAYGPMCDILWSDPLEDFGNEK (Met_{227}) and VTEMLVNVLNICSDDELGSEEDGFDGATAAARK (Met_{364}), as well as the calcineurin-B peptide LRFAFRIYDMDK (Met_{101}), was also determined (Figures 7.4-7.7).

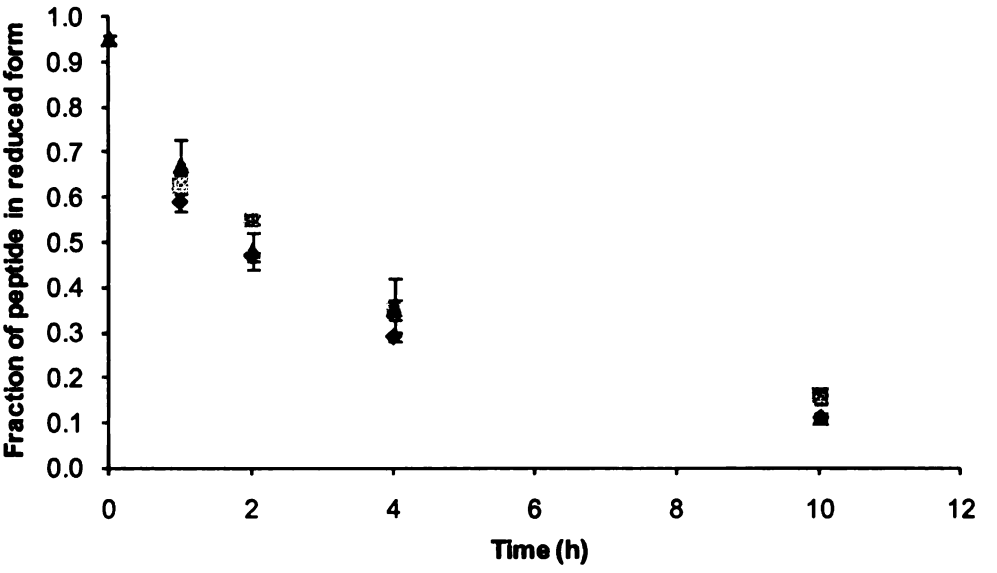

Figure 7.4 Fraction of the calcineurin-A peptide GLTPTGM$_{431}$LPSGVLSGGK remaining in the reduced form following treatment of calcineurin with 12 mM H_2O_2 for 0, 1, 2, 4 or 10 h calculated using either the peptide mapping procedure described in Carruthers *et al.* (▲), the fixed-charge chemical derivatization-MS (♦) or the fixed-charge chemical derivatization-MS/MS (■) approach. All data are the mean of three experiments each analyzed in triplicate. Error bars are ± the standard deviation.

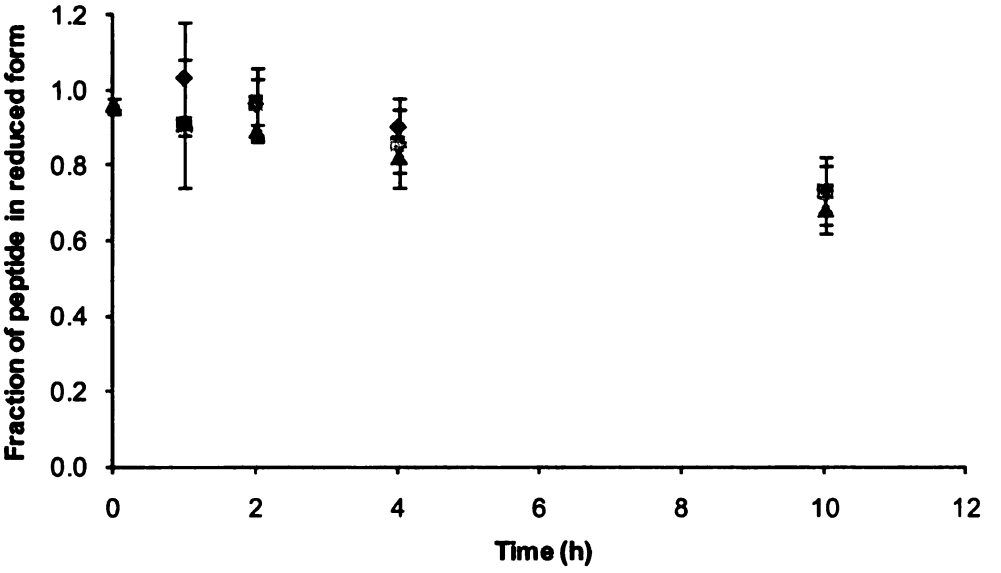

Figure 7.5 Fraction of the calcineurin-A peptide EPPAYGPM$_{227}$CDILWSD-PLEDFGNEK remaining in the reduced form following treatment of calcineurin with 12 mM H_2O_2 for 0, 1, 2, 4 or 10 h calculated using either the peptide mapping procedure described in Carruthers *et al.* (▲), the fixed-charge chemical derivatization-MS (♦) or the fixed-charge chemical derivatization-MS/MS (■) approach. All data are the mean of three experiments each analyzed in triplicate. Error bars are ± the standard deviation.

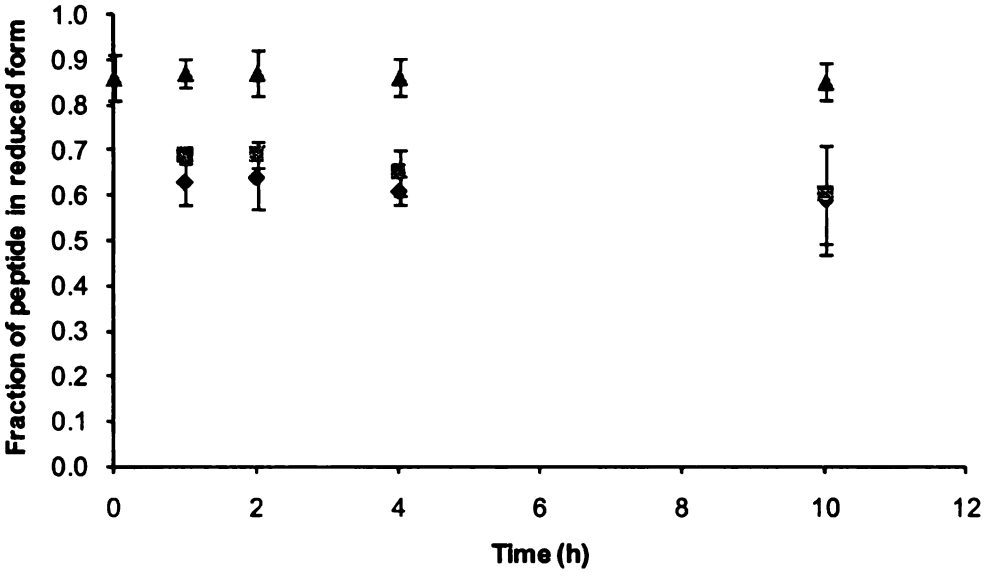

Figure 7.6 Fraction of the calcineurin-A peptide VTEM$_{364}$LVNVLNICSDDELGSE-EDGFDGATAAARK remaining in the reduced form following treatment of calcineurin with 12 mM H_2O_2 for 0, 1, 2, 4 or 10 h calculated using either the peptide mapping procedure described in Carruthers *et al.* (▲), the fixed-charge chemical derivatization-MS (♦) or fixed-charge chemical derivatization-MS/MS (■) approach. All data are the mean of three experiments each analyzed in triplicate. Error bars are ± the standard deviation.

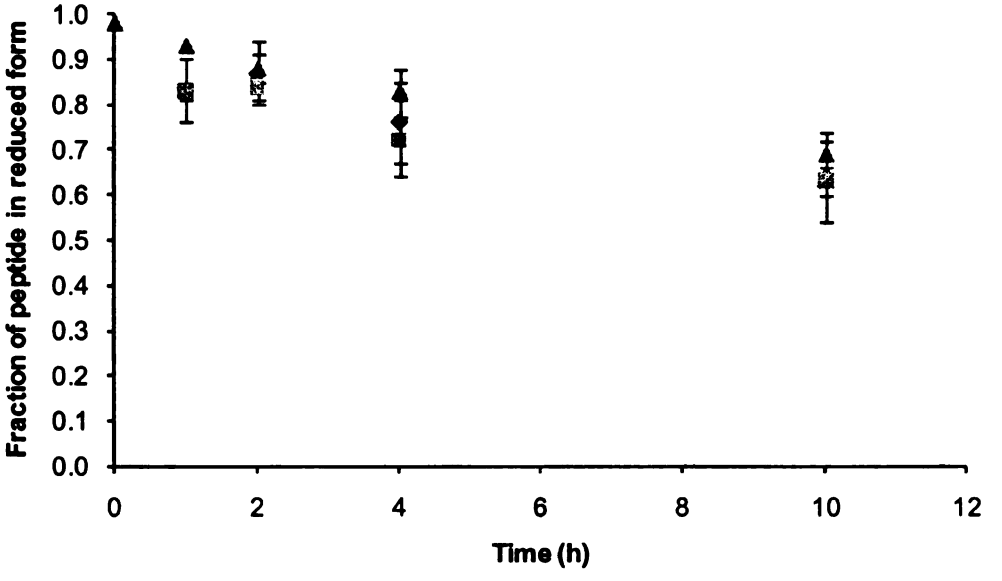

Figure 7.7 Fraction of the calcineurin-B peptide LRFAFRIYDM$_{101}$DK remaining in the reduced form following treatment of calcineurin with 12 mM H_2O_2 for 0, 1, 2, 4 or 10 h calculated using either the peptide mapping procedure described in Carruthers *et al.* (▲), the fixed-charge chemical derivatization-MS (♦) or the fixed-charge chemical derivatization-MS/MS (■) approach. All data are the mean of three experiments each analyzed in triplicate. Error bars are ± the standard deviation.

7.3 Comparison of the Results Obtained for the Quantitative Analysis of Methionine Oxidation Using Different Measurement Strategies

In general, there was a very good correlation between the results obtained using the abundances of the fixed-charge methionine-containing precursor ions (MS-based quantitation) and the abundances of the characteristic neutral loss product ions (MS/MS-based quantitation) to calculate methionine oxidation as demonstrated in Figure 7.4 for the Met_{431} peptide derived from subunit A of calcineurin. However, it is important to note that a discrepancy was observed between the results obtained using the fixed-charge MS- and MS/MS-based approaches for the Met_{406} peptide (Figure 7.3). One potential explanation for this discrepancy could be ionization suppression resulting from slight changes in the chromatographic retention time from run to run, therefore precluding accurate quantitative analysis by MS. Furthermore, the isolation width used to isolate the fixed-charge methionine containing precursor ion for fragmentation could also have played a role in the observed differences. The isolation width of 2.0 used in this study may have been too narrow to account for slight changes in the m/z value of the precursor ion during isolation and subsequent fragmentation. Although likely not an issue in this particular study, where a relatively simple peptide mixture was subjected to analysis, the isolation width may have been too wide therefore resulting in interference from co-eluting peptides with nearly identical m/z values.

There was also a very good correlation between the results obtained using either of the fixed-charge chemical derivatization approaches and those obtained using the peptide mapping procedure described in Carruthers *et al.* with the exception of the Met_{364} calcineurin-A peptide (Figure 7.6). A possible explanation for the observed differences

could be that the reduced and oxidized forms of the Met_{364} peptide, the abundances of which were used to calculate the extent of methionine oxidation using the peptide mapping procedure, may exhibit different ionization efficiencies. Also, the reduced and oxidized forms of the Met_{364} peptide may experience differences in ionization suppression given that they elute at different chromatographic retention times.

7.4 Conclusions and Future Directions

The results from this initial investigation indicate that the fixed-charge chemical derivatization and tandem mass spectrometry-based approach holds promise for the quantitative analysis of calcineurin methionine oxidation. In addition, it also addresses several of the limitations associated with the peptide mapping procedure described in Carruthers *et al.* It is important to note that despite the initial success of this approach, several of the methionine-containing peptides identified in the study by Carruthers *et al.* were not identified here. However, this is likely attributed to differences in the chromatographic separation used in each individual study as opposed to the experimental approach.

As an extension of this initial investigation, it would be beneficial to subject the native and oxidized peptide mixtures to alkylation with $^{12}C_6$- and $^{13}C_6$-phenacylbromide, respectively so that these samples could be combined prior to LC-MS and MS/MS analysis. Analyzing the native and oxidized peptide mixtures in a single run would eliminate differences caused by sample preparation, shifts in retention time and fluctuations in MS signal intensity. It would also be beneficial to analyze native and oxidized calcineurin using the automated neutral loss MS/MS and data dependent energy-

resolved pseudo MS^3 analysis method as described in Chapter 6 in an effort to increase protein sequence coverage and to identify/quantify additional methionine residues, particularly those present at low abundance.

APPENDIX

Cartesian Coordinates of Optimized Precursor, Transition State and Product Ion Structures

Chapter 5

B3LYP/6-31 + G(d,p) Optimized Structures

A

C	3.336	-2.137	1.136
C	2.114	-1.250	0.990
N	1.076	-1.771	0.278
O	2.067	-0.115	1.473
C	-0.204	-1.096	0.175
C	-1.210	-2.150	-0.364
C	-0.094	0.170	-0.712
S	-1.149	1.546	-0.074
O	-0.840	-3.314	-0.561
N	-2.463	-1.719	-0.579
O	-2.609	1.090	-0.216
C	-0.845	2.709	-1.453
C	-3.495	-2.622	-1.068
H	3.509	-2.318	2.201
H	3.241	-3.096	0.620
H	4.208	-1.603	0.748
H	1.052	-2.745	-0.013
H	-0.526	-0.794	1.181
H	0.929	0.551	-0.660
H	-0.374	-0.025	-1.752
H	-2.691	-0.731	-0.422
H	-1.458	3.591	-1.256
H	-1.149	2.246	-2.395
H	0.213	2.985	-1.467
H	-3.211	-3.058	-2.032
H	-4.419	-2.056	-1.186
H	-3.661	-3.443	-0.364

B

C	2.437	-3.229	-1.146
C	1.369	-2.153	-1.077
N	1.415	-1.328	0.023
O	0.508	-2.026	-1.943
C	0.612	-0.108	0.138
C	-0.889	-0.343	0.402
C	0.827	0.880	-1.022
S	1.710	2.414	-0.417
O	-1.688	0.582	0.251
N	-1.233	-1.552	0.903
O	2.493	1.974	0.822
C	0.247	3.334	0.192
C	-2.616	-1.904	1.188
H	3.137	-2.976	-1.950
H	3.000	-3.348	-0.215
H	1.965	-4.178	-1.409
H	2.236	-1.372	0.612
H	0.995	0.375	1.050
H	1.477	0.455	-1.786
H	-0.114	1.189	-1.480
H	-0.533	-2.279	0.890
H	0.637	4.178	0.764
H	-0.379	2.691	0.813
H	-0.325	3.693	-0.669
H	-3.137	-1.020	1.560
H	-2.639	-2.688	1.950
H	-3.137	-2.259	0.290

TS1

C	2.571	-2.471	-2.213
C	1.402	-1.620	-1.741
N	1.576	-0.999	-0.522
O	0.381	-1.498	-2.408
C	0.637	-0.066	0.061
C	-0.399	-0.590	1.012
C	0.219	1.039	-0.746
S	1.217	2.752	0.267
O	-1.248	0.166	1.504
N	-0.314	-1.907	1.349
O	1.970	1.747	1.256
C	-0.220	3.320	1.233
C	-1.291	-2.543	2.217

H	3.011	-2.001	-3.099
H	3.354	-2.603	-1.461
H	2.192	-3.450	-2.517
H	2.481	-1.102	-0.080
H	0.640	1.131	-1.741
H	-0.813	1.363	-0.653
H	0.299	-2.486	0.794
H	1.465	0.738	0.952
H	0.139	3.918	2.073
H	-0.786	2.449	1.573
H	-0.827	3.943	0.568
H	-1.610	-1.824	2.972
H	-0.834	-3.407	2.707
H	-2.179	-2.875	1.663

C

C	3.753	-3.320	-0.664
C	3.100	-2.023	-1.111
N	1.784	-1.866	-0.707
O	3.701	-1.193	-1.777
C	0.967	-0.717	-0.877
C	-0.514	-0.983	-0.847
C	1.418	0.525	-1.103
O	-1.346	-0.123	-0.540
N	-0.899	-2.254	-1.164
C	-2.311	-2.605	-1.269
H	4.530	-3.085	0.070
H	3.058	-4.040	-0.220
H	4.244	-3.777	-1.526
H	1.425	-2.570	-0.076
H	2.476	0.737	-1.172
H	0.709	1.332	-1.244
H	-0.227	-2.837	-1.646
H	-2.838	-2.240	-0.386
H	-2.400	-3.691	-1.323
H	-2.777	-2.155	-2.153
S	-2.652	3.341	-0.898
O	-1.250	2.640	-0.266
C	-3.641	3.541	0.614
H	-1.343	1.664	-0.312
H	-3.099	4.141	1.350
H	-3.920	2.575	1.046
H	-4.551	4.076	0.317

D

C	0.848	0.676	-0.438
C	0.665	-0.746	-1.002
S	-0.701	1.498	0.179
C	0.938	-1.867	0.011
O	-1.558	0.418	0.846
C	-1.488	1.825	-1.442
O	1.872	-2.650	-0.152
N	0.089	-1.918	1.066
H	1.527	0.682	0.419
H	1.257	1.364	-1.187
H	-0.342	-0.878	-1.415
H	1.377	-0.901	-1.815
H	-1.591	0.895	-2.007
H	-2.477	2.232	-1.224
H	-0.894	2.560	-1.993
H	-0.664	-1.239	1.173
H	0.240	-2.635	1.761

E

C	0.672	0.648	-1.237
C	1.061	-0.678	-0.596
S	0.664	2.063	-0.022
C	-0.137	-1.481	-0.088
O	1.778	1.772	0.979
C	-0.915	1.711	0.842
O	-1.262	-1.371	-0.567
N	0.142	-2.366	0.912
H	1.419	0.955	-1.975
H	-0.309	0.600	-1.718
H	1.561	-1.306	-1.345
H	1.789	-0.495	0.206
H	-0.862	0.746	1.346
H	-1.039	2.509	1.578
H	-1.741	1.725	0.126
H	1.044	-2.402	1.362
H	-0.604	-2.947	1.265

TS2

C	0.337	0.145	-1.131
C	1.043	-0.534	-0.089
S	0.600	2.269	-0.541
C	0.222	-1.143	0.987
O	1.627	1.846	0.600
C	-0.986	2.473	0.337
O	-0.920	-0.755	1.261
N	0.807	-2.161	1.694
H	0.783	0.178	-2.121
H	-0.750	0.098	-1.124
H	1.964	-1.044	-0.369
H	1.553	0.661	0.539
H	-1.225	1.552	0.876
H	-0.899	3.324	1.015
H	-1.748	2.682	-0.422
H	1.761	-2.444	1.538
H	0.316	-2.523	2.497

F

C	1.539	0.848	-1.408
C	2.004	0.015	-0.469
C	1.162	-1.111	0.051
O	-0.012	-1.271	-0.273
N	1.799	-1.950	0.921
H	2.144	1.661	-1.794
H	0.535	0.722	-1.804
H	3.011	0.129	-0.073
H	2.758	-1.823	1.199
H	1.277	-2.723	1.310
S	-1.586	2.548	0.353
O	-0.166	2.328	1.264
C	-2.506	1.039	0.784
H	0.455	1.826	0.710
H	-1.977	0.144	0.446
H	-2.693	0.999	1.860
H	-3.464	1.115	0.258

G

C	1.352	0.178	-0.127
C	0.175	-0.044	-1.091
S	1.191	1.813	0.740
C	-1.164	-0.220	-0.407
O	1.108	2.865	-0.358
C	2.901	1.858	1.401
C	-2.067	0.844	-0.280
C	-1.551	-1.451	0.137
C	-2.788	-1.561	0.773
C	-3.282	0.631	0.376
N	-3.653	-0.544	0.901
H	1.400	-0.595	0.649
H	2.295	0.200	-0.682
H	0.403	-0.938	-1.684
H	0.137	0.802	-1.784
H	3.611	1.833	0.569
H	3.004	2.798	1.946
H	3.056	1.015	2.080
H	-1.826	1.824	-0.679
H	-0.904	-2.322	0.061
H	-3.103	-2.513	1.197
H	-3.993	1.448	0.484

TS3

C	1.406	0.097	-0.810
C	0.054	0.551	-0.825
S	2.350	1.671	0.583
C	-1.023	-0.211	-0.137
O	0.937	2.371	0.725
C	3.207	2.638	-0.708
C	-0.809	-0.975	1.023
C	-2.342	-0.168	-0.616
C	-3.344	-0.873	0.050
C	-1.880	-1.645	1.613
N	-3.138	-1.611	1.150
H	1.671	-0.801	-0.259
H	2.032	0.279	-1.678
H	-0.265	1.031	-1.751
H	0.245	1.647	-0.014
H	2.568	2.737	-1.588
H	3.451	3.625	-0.310
H	4.129	2.106	-0.967

H	0.175	-1.048	1.477
H	-2.586	0.407	-1.506
H	-4.367	-0.845	-0.322
H	-1.718	-2.240	2.510

H

C	2.264	1.383	-1.425
C	2.537	0.294	-0.691
C	1.562	-0.658	-0.130
C	0.169	-0.540	-0.300
C	2.011	-1.753	0.623
C	1.088	-2.653	1.157
C	-0.666	-1.495	0.273
N	-0.238	-2.544	0.994
H	1.253	1.681	-1.686
H	3.068	2.015	-1.786
H	3.578	0.061	-0.469
H	-0.261	0.279	-0.868
H	3.074	-1.905	0.794
H	1.430	-3.505	1.741
H	-1.744	-1.417	0.147
S	-1.597	3.704	-1.439
O	-1.184	2.176	-2.078
C	-2.817	3.219	-0.184
H	-1.731	2.022	-2.863
H	-3.716	2.791	-0.633
H	-2.376	2.521	0.533
H	-3.085	4.144	0.339

I

C	1.560	0.582	1.006
C	1.121	-0.547	0.040
S	1.743	2.239	0.162
C	-0.358	-0.846	0.063
O	0.689	2.246	-0.944
C	3.346	1.943	-0.666
C	-1.297	0.096	-0.405
C	-0.839	-2.083	0.534
C	-2.195	-2.352	0.532
C	-2.643	-0.212	-0.396
N	-3.055	-1.417	0.069
H	0.829	0.748	1.803

H	2.519	0.351	1.480
H	1.675	-1.459	0.281
H	1.381	-0.270	-0.990
H	3.299	1.044	-1.284
H	3.520	2.813	-1.302
H	4.134	1.871	0.087
H	-0.948	1.059	-0.774
H	-0.158	-2.843	0.901
H	-2.623	-3.284	0.879
H	-3.414	0.464	-0.748
H	-4.050	-1.626	0.068

TS4

C	1.928	-0.356	-0.452
C	0.449	-0.244	-0.480
S	2.552	1.397	0.245
C	-0.392	-1.035	0.380
O	1.110	1.919	0.628
C	2.951	2.228	-1.326
C	0.025	-1.567	1.636
C	-1.756	-1.268	0.029
C	-2.594	-1.965	0.858
C	-0.848	-2.261	2.434
N	-2.134	-2.452	2.043
H	2.348	-1.083	0.242
H	2.402	-0.463	-1.428
H	0.026	-0.058	-1.466
H	0.432	1.024	0.142
H	2.134	2.100	-2.039
H	3.101	3.286	-1.107
H	3.880	1.794	-1.708
H	1.038	-1.429	1.995
H	-2.146	-0.895	-0.911
H	-3.632	-2.165	0.621
H	-0.566	-2.676	3.394
H	-2.766	-2.967	2.647

J

C	0.829	-1.344	-1.483
C	-0.264	-2.050	-1.143
C	-1.504	-1.486	-0.617
C	-1.698	-0.100	-0.389

C	-2.581	-2.353	-0.313
C	-3.764	-1.856	0.185
C	-2.898	0.352	0.108
N	-3.899	-0.523	0.383
H	0.888	-0.263	-1.393
H	1.708	-1.851	-1.866
H	-0.254	-3.131	-1.258
H	-0.921	0.630	-0.597
H	-2.487	-3.422	-0.467
H	-4.618	-2.477	0.432
H	-3.103	1.398	0.300
H	-4.777	-0.167	0.749
S	1.913	2.302	0.114
O	0.539	2.205	-0.913
C	1.439	3.674	1.201
H	0.692	2.784	-1.676
H	1.356	4.614	0.651
H	0.514	3.454	1.739
H	2.257	3.761	1.925

REFERENCES

REFERENCES

1. Gygi, S. P.; Rochon, Y.; Franza, B. R.; Aebersold, R. Correlation between Protein and mRNA Abundance in Yeast. *Mol. Cell. Biol.* **1999,** *19,* 1720-1730.

2. Aebersold, R.; Mann, M. Mass Spectrometry-based Proteomics. *Nature* **2003,** *422,* 198-207.

3. Simpson, R. J.; Connelly, L. M.; Eddes, J. S.; Pereira, J. J.; Moritz, R. L.; Reid, G. E. Proteomic Analysis of the Human Colon Carcinoma Cell Line (LIM 1215): Development of a Membrane Protein Database. *Electrophoresis* **2000,** *21,* 1707-1732.

4. Reid, G. E.; Rasmussen, R. K.; Dorow, D. S.; Simpson, R. J. Capillary Column Chromatrography Improves Sample Preparation for Mass Spectrometric Analysis: Complete Characterization of Human α-Enolase from Two-Dimensional Gels Following In Situ Proteolytic Digestion. *Electrophoresis* **1998,** *19,* 946-955.

5. Zugaro, L. M.; Reid, G. E.; Ji, H.; Eddes, J. S.; Murphy, A. C.; Burgess, A. W.; Simpson, R. J. Characterization of Rat Brain Stathmin Isoforms by Two-Dimensional Gel Electrophoresis-Matrix Assisted Laser Desorption/Ionization and Electrospray Ionizationion Trap Mass Spectrometry. *Electrophoresis* **1998,** *19,* 867-876.

6. Rasmussen, R. K.; Ji, H.; Eddes, J. S.; Moritz, R. L.; Reid, G. E.; Simpson, R. J.; Dorow, D. S. Two-Dimensional Electrophoretic Analysis of Mixed Lineage Kinase 2 N-terminal Domain Binding Proteins. *Electrophoresis* **1998,** *19,* 809-817.

7. Hunt, D. F.; Yates, J. R., III; Shabanowitz, J.; Winston, S.; Hauer, C. R. Protein Sequencing by Tandem Mass Spectrometry. *Proc. Natl. Acad. Sci. U.S.A.* **1986,** *83,* 6233-6237.

8. Steen, H.; Mann, M. The ABC's (and XYZ's) of Peptide Sequencing. *Nat. Rev. Mol. Cell Biol.* **2004,** *5,* 699-711.

9. Eng, J. K.; McCormack, A. L.; Yates, J. R. An Approach to Correlate Tandem Mass Spectral Data of Peptides with Amino Acid Sequences in a Protein Database. *J. Am. Soc. Mass Spectrom.* **1994,** *5,* 976-989.

10. Perkins, D. N.; Pappin, D. J. C.; Creasy, D. M.; Cottrell, J. S. Probability-Based Protein Identification by Searching Sequence Databases using Mass Spectrometry Data. *Electrophoresis* **1999,** *20,* 3551-3567.

11. MacCoss, M. J.; Wu, C. C.; Yates, J. R. Probability-Based Validation of Protein Identifications Using a Modified SEQUEST Algorithm. *Anal. Chem.* **2002,** *74,* 5593-5599.

12. Creasy, D. M.; Cottrell, J. S. Error Tolerant Searching of Uninterpreted Tandem Mass Spectrometry Data. *Proteomics* **2002,** *2,* 1426-1434.

13. Washburn, M. P.; Walters, D.; Yates, J. R. Large-Scale Analysis of the Yeast Proteome by Multidimensional Protein Identification Technology. *Nat. Biotechnol.* **2001,** *19,* 242-247.

14. Spahr, C. S.; Susin, S. A.; Bures, E. J.; Robinson, J. H.; Davis, M. T.; McGinley, M. D.; Kroemer, G.; Patterson, S. D. Simplification of Complex Peptide Mixtures for Proteomic Analysis: Reversible Biotinylation of Cysteinyl Peptides. *Electrophoresis* **2000,** *21,* 1635-1650.

15. Spahr, C. S.; Davis, M. T.; McGinley, M. D.; Robinson, J. H.; Bures, E. J.; Beierle, J.; Mort, J.; Courchesne, P. L.; Chen, K.; Wahl, R. C.; Yu, W.; Luethy, R.; Patterson, S. D. Towards Defining the Urinary Proteome using Liquid Chromatography-Tandem Mass Spectrometry I.Profiling an Unfractionated Tryptic Digest. *Proteomics* **2001,** *1,* 93-107.

16. Davis, M. T.; Spahr, C. S.; McGinley, M. D.; Robinson, J. H.; Bures, E. J.; Beierle, J.; Mort, J.; Yu, W.; Luethy, R.; Patterson, S. D. Towards Defining the Urinary Proteome using Liquid Chromatography-Tandem Mass Spectrometry II.Limitations of Complex Mixture Analyses. *Proteomics* **2001,** *1,* 108-117.

17. Wang, N.; Li, L. Exploring the Precursor Ion Exclusion Feature of Liquid Chromatography-Electrospray Ionization Quadrupole Time-of-Flight Mass Spectrometry for Improving Protein Identification in Shotgun Proteome Analysis. *Anal. Chem.* **2008,** *80,* 4696-4710.

18. Ahmed, N.; Barker, G.; Oliva, K.; Garfin, D.; Talmadge, K.; Georgiou, H.; Quinn, M.; Rice, G. An Approach to Remove Albumin for the Proteomic Analysis of Low Abundance Biomarkers in Human Serum. *Proteomics* **2003,** *3,* 1980-1987.

19. Maccarrone, G.; Mifay, D.; Birg, I.; Rosenhagen, M.; Holsboer, F.; Grimm, R.; Bailey, J.; Zolotarjova, N.; Turck, C. W. Mining the Human Cerebrospinal Fluid Proteome by Immunodepletion and Shotgun Mass Spectrometry. *Electrophoresis* **2004,** *25,* 2402-2412.

20. Björhall, K.; Miliotis, T.; Davidsson, P. Comparison of Different Depletion Strategies for Improved Resolution in Proteomic Analysis of Human Serum Samples. *Proteomics* **2005,** *5,* 307-317.

21. Thulasiraman, V.; Lin, S.; Gheorghiu, L.; Lathrop, J.; Lomas, L.; Hammond, D.; Boschetti, E. Reduction of the Concentration of Proteins in Biological Fluids Using a Library of Combinatorial Ligands. *Electrophoresis* **2005,** *26,* 3561-3571.

22. Guerrier, L.; Claverol, S.; Fortis, F.; Rinalducci, S.; Timperio, A. M.; Antonioli, P.; Jandrot-Perrus, M.; Boschetti, E.; Righetti, P. G. Exploring the Platelet Proteome via Combinatorial, Hexapeptide Ligand Libraries. *J. Proteome Res.* **2007,** *6,* 4290-4303.

23. Shores, K. S.; Udugamasooriya, D. G.; Kodadek, T.; Knapp, D. R. Use of Peptide Analogue Diversity Library Beads for Increased Depth of Proteomic Analysis: Application to Cerebrospinal Fluid. *J. Proteome Res.* **2008,** *7,* 1922-1931.

24. Ndassa, Y. M.; Orsi, C.; Marto, J. A.; Chen, S.; Ross, M. M. Improved Immobilized Metal Affinity Chromatography for Large-Scale Phosphoproteomics Applications. *J. Proteome Res.* **2006,** *5,* 2789-2799.

25. Lee, J.; Xu, Y.; Chen, Y.; Sprung, R.; Kim, S. C.; Xie, S.; Zhao, Y. Mitochondrial Phosphoproteome Revealed by an Improved IMAC Method and MS/MS/MS. *Mol. Cell. Proteomics* **2007,** *6,* 669-676.

26. Ren, D.; Penner, N. A.; Slentz, B. E.; Mirzaei, H.; Regnier, F. Evaluating Immobilized Metal Affinity Chromatography for the Selection of Histidine-Containing Peptides in Comparative Proteomics. *J. Proteome Res.* **2003,** *2,* 321-329.

27. Raftery, M. J. Enrichment by Organomercurial Agarose and Identification of Cys-Containing Peptides from Yeast Cell Lysates. *Anal. Chem.* **2008,** *80,* 3334-3341.

28. Olsen, J. V.; Blagoev, B.; Gnad, F.; Macek, B.; Kumar, C.; Mortensen, P.; Mann, M. Global, In Vivo, and Site-Specific Phosphorylation Dynamics in Signaling Networks. *Cell* **2006,** *127,* 635-648.

29. Kweon, H. K.; Hakansson, K. Selective Zirconium Dioxide-Based Enrichment of Phosphorylated Peptides for Mass Spectrometric Analysis. *Anal. Chem.* **2006,** *78,* 1743-1749.

30. Li, Y.; Xu, X.; Qi, D.; Deng, C.; Yang, P.; Zhang, X. Novel Fe_3O_4@TiO_2 Core-Shell Microspheres for Selective Enrichment of Phosphopeptides in Phosphoproteome Analysis. *J. Proteome Res.* **2008,** *7,* 2526-2538.

31. Qiu, R.; Regnier, F. E. Use of Multidimensional Lectin Affinity Chromatography in Differential Glycoproteomics. *Anal. Chem.* **2005,** *77,* 2802-2809.

32. Gygi, S. P.; Rist, B.; Gerber, S. A.; Turecek, F.; Gelb, M. H.; Aebersold, R. Quantitative Analysis of Complex Protein Mixtures using Isotope-Coded Affinity Tags. *Nat Biotech* **1999,** *17,* 994-999.

33. Hansen, K. C.; Schmitt-Ulms, G.; Chalkley, R. J.; Hirsch, J.; Baldwin, M. A.; Burlingame, A. L. Mass Spectrometric Analysis of Protein Mixtures at Low Levels Using Cleavable ^{13}C-Isotope-coded Affinity Tag and Multidimensional Chromatography. *Mol. Cell. Proteomics* **2003,** *2,* 299-314.

34. Bernhard, O. K.; Kapp, E. A.; Simpson, R. J. Enhanced Analysis of the Mouse Plasma Proteome Using Cysteine-Containing Tryptic Glycopeptides. *J. Proteome Res.* **2007,** *6,* 987-995.

35. Qian, W.-J.; Goshe, M. B.; Camp, D. G.; Yu, L.-R.; Tang, K.; Smith, R. D. Phosphoprotein Isotope-Coded Solid-Phase Tag Approach for Enrichment and Quantitative Analysis of Phosphopeptides from Complex Mixtures. *Anal. Chem.* **2003,** *75,* 5441-5450.

36. Jalili, P. R.; Ball, H. L. Novel Reversible Biotinylated Probe for the Selective Enrichment of Phosphorylated Peptides from Complex Mixtures. *J. Am. Soc. Mass Spectrom.* **2008,** *19,* 741-750.

37. Jalili, P. R.; Sharma, D.; Ball, H. L. Enhancement of Ionization Efficiency and Selective Enrichment of Phosphorylated Peptides from Complex Protein Mixtures Using a Reversible Poly-Histidine Tag. *J. Am. Soc. Mass Spectrom.* **2007,** *18,* 1007-1017.

38. Ren, D.; Julka, S.; Inerowicz, H. D.; Regnier, F. E. Enrichment of Cysteine-Containing Peptides from Tryptic Digests Using a Quaternary Amine Tag. *Anal. Chem.* **2004,** *76,* 4522-4530.

39. Brittain, S. M.; Ficarro, S. B.; Brock, A.; Peters, E. C. Enrichment and Analysis of Peptide Subsets using Fluorous Affinity Tags and Mass Spectrometry. *Nat. Biotechnol.* **2005,** *23,* 463-468.

40. Weinberger, S. R.; Viner, R. I.; Ho, P. Tagless Extraction-Retentate Chromatography: A New Global Protein Digestion Strategy for Monitoring Differential Protein Expression. *Electrophoresis* **2002,** *23,* 3182-3192.

41. Zhou, H.; Ranish, J. A.; Watts, J. D.; Aebersold, R. Quantitative Proteome Analysis by Solid-Phase Isotope Tagging and Mass Spectrometry. *Nat. Biotechnol.* **2002,** *20,* 512-515.

42. Qiu, Y.; Sousa, E. A.; Hewick, R. M.; Wang, J. H. Acid-Labile Isotope-Coded Extractants: A Class of Reagents for Quantitative Mass Spectrometric Analysis of Complex Protein Mixtures. *Anal. Chem.* **2002,** *74,* 4969-4979.

43. Shi, Y.; Xiang, R.; Horvath, C.; Wilkins, J. A. Quantitative Analysis of Membrane Proteins from Breast Cancer Cell Lines BT474 and MCF7 Using Multistep Solid Phase Mass Tagging and 2D LC/MS. *J. Proteome Res.* **2005,** *4,* 1427-1433.

44. Wang, H.; Qian, W.-J.; Chin, M. H.; Petyuk, V. A.; Barry, R. C.; Liu, T.; Gritsenko, M. A.; Mottaz, H. M.; Moore, R. J.; Camp, D. G.; Khan, A. H.; Smith, D. J.; Smith, R. D. Characterization of the Mouse Brain Proteome Using Global Proteomic Analysis Complemented with Cysteinyl-Peptide Enrichment. *J. Proteome Res.* **2006,** *5,* 361-369.

45. Lansdell, T. A.; Tepe, J. J. Isolation of Phosphopeptides using Solid Phase Enrichment. *Tetrahedron Lett.* **2004,** *45,* 91-93.

46. Shen, M.; Guo, L.; Wallace, A.; Fitzner, J.; Eisenman, J.; Jacobson, E.; Johnson, R. S. Isolation and Isotope Labeling of Cysteine- and Methionine-Containing Tryptic Peptides: Application to the Study of Cell Surface Proteolysis. *Mol. Cell. Proteomics* **2003,** *2,* 315-324.

47. Gevaert, K.; Ghesquière, B.; Staes, A.; Martens, L.; Van Damme, J.; Thomas, G. R.; Vandekerckhove, J. Reversible Labeling of Cysteine-Containing Peptides Allows their Specific Chromatographic Isolation for Non-Gel Proteome Studies. *Proteomics* **2004,** *4,* 897-908.

48. Gevaert, K.; Pinxteren, J.; Demol, H.; Hugelier, K.; Staes, A.; Damme, J. V.; Martens, L.; Vandekerckhove, J. Four Stage Liquid Chromatographic Selection of Methionyl Peptides for Peptide-Centric Proteome Analysis: The Proteome of Human Multipotent Adult Progenitor Cells. *J. Proteome Res.* **2006,** *5,* 1415-1428.

49. Unlu, M.; Morgan, M. E.; Minden, J. S. Differential Gel Electrophoresis: A Single Gel Method for Detecting Changes in Protein Extracts. *Electrophoresis* **1997,** *18,* 2071-2077.

50. Tonge, R.; Shaw, J.; Middleton, B.; Rowlinson, R.; Rayner, S.; Young, J.; Pognan, F.; Hawkins, E.; Currie, I.; Davison, M. Validation and Development of Fluorescence Two-Dimensional Differential Gel Electrophoresis Proteomics Technology. *Proteomics* **2001,** *1,* 377-396.

51. Zhou, G.; Li, H.; DeCamp, D.; Chen, S.; Shu, H.; Gong, Y.; Flaig, M.; Gillespie, J. W.; Hu, N.; Taylor, P. R.; Emmert-Buck, M. R.; Liotta, L. A.; Petricoin, E. F., III; Zhao, Y. 2D Differential In-gel Electrophoresis for the Identification of Esophageal Scans Cell Cancer-specific Protein Markers. *Mol. Cell. Proteomics* **2002,** *1,* 117-123.

52. Chelius, D.; Zhang, T.; Wang, G.; Shen, R.-F. Global Protein Identification and Quantification Technology Using Two-Dimensional Liquid Chromatography Nanospray Mass Spectrometry. *Anal. Chem.* **2003,** *75,* 6658-6665.

53. Colinge, J.; Chiappe, D.; Lagache, S.; Moniatte, M.; Bougueleret, L. Differential Proteomics via Probabilistic Peptide Identification Scores. *Anal. Chem.* **2005,** *77,* 596-606.

54. Liu, H.; Sadygov, R. G.; Yates, J. R. A Model for Random Sampling and Estimation of Relative Protein Abundance in Shotgun Proteomics. *Anal. Chem.* **2004,** *76,* 4193-4201.

55. Old, W. M.; Meyer-Arendt, K.; Aveline-Wolf, L.; Pierce, K. G.; Mendoza, A.; Sevinsky, J. R.; Resing, K. A.; Ahn, N. G. Comparison of Label-free Methods for Quantifying Human Proteins by Shotgun Proteomics. *Mol. Cell. Proteomics* **2005,** *4,* 1487-1502.

56. Oda, Y.; Huang, K.; Cross, F. R.; Cowburn, D.; Chait, B. T. Accurate Quantitation of Protein Expression and Site-Specific Phosphorylation. *Proc. Natl. Acad. Sci. U. S. A.* **1999,** *96,* 6591-6596.

57. Ong, S.-E.; Blagoev, B.; Kratchmarova, I.; Kristensen, D. B.; Steen, H.; Pandey, A.; Mann, M. Stable Isotope Labeling by Amino Acids in Cell Culture, SILAC, as a Simple and Accurate Approach to Expression Proteomics. *Mol. Cell. Proteomics* **2002,** *1,* 376-386.

58. Julka, S.; Regnier, F. Quantification in Proteomics through Stable Isotope Coding: A Review. *J. Proteome Res.* **2004,** *3,* 350-363.

59. Kuhn, K.; Prinz, T.; Schäfer, J.; Baumann, C.; Schärfke, M.; Kienle, S.; Schwarz, J.; Steiner, S.; Hamon, C. Protein Sequence Tags: A Novel Solution for Comparative Proteomics. *Proteomics* **2005,** *5,* 2364-2368.

60. Simons, B. L.; Wang, G.; Shen, R.-F.; Knepper, M. A. *In Vacuo* Isotope Coded Alkylation Technique (IVICAT); An N-terminal Stable Isotopic Label for Quantitative Liquid Chromatography/Mass Spectrometry Proteomics. *Rapid Commun. Mass Spectrom.* **2006,** *20,* 2463-2477.

61. Shi, Y.; Yao, X. Oxygen Isotopic Substitution of Peptidyl Phosphates for Modification-Specific Mass Spectrometry. *Anal. Chem.* **2007,** *79,* 8454-8462.

62. Thompson, A.; Schafer, J.; Kuhn, K.; Kienle, S.; Schwarz, J.; Schmidt, G.; Neumann, T.; Hamon, C. Tandem Mass Tags: A Novel Quantification Strategy for Comparative Analysis of Complex Protein Mixtures by MS/MS. *Anal. Chem.* **2003,** *75,* 1895-1904.

63. Dayon, L.; Hainard, A.; Licker, V.; Turck, N.; Kuhn, K.; Hochstrasser, D. F.; Burkhard, P. R.; Sanchez, J.-C. Relative Quantification of Proteins in Human Cerebrospinal Fluids by MS/MS Using 6-Plex Isobaric Tags. *Anal. Chem.* **2008,** *80,* 2921-2931.

64. Ross, P. L.; Huang, Y. N.; Marchese, J. N.; Williamson, B.; Parker, K.; Hattan, S.; Khainovski, N.; Pillai, S.; Dey, S.; Daniels, S.; Purkayastha, S.; Juhasz, P.; Martin, S.; Bartlet-Jones, M.; He, F.; Jacobson, A.; Pappin, D. J. Multiplexed Protein Quantitation in *Saccharomyces cerevisiae* Using Amine-reactive Isobaric Tagging Reagents. *Mol. Cell. Proteomics* **2004,** *3,* 1154-1169.

65. Sachon, E.; Mohammed, S.; Bache, N.; Jensen, O. N. Phosphopeptide Quantitation using Amine-Reactive Isobaric Tagging Reagents and Tandem Mass Spectrometry: Application to Proteins Isolated by Gel Electrophoresis. *Rapid Commun. Mass Spectrom.* **2006,** *20,* 1127-1134.

66. Choe, L.; D'Ascenzo, M.; Relkin, N. R.; Pappin, D.; Ross, P.; Williamson, B.; Guertin, S.; Pribil, P.; Lee, K. H. 8-Plex Quantitation of Changes in Cerebrospinal Fluid Protein Expression in Subjects Undergoing Intravenous Immunoglobulin Treatment for Alzheimer's Disease. *Proteomics* **2007,** *7,* 3651-3660.

67. Li, S.; Zeng, D. CILAT-A New Reagent for Quantitative Proteomics. *Chem. Commun.* **2007,** *21,* 2181-2183.

68. Hernandez, P.; Müller, M.; Appel, R. D. Automated Protein Identification by Tandem Mass Spectrometry: Issues and Strategies. *Mass Spectrom. Rev.* **2006,** *25,* 235-254.

69. Sadygov, R. G.; Cociorva, D.; Yates, J. R. Large-Scale Database Searching using Tandem Mass Spectra: Looking up the Answer in the Back of the Book. *Nat. Methods* **2004,** *1,* 195-202.

70. Paizs, B.; Suhai, S. Fragmentation Pathways of Protonated Peptides. *Mass Spectrom. Rev.* **2005,** *24,* 508-548.

71. McLuckey, S. A. Principles of Collisional Activation in Analytical Mass Spectrometry. *J. Am. Soc. Mass Spectrom.* **1992,** *3,* 599-614.

72. Dongre, A. R.; Jones, J. L.; Somogyi, A.; Wysocki, V. H. Influence of Peptide Composition, Gas-Phase Basicity, and Chemical Modification on Fragmentation Efficiency: Evidence for the Mobile Proton Model. *J. Am. Chem. Soc.* **1996,** *118,* 8365-8374.

73. Wysocki, V. H.; Tsaprailis, G.; Smith, L. L.; Breci, L. A. Mobile and Localized Protons: A Framework for Understanding Peptide Dissociation. *J. Mass Spectrom.* **2000,** *35,* 1399-1406.

74. Cox, K. A.; Gaskell, S. J.; Morris, M.; Whiting, A. Role of the Site of Protonation in the Low-Energy Decompositions of Gas-Phase Peptide Ions. *J. Am. Soc. Mass Spectrom.* **1996,** *7,* 522-531.

75. Polfer, N. C.; Oomens, J.; Suhai, S.; Paizs, B. Infrared Spectroscopy and Theoretical Studies on Gas-Phase Protonated Leu-enkephalin and Its Fragments: Direct Experimental Evidence for the Mobile Proton. *J. Am. Chem. Soc.* **2007,** *129,* 5887-5897.

76. Kapp, E. A.; Schutz, F.; Reid, G. E.; Eddes, J. S.; Moritz, R. L.; O'Hair, R. A. J.; Speed, T. P.; Simpson, R. J. Mining a Tandem Mass Spectrometry Database To Determine the Trends and Global Factors Influencing Peptide Fragmentation. *Anal. Chem.* **2003,** *75,* 6251-6264.

77. O'Hair, R. A. J. The Role of Nucleophile-Electrophile Interactions in the Unimolecular and Bimolecular Gas-Phase Ion Chemistry of Peptides and Related Systems. *J. Mass Spectrom.* **2000,** *35,* 1377-1381.

78. Lioe, H.; O'Hair, R. A. J.; Reid, G. E. A Mass Spectrometric and Molecular Orbital Study of H_2O Loss from Protonated Tryptophan and Oxidized Tryptophan Derivatives. *Rapid Commun. Mass Spectrom.* **2004,** *18,* 978-988.

79. Reid, G. E.; Simpson, R. J.; O'Hair, R. A. J. Leaving Group and Gas Phase Neighboring Group Effects in the Side Chain Losses from Protonated Serine and its Derivatives. *J. Am. Soc. Mass Spectrom.* **2000,** *11,* 1047-1060.

80. Palumbo, A. M.; Tepe, J. J.; Reid, G. E. Mechanistic Insights into the Multistage Gas-Phase Fragmentation Behavior of Phosphoserine- and Phosphothreonine-Containing Peptides. *J. Proteome Res.* **2008,** *7,* 771-779.

81. Reid, G. E.; Roberts, K. D.; Kapp, E. A.; Simpson, R. J. Statistical and Mechanistic Approaches to Understanding the Gas-Phase Fragmentation Behavior of Methionine Sulfoxide Containing Peptides. *J. Proteome Res.* **2004,** *3,* 751-759.

82. Green, M. K.; Lebrilla, C. B. Ion-Molecule Reactions as Probes of Gas-Phase Structures of Peptides and Proteins. *Mass Spectrom. Rev.* **1997,** *16,* 53-71.

83. Polce, M. J.; Beranová, S.; Nold, M. J.; Wesdemiotis, C. Characterization of Neutral Fragments in Tandem Mass Spectrometry: A Unique Route to Mechanistic and Structural Information. *J. Mass Spectrom.* **1996,** *31,* 1073-1085.

84. Bailey, T. H.; Laskin, J.; Futrell, J. H. Energetics of Selective Cleavage at Acidic Residues Studied by Time- and Energy-Resolved Surface-Induced Dissociation in FT-ICR MS. *Int. J. Mass Spectrom.* **2003,** *222,* 313-327.

85. Vékey, K.; Somogyi, A.; Wysocki, V. H. Average Activation Energies of Low-energy Fragmentation Processes of Protonated Peptides Determined by a New Approach. *Rapid Commun. Mass Spectrom.* **1996,** *10,* 911-918.

86. Tabb, D. L.; Smith, L. L.; Breci, L. A.; Wysocki, V. H.; Lin, D.; Yates, J. R. Statistical Characterization of Ion Trap Tandem Mass Spectra from Doubly Charged Tryptic Peptides. *Anal. Chem.* **2003,** *75,* 1155-1163.

87. Huang, Y.; Triscari, J. M.; Tseng, G. C.; Pasa-Tolic, L.; Lipton, M. S.; Smith, R. D.; Wysocki, V. H. Statistical Characterization of the Charge State and Residue Dependence of Low-Energy CID Peptide Dissociation Patterns. *Anal. Chem.* **2005,** *77,* 5800-5813.

88. Roepstorff, P.; Fohlman, J. Proposal for a Common Nomenclature for Sequence Ions in Mass Spectra of Peptides. *Biomed. Mass Spectrom.* **1984,** *11,* 601.

89. Biemann, K.; Papayannopoulos, I. A. Amino Acid Sequencing of Proteins. *Acc. Chem. Res.* **1994,** *27,* 370-378.

90. Schlosser, A.; Lehmann, W. D. Five-Membered Ring Formation in Unimolecular Reactions of Peptides: A Key Structural Element Controlling Low-Energy Collision-Induced Dissociation of Peptides. *J. Mass Spectrom.* **2000,** *35,* 1382-1390.

91. Polce, M. J.; Ren, D.; Wesdemiotis, C. Dissociation of the Peptide Bond in Protonated Peptides. *J. Mass Spectrom.* **2000,** *35,* 1391-1398.

92. Paizs, B.; Suhai, S. Towards Understanding the Tandem Mass Spectra of Protonated Oligopeptides. 1: Mechanism of Amide Bond Cleavage. *J. Am. Soc. Mass Spectrom.* **2004,** *15,* 103-113.

93. Yalcin, T.; Khouw, C.; Csizmadia, I. G.; Peterson, M. R.; Harrison, A. G. Why Are B Ions Stable Species in Peptide Spectra? *J. Am. Soc. Mass Spectrom.* **1995,** *6,* 1165-1174.

94. Yalcin, T.; Csizmadia, I. G.; Peterson, M. R.; Harrison, A. G. The Structure and Fragmentation of B_n (n >= 3) Ions in Peptide Spectra. *J. Am. Soc. Mass Spectrom.* **1996,** *7,* 233-242.

95. Harrison, A. G.; Csizmadia, I. G.; Tang, T.-H. Structure and Fragmentation of b_2 Ions in Peptide Mass Spectra. *J. Am. Soc. Mass Spectrom.* **2000,** *11,* 427-436.

96. Polfer, N. C.; Oomens, J.; Suhai, S.; Paizs, B. Spectroscopic and Theoretical Evidence for Oxazolone Ring Formation in Collision-Induced Dissociation of Peptides. *J. Am. Chem. Soc.* **2005,** *127,* 17154-17155.

97. Morgan, D. G.; Bursey, M. M. A Linear Free-Energy Correlation in the Low-Energy Tandem Mass Spectra of Protonated Tripeptides Gly-Gly-Xxx. *Org. Mass Spectrom.* **1994,** *29,* 354-359.

98. Harrison, A. G.; Young, A. B.; Bleiholder, C.; Suhai, S.; Paizs, B. Scrambling of Sequence Information in Collision-Induced Dissociation of Peptides. *J. Am. Chem. Soc.* **2006,** *128,* 10364-10365.

99. Vékey, K.; Gömöry, A. Theoretical Modelling of Mass Spectrometric Behaviour of Peptides: Singly and Doubly Protonated Tetraglycine. *Rapid Commun. Mass Spectrom.* **1996,** *10,* 1485-1496.

100. Paizs, B.; Lendvay, G.; Vékey, K.; Suhai, S. Formation of b_2^+ Ions from Protonated Peptides: An *ab initio* Study. *Rapid Commun. Mass Spectrom.* **1999,** *13,* 525-533.

101. Csonka, I. P.; Paizs, B.; Lendvay, G.; Suhai, S. Proton Mobility in Protonated Peptides: A Joint Molecular Orbital and RRKM Study. *Rapid Commun. Mass Spectrom.* **2000,** *14,* 417-431.

102. Somogyi, Á.; Wysocki, V. H.; Mayer, I. The Effect of Protonation Site on Bond Strengths in Simple Peptides: Application of ab initio and Modified Neglect of Differential Overlap Bond Orders and Modified Neglect of Differential Overlap Energy Partitioning. *J. Am. Soc. Mass Spectrom.* **1994,** *5,* 704-717.

103. Reid, G.; Simpson, R.; O'Hair, R. J. A Mass Spectrometric and ab initio Study of the Pathways for Dehydration of Simple Glycine and Cysteine-Containing Peptide $[M+H]^+$ Ions. *J. Am. Soc. Mass Spectrom.* **1998,** *9,* 945-956.

104. Reid, G. E.; Simpson, R. J.; O'Hair, R. A. J. Probing the Fragmentation Reactions of Protonated Glycine Oligomers via Multistage Mass Spectrometry and Gas Phase Ion Molecule Hydrogen/Deuterium Exchange. *Int. J. Mass Spectrom.* **1999,** *190-191,* 209-230.

105. Breci, L. A.; Tabb, D. L.; Yates, J. R.; Wysocki, V. H. Cleavage N-Terminal to Proline: Analysis of a Database of Peptide Tandem Mass Spectra. *Anal. Chem.* **2003,** *75,* 1963-1971.

106. Tsaprailis, G.; Nair, H.; Somogyi, A.; Wysocki, V. H.; Zhong, W.; Futrell, J. H.; Summerfield, S. G.; Gaskell, S. J. Influence of Secondary Structure on the Fragmentation of Protonated Peptides. *J. Am. Chem. Soc.* **1999,** *121,* 5142-5154.

107. Yu, W.; Vath, J. E.; Huberty, M. C.; Martin, S. A. Identification of the Facile Gas-Phase Cleavage of the Asp-Pro and Asp-Xxx Peptide Bonds in Matrix-Assisted Laser Desorption Time-of-Flight Mass Spectrometry. *Anal. Chem.* **1993,** *65,* 3015-3023.

108. Summerfield, S. G.; Whiting, A.; Gaskell, S. J. Intra-Ionic Interactions in Electrosprayed Peptide Ions. *Int. J. Mass Spectrom. Ion Processes* **1997,** *162,* 149-161.

109. Paizs, B.; Suhai, S.; Hargittai, B.; Hruby, V. J.; Somogyi, Á. Ab Initio and MS/MS Studies on Protonated Peptides Containing Basic and Acidic Amino Acid Residues: I. Solvated Proton vs. Salt-Bridged Structures and the Cleavage of the Terminal Amide Bond of Protonated RD-NH_2. *Int. J. Mass Spectrom.* **2002,** *219,* 203-232.

110. Qin, J.; Chait, B. T. Preferential Fragmentation of Protonated Gas-Phase Peptide Ions Adjacent to Acidic Amino Acid Residues. *J. Am. Chem. Soc.* **1995,** *117,* 5411-5412.

111. Tsaprailis, G.; Somogyi, Á.; Nikolaev, E. N.; Wysocki, V. H. Refining the Model for Selective Cleavage at Acidic Residues in Arginine-Containing Protonated Peptides. *Int. J. Mass Spectrom.* **2000,** *195-196,* 467-479.

112. Huang, Y.; Wysocki, V. H.; Tabb, D. L.; Yates, J. R. The Influence of Histidine on Cleavage C-terminal to Acidic Residues in Doubly Protonated Tryptic Peptides. *Int. J. Mass Spectrom.* **2002,** *219,* 233-244.

113. Gu, C.; Tsaprailis, G.; Breci, L.; Wysocki, V. H. Selective Gas-Phase Cleavage at the Peptide Bond C-Terminal to Aspartic Acid in Fixed-Charge Derivatives of Asp-Containing Peptides. *Anal. Chem.* **2000,** *72,* 5804-5813.

114. Sullivan, A. G.; Brancia, F. L.; Tyldesley, R.; Bateman, R.; Sidhu, K.; Hubbard, S. J.; Oliver, S. G.; Gaskell, S. J. The Exploitation of Selective Cleavage of Singly Protonated Peptide Ions Adjacent to Aspartic Acid Residues using a Quadrupole Orthogonal Time-of-Flight Mass Spectrometer Equipped with a Matrix-Assisted Laser Desorption/Ionization Source. *Int. J. Mass Spectrom.* **2001,** *210-211,* 665-676.

115. Sidhu, K. S.; Sangvanich, P.; Brancia, F. L.; Sullivan, A. G.; Gaskell, S. J.; Wolkenhauer, O.; Oliver, S. G.; Hubbard, S. J. Bioinformatic Assessment of Mass Spectrometric Chemical Derivatisation Techniques for Proteome Database Searching. *Proteomics* **2001,** *1,* 1368-1377.

116. Burlet, O.; Yang, C.-Y.; Gaskell, S. J. Influence of Cysteine to Cysteic Acid Oxidation on the Collision-Activated Decomposition of Protonated Peptides: Evidence for Intraionic Interactions. *J. Am. Soc. Mass Spectrom.* **1992,** *3,* 337-344.

117. Summerfield, S. G.; Cox, K. A.; Gaskell, S. J. The Promotion of d-type Ions during the Low Energy Collision-Induced Dissociation of Some Cysteic Acid-Containing Peptides. *J. Am. Soc. Mass Spectrom.* **1997,** *8,* 25-31.

118. Wang, Y.; Vivekananda, S.; Men, L.; Zhang, Q. Fragmentation of Protonated Ions of Peptides Containing Cysteine, Cysteine Sulfinic Acid, and Cysteine Sulfonic Acid. *J. Am. Soc. Mass Spectrom.* **2004,** *15,* 697-702.

119. Men, L.; Wang, Y. Further Studies on the Fragmentation of Protonated Ions of Peptides Containing Aspartic Acid, Glutamic Acid, Cysteine Sulfinic Acid, and Cysteine Sulfonic Acid. *Rapid Commun. Mass Spectrom.* **2005,** *19,* 23-30.

120. Srikanth, R.; Wilson, J.; Bridgewater, J. D.; Numbers, J. R.; Lim, J.; Olbris, M. R.; Kettani, A.; Vachet, R. W. Improved Sequencing of Oxidized Cysteine and Methionine Containing Peptides Using Electron Transfer Dissociation. *J. Am. Soc. Mass Spectrom.* **2007,** *18,* 1499-1506.

121. Bridgewater, J. D.; Srikanth, R.; Lim, J.; Vachet, R. W. The Effect of Histidine Oxidation on the Dissociation Patterns of Peptide Ions. *J. Am. Soc. Mass Spectrom.* **2007,** *18,* 553-562.

122. Swiderek, K. M.; Davis, M. T.; Lee, T. D. The Identification of Peptide Modifications Derived from Gel-Separated Proteins Using Electrospray Triple Quadrupole and Ion Trap Analyses. *Electrophoresis* **1998,** *19,* 989-997.

123. Mann, M.; Jensen, O. N. Proteomic Analysis of Post-Translational Modifications. *Nat Biotech* **2003,** *21,* 255-261.

124. Annan, R. S.; Carr, S. A. Phosphopeptide Analysis by Matrix-Assisted Laser Desorption Time-of-Flight Mass Spectrometry. *Anal. Chem.* **1996,** *68,* 3413-3421.

125. DeGnore, J. P.; Qin, J. Fragmentation of Phosphopeptides in an Ion Trap Mass Spectrometer. *J. Am. Soc. Mass Spectrom.* **1998,** *9,* 1175-1188.

126. Tholey, A.; Reed, J.; Lehmann, W. D. Electrospray Tandem Mass Spectrometric Studies of Phosphopeptides and Phosphopeptide Analogues. *J. Mass Spectrom.* **1999,** *34,* 117-123.

127. Metzger, S.; Hoffmann, R. Studies on the Dephosphorylation of Phosphotyrosine-Containing Peptides during Post-Source Decay in Matrix-Assisted Laser Desorption/Ionization. *J. Mass Spectrom.* **2000,** *35,* 1165-1177.

128. Medzihradszky, K. F.; Darula, Z.; Perlson, E.; Fainzilber, M.; Chalkley, R. J.; Ball, H.; Greenbaum, D.; Bogyo, M.; Tyson, D. R.; Bradshaw, R. A.; Burlingame, A. L. O-Sulfonation of Serine and Threonine: Mass Spectrometric Detection and Characterization of a New Posttranslational Modification in Diverse Proteins Throughout the Eukaryotes. *Mol. Cell. Proteomics* **2004,** *3,* 429-440.

129. Medzihradszky, K. F.; Guan, S.; Maltby, D. A.; Burlingame, A. L. Sulfopeptide Fragmentation in Electron-Capture and Electron-Transfer Dissociation. *J. Am. Soc. Mass Spectrom.* **2007,** *18,* 1617-1624.

130. Raftery, M. J. Selective Detection of Thiosulfate-Containing Peptides using Tandem Mass Spectrometry. *Rapid Commun. Mass Spectrom.* **2005,** *19,* 674-682.

131. Hanisch, F.-G.; Green, B. N.; Bateman, R.; Peter-Katalinic, J. Localization of *O*-glycosylation Sites of MUC1 Tandem Repeats by QTOF ESI Mass Spectrometry. *J. Mass Spectrom.* **1998,** *33,* 358-362.

132. Rademaker, G. J.; Pergantis, S. A.; Blok-Tip, L.; Langridge, J. I.; Kleen, A.; Thomas-Oates, J. E. Mass Spectrometric Determination of the Sites of O-Glycan Attachment with Low Picomolar Sensitivity. *Anal. Biochem.* **1998,** *257,* 149-160.

133. Steen, H.; Mann, M. Similarity Between Condensed Phase and Gas Phase Chemistry: Fragmentation of Peptides Containing Oxidized Cysteine Residues and its Implications for Proteomics. *J. Am. Soc. Mass Spectrom.* **2001,** *12,* 228-232.

134. Yagüe, J.; Núñez, A.; Boix, M.; Esteller, M.; Alfonso, P.; Ignacio Casal, J. Oxidation of Carboxyamidomethyl Cysteine may add Complexity to Protein Identification. *Proteomics* **2005,** *5,* 2761-2768.

135. Chowdhury, S. M.; Munske, G. R.; Ronald, R. C.; Bruce, J. E. Evaluation of Low Energy CID and ECD Fragmentation Behavior of Mono-Oxidized Thio-Ether Bonds in Peptides. *J. Am. Soc. Mass Spectrom.* **2007,** *18,* 493-501.

136. Shetty, V.; Spellman, D. S.; Neubert, T. A. Characterization by Tandem Mass Spectrometry of Stable Cysteine Sulfenic Acid in a Cysteine Switch Peptide of Matrix Metalloproteinases. *J. Am. Soc. Mass Spectrom.* **2007,** *18,* 1544-1551.

137. Gruhler, A.; Olsen, J. V.; Mohammed, S.; Mortensen, P.; Faergeman, N. J.; Mann, M.; Jensen, O. N. Quantitative Phosphoproteomics Applied to the Yeast Pheromone Signaling Pathway. *Mol. Cell. Proteomics* **2005,** *4,* 310-327.

138. Chang, E. J.; Archambault, V.; McLachlin, D. T.; Krutchinsky, A. N.; Chait, B. T. Analysis of Protein Phosphorylation by Hypothesis-Driven Multiple-Stage Mass Spectrometry. *Anal. Chem.* **2004,** *76,* 4472-4483.

139. Schroeder, M. J.; Shabanowitz, J.; Schwartz, J. C.; Hunt, D. F.; Coon, J. J. A Neutral Loss Activation Method for Improved Phosphopeptide Sequence Analysis by Quadrupole Ion Trap Mass Spectrometry. *Anal. Chem.* **2004,** *76,* 3590-3598.

140. Wolschin, F.; Lehmann, U.; Glinski, M.; Weckwerth, W. An Integrated Strategy for Identification and Relative Quantification of Site-Specific Protein Phosphorylation using Liquid Chromatography Coupled to MS^2/MS^3. *Rapid Commun. Mass Spectrom.* **2005,** *19,* 3626-3632.

141. Stensballe, A.; Jensen, O. N.; Olsen, J. V.; Haselmann, K. F.; Zubarev, R. A. Electron Capture Dissociation of Singly and Multiply Phosphorylated Peptides. *Rapid Commun. Mass Spectrom.* **2000,** *14,* 1793-1800.

142. Bakhtiar, R.; Guan, Z. Electron Capture Dissociation Mass Spectrometry in Characterization of Post-Translational Modifications. *Biochem. Biophys. Res. Commun.* **2005,** *334,* 1-8.

143. Mirgorodskaya, E.; Roepstorff, P.; Zubarev, R. A. Localization of O-Glycosylation Sites in Peptides by Electron Capture Dissociation in a Fourier Transform Mass Spectrometer. *Anal. Chem.* **1999,** *71,* 4431-4436.

144. Cooper, H. J.; Håkansson, K.; Marshall, A. G. The Role of Electron Capture Dissociation in Biomolecular Analysis. *Mass Spectrom. Rev.* **2005,** *24,* 201-222.

145. Bakhtiar, R.; Guan, Z. Electron Capture Dissociation Mass Spectrometry in Characterization of Peptides and Proteins. *Biotechnol. Lett.* **2006,** *28,* 1047-1060.

146. Chamot-Rooke, J.; van der Rest, G.; Dalleu, A.; Bay, S.; Lemoine, J. The Combination of Electron Capture Dissociation and Fixed Charge Derivatization Increases Sequence Coverage for O-Glycosylated and O-Phosphorylated Peptides. *J. Am. Soc. Mass Spectrom.* **2007,** *18,* 1405-1413.

147. Syka, J. E. P.; Coon, J. J.; Schroeder, M. J.; Shabanowitz, J.; Hunt, D. F. Peptide and Protein Sequence Analysis by Electron Transfer Dissociation Mass Spectrometry. *Proc. Natl. Acad. Sci. U. S. A.* **2004,** *101,* 9528-9533.

148. Gunawardena, H. P.; Emory, J. F.; McLuckey, S. A. Phosphopeptide Anion Characterization via Sequential Charge Inversion and Electron-Transfer Dissociation. *Anal. Chem.* **2006,** *78,* 3788-3793.

149. Zhang, Q.; Frolov, A.; Tang, N.; Hoffmann, R.; van de Goor, T.; Metz, T. O.; Smith, R. D. Application of Electron Transfer Dissociation Mass Spectrometry in Analyses of Non-Enzymatically Glycated Peptides. *Rapid Commun. Mass Spectrom.* **2007,** *21,* 661-666.

150. Hogan, J. M.; Pitteri, S. J.; Chrisman, P. A.; McLuckey, S. A. Complementary Structural Information from a Tryptic N-Linked Glycopeptide via Electron Transfer Ion/Ion Reactions and Collision-Induced Dissociation. *J. Proteome Res.* **2005,** *4,* 628-632.

151. O'Connor, P. B.; Cournoyer, J. J.; Pitteri, S. J.; Chrisman, P. A.; McLuckey, S. A. Differentiation of Aspartic and Isoaspartic Acids Using Electron Transfer Dissociation. *J. Am. Soc. Mass Spectrom.* **2006,** *17,* 15-19.

152. Chi, A.; Huttenhower, C.; Geer, L. Y.; Coon, J. J.; Syka, J. E. P.; Bai, D. L.; Shabanowitz, J.; Burke, D. J.; Troyanskaya, O. G.; Hunt, D. F. Analysis of Phosphorylation Sites on Proteins from Saccharomyces cerevisiae by Electron Transfer Dissociation (ETD) Mass Spectrometry. *Proc. Natl. Acad. Sci. U.S.A.* **2007,** *104,* 2193-2198.

153. Dikler, S.; Kelly, J. W.; Russell, D. H. Improving Mass Spectrometric Sequencing of Arginine-Containing Peptides by Derivatization with Acetylacetone. *J. Mass Spectrom.* **1997,** *32,* 1337-1349.

154. Foettinger, A.; Leitner, A.; Lindner, W. Derivatisation of Arginine Residues with Malondialdehyde for the Analysis of Peptides and Protein Digests by LC-ESI-MS/MS. *J. Mass Spectrom.* **2006,** *41,* 623-632.

155. Peters, E. C.; Horn, D. M.; Tully, D. C.; Brock, A. A Novel Multifunctional Labeling Reagent for Enhanced Protein Characterization with Mass Spectrometry. *Rapid Commun. Mass Spectrom.* **2001,** *15,* 2387-2392.

156. Conrotto, P.; Hellman, U. Lys Tag: An Easy and Robust Chemical Modification for Improved *de novo* Sequencing with a Matrix-Assisted Laser Desorption/Ionization Tandem Time-of-Flight Mass Spectrometer. *Rapid Commun. Mass Spectrom.* **2008,** *22,* 1823-1833.

157. Roth, K. D. W.; Huang, Z.-H.; Sadagopan, N.; Watson, J. T. Charge Derivatization of Peptides for Analysis by Mass Spectrometry. *Mass Spectrom. Rev.* **1998,** *17,* 255-274.

158. Huang, Z.-H.; Wu, J.; Roth, K. D. W.; Yang, Y.; Gage, D. A.; Watson, J. T. A Picomole-Scale Method for Charge Derivatization of Peptides for Sequence Analysis by Mass Spectrometry. *Anal. Chem.* **1997,** *69,* 137-144.

159. Sadagopan, N.; Watson, J. T. Investigation of the Tris(trimethoxyphenyl)phosphonium Acetyl Charged Derivatives of Peptides by Electrospray Ionization Mass Spectrometry and Tandem Mass Spectrometry. *J. Am. Soc. Mass Spectrom.* **2000,** *11,* 107-119.

160. Adamczyk, M.; Gebler, J. C.; Wu, J. Charge Derivatization of Peptides to Simplify their Sequencing with an Ion Trap Mass Spectrometer. *Rapid Commun. Mass Spectrom.* **1999,** *13,* 1413-1422.

161. Kuyama, H.; Sonomura, K.; Shima, K.; Nishimura, O.; Tsunasawa, S. An Improved Method for *de novo* Sequencing of Arginine-Containing, N^{α}-tris(2,4,6-trimethoxyphenyl)phosphonium-acetylated Peptides. *Rapid Commun. Mass Spectrom.* **2008,** *22,* 2063-2072.

162. Munchbach, M.; Quadroni, M.; Miotto, G.; James, P. Quantitation and Facilitated de Novo Sequencing of Proteins by Isotopic N-Terminal Labeling of Peptides with a Fragmentation-Directing Moiety. *Anal. Chem.* **2000,** *72,* 4047-4057.

163. Lee, Y. H.; Kim, M.-S.; Choie, W.-S.; Min, H.-K.; Lee, S.-W. Highly Informative Proteome Analysis by Combining Improved N-terminal Sulfonation for *de novo* Peptide Sequencing and Online Capillary Reverse-Phase Liquid Chromatography/Tandem Mass Spectrometry. *Proteomics* **2004,** *4,* 1684-1694.

164. Keough, T.; Youngquist, R. S.; Lacey, M. P. A Method for High-Sensitivity Peptide Sequencing using Postsource Decay Matrix-Assisted Laser Desorption Ionization Mass Spectrometry. *Proc. Natl. Acad. Sci. U. S. A.* **1999,** *96,* 7131-7136.

165. Bauer, M. D.; Sun, Y.; Keough, T.; Lacey, M. P. Sequencing of Sulfonic Acid Derivatized Peptides by Electrospray Mass Spectrometry. *Rapid Commun. Mass Spectrom.* **2000,** *14,* 924-929.

166. Keough, T.; Lacey, M. P.; Fieno, A. M.; Grant, R. A.; Sun, Y.; Bauer, M. D.; Begley, K. B. Tandem Mass Spectrometry Methods for Definitive Protein Identification in Proteomics Research. *Electrophoresis* **2000,** *21,* 2252-2265.

167. Summerfield, S. G.; Bolgar, M. S.; Gaskell, S. J. Promotion and Stabilization of b_1 Ions in Peptide Phenythiocarbamoyl Derivatives: Analogies with Condensed-phase Chemistry. *J. Mass Spectrom.* **1997,** *32,* 225-231.

168. Summerfield, S. G.; Steen, H.; O'Malley, M.; Gaskell, S. J. Phenyl Thiocarbamoyl and Related Derivatives of Peptides: Edman Chemistry in the Gas Phase. *Int. J. Mass Spectrom.* **1999,** *188,* 95-103.

169. Reid, G. E.; Roberts, K. D.; Simpson, R. J.; O'Hair, R. A. J. Selective Identification and Quantitative Analysis of Methionine Containing Peptides by Charge Derivatization and Tandem Mass Spectrometry. *J. Am. Soc. Mass Spectrom.* **2005,** *16,* 1131-1150.

170. Amunugama, M.; Roberts, K. D.; Reid, G. E. Mechanisms for the Selective Gas-Phase Fragmentation Reactions of Methionine Side Chain Fixed Charge Sulfonium Ion Containing Peptides. *J. Am. Soc. Mass Spectrom.* **2006,** *17,* 1631-1642.

171. Sierakowski, J.; Amunugama, M.; Roberts, K. D.; Reid, G. E. Substituent Effects on the Gas-Phase Fragmentation Reactions of Sulfonium Ion Containing Peptides. *Rapid Commun. Mass Spectrom.* **2007,** *21,* 1230-1238.

172. Roberts, K. D.; Reid, G. E. Leaving Group Effects on the Selectivity of the Gas-Phase Fragmentation Reactions of Side Chain Fixed-Charge-Containing Peptide Ions. *J. Mass Spectrom.* **2007,** *42,* 187-198.

173. Chu, I. K.; Rodriguez, C. F.; Hopkinson, A. C.; Siu, K. W. M.; Lau, T.-C. Formation of Molecular Radical Cations of Enkephalin Derivatives via Collision-Induced Dissociation of Electrospray-Generated Copper (II) Complex Ions of Amines and Peptides. *J. Am. Soc. Mass Spectrom.* **2001,** *12,* 1114-1119.

174. Yin, H.; Chacon, A.; Porter, N. A.; Masterson, D. S. Free Radical-Induced Site-Specific Peptide Cleavage in the Gas Phase: Low-Energy Collision-Induced Dissociation in ESI- and MALDI Mass Spectrometry. *J. Am. Soc. Mass Spectrom.* **2007,** *18,* 807-816.

175. Ly, T.; Julian, R. R. Residue-Specific Radical-Directed Dissociation of Whole Proteins in the Gas-Phase. *J. Am. Chem. Soc.* **2008,** *130,* 351-358.

176. Diedrich, J. K.; Julian, R. R. Site-Specific Radical Directed Dissociation of Peptides at Phosphorylated Residues. *J. Am. Chem. Soc.* **2008,** *130,* 12212-12213.

177. Jones, A. M. E.; Bennett, M. H.; Mansfield, J. W.; Grant, M. Analysis of the Defence Phosphoproteome of *Arabidopsis thaliana* using Differential Mass Tagging. *Proteomics* **2006,** *6,* 4155-4165.

178. Champion, P. A. D.; Stanley, S. A.; Champion, M. M.; Brown, E. J.; Cox, J. S. C-Terminal Signal Sequence Promotes Virulence Secretion in Mycobacterium Tuberculosis. *Science* **2006,** *313,* 1632-1636.

179. Corvey, C.; Koetter, P.; Beckhaus, T.; Hack, J.; Hofmann, S.; Hampel, M.; Stein, T.; Karas, M.; Entian, K.-D. Carbon Source-Dependent Assembly of the Snf1p Kinase Complex in *Candida albicans*. *J. Biol. Chem.* **2005,** *280,* 25323-25330.

180. Williamson, B. L.; Marchese, J.; Morrice, N. A. Automated Identification and Quantification of Protein Phosphorylation Sites by LC/MS on a Hybrid Triple Quadrupole Linear Ion Trap Mass Spectrometer. *Mol. Cell. Proteomics* **2006,** *5,* 337-346.

181. Wolf-Yadlin, A.; Hautaniemi, S.; Lauffenburger, D. A.; White, F. M. Multiple Reaction Monitoring for Robust Quantitative Proteomic Analysis of Cellular Signaling Networks. *Proc. Natl. Acad. Sci. U. S. A.* **2007,** *104,* 5860-5865.

182. Cunningham, J. C.; Glish, G. L.; Burinsky, D. J. High Amplitude Short Time Excitation: A Method to Form and Detect Low Mass Product Ions in a Quadrupole Ion Trap Mass Spectrometer. *J. Am. Soc. Mass Spectrom.* **2006,** *17,* 81-84.

183. Meany, D. L.; Xie, H.; Thompson, L. V.; Arriaga, E. A.; Griffin, T. J. Identification of Carbonylated Proteins from Enriched Rat Skeletal Muscle Mitochondria using Affinity Chromatography-Stable Isotope Labeling and Tandem Mass Spectrometry. *Proteomics* **2007,** *7,* 1150-1163.

184. Griffin, T. J.; Xie, H.; Bandhakavi, S.; Popko, J.; Mohan, A.; Carlis, J. V.; Higgins, L. iTRAQ Reagent-Based Quantitative Proteomic Analysis on a Linear Ion Trap Mass Spectrometer. *J. Proteome Res.* **2007,** *6,* 4200-4209.

185. Bantscheff, M.; Eberhard, D.; Abraham, Y.; Bastuck, S.; Boesche, M.; Hobson, S.; Mathieson, T.; Perrin, J.; Raida, M.; Rau, C.; Reader, V.; Sweetman, G.; Bauer, A.; Bouwmeester, T.; Hopf, C.; Kruse, U.; Neubauer, G.; Ramsden, N.; Rick, J.; Kuster, B.; Drewes, G. Quantitative Chemical Proteomics Reveals Mechanisms of Action of Clinical ABL Kinase Inhibitors. *Nat Biotech* **2007,** *25,* 1035-1044.

186. Chang, B.; Ünlü, M.; Clauser, K.; Carr, S. A., iTRAQ-IT: Implementation of iTRAQ Quantitation Tags on Ion Trap Instruments via MS^3. In *53rd ASMS Conference on Mass Spectrometry*, San Antonio, Texas, 2005.

187. Fenn, J. B.; Mann, M.; Meng, C. K.; Wong, S. F.; Whitehouse, C. M. Electrospray Ionization for Mass Spectrometry of Large Biomolecules. *Science* **1989,** *246,* 64-71.

188. Wilm, M. S.; Mann, M. Electrospray and Taylor Cone Theory, Dole's Beam of Macromolecules at Last? *Int. J. Mass Spectrom. Ion Processes* **1994,** *136,* 167-180.

189. Gomez, A.; Tang, K. Charge and Fission of Droplets in Electrostatic Sprays. *Phys. Fluids* **1994,** *6,* 404-414.

190. Iribarne, J. V.; Thompson, B. A. On the Evaporation of Small Ions from Charged Droplets. *J. Chem. Phys.* **1976,** *64,* 2287-2294.

191. Thompson, B. A.; Iribarne, J. V. Field Induced Ion Evaporation from Liquid Surfaces at Atmospheric Pressure. *J. Chem. Phys.* **1979,** *71,* 4451-4463.

192. Kebarle, P. A Brief Overview of the Present Status of the Mechanisms Involved in Electrospray Mass Spectrometry. *J. Mass Spectrom.* **2000,** *35,* 804-817.

193. Karas, M.; Hillencamp, F. Laser Desorption Ionization of Proteins with Molecular Masses Exceeding 10 000 Daltons. *Anal. Chem.* **1988,** *60,* 2299-2301.

194. Zenobi, R.; Knochenmuss, R. Ion Formation in MALDI Mass Spectrometry. *Mass Spectrom. Rev.* **1998,** *17,* 337-366.

195. de Hoffmann, E. D.; Stroobant, V., *Mass Spectrometry Principles and Applications*. 2nd ed.; John Wiley and Sons: New York, 2002.

196. March, R. E. An Introduction to Quadrupole Ion Trap Mass Spectrometry. *J. Mass Spectrom.* **1997,** *32,* 351-369.

197. Hager, J. W. A New Linear Ion Trap Mass Spectrometer. *Rapid Commun. Mass Spectrom.* **2002,** *16,* 512-526.

198. Schwartz, J. C.; Senko, M. W.; Syka, J. E. A Two-Dimensional Quadrupole Ion Trap Mass Spectrometer. *J. Am. Soc. Mass Spectrom.* **2002,** *13,* 659-669.

199. Finkielsztein, L. M.; Aguirre, J. M.; Lantaño, B.; Alesso, E. N.; Iglesias, G. Y. M. $ZnI_2/NaCNBH_3$ as an Efficient Reagent for Regioselective Ring Opening of the Benzylic Epoxide Moiety. *Synth. Commun.* **2004,** *34,* 895-901.

200. Shechter, Y. Selective Oxidation and Reduction of Methionine Residues in Peptides and Proteins by Oxygen Exchange Between Sulfoxide and Sulfide. *J. Biol. Chem.* **1986,** *261,* 66-70.

201. Frisch, M. J.; Trucks, G. W.; Schlegel, H. B.; Scuseria, G. E.; Robb, M. A.; Cheeseman, J. R.; Zakrzewski, V. G.; Montgomery, J. A.; Stratman, R. E.; Burant, J. C.; Dapprich, S.; Millam, J. M.; Daniels, A. D.; Kudin, K. N.; Strain, M. C.; Farkas, O.; Tomasi, J.; Barone, V.; Cossi, M.; Cammi, R.; Mennucci, B.; Pomelli, C.; Adamo, C.; Clifford, S.; Ochterski, J.; Peterson, G. A.; Ayala, P. Y.; Cui, Q.; Morokuma, K.; Malick, D. K.; Rabuck, A. D.; Raghavachari, K.; Foresman, J. B.; Cioslowski, J.; Oritz, J. V.; Baboul, A. G.; Stefanov, B. B.; Liu, G.; Liashenko, A.; Piskorz, P.; Komaromi, I.; Gomperts, R.; Martin, R. L.; Fox, D. J.; Keith, T.; Al-Laham, M. A.; Peng, C. Y.; Nanayakkara, A.; Gonzalez, C.; Challacombe, M.; Gill, P. M. W.; Johnson, B.; Chen, W.; Wong, M. W.; Andres, J. L.; Gonzalez, C.; Head-Gordon, M.; Replogle, E. S.; Pople, J. A. *Gaussian 98, Revision A.7*, Gaussian Inc.: Pittsburg PA, 1998.

202. Carruthers, N. J.; Stemmer, P. M. Methionine Oxidation in the Calmodulin-Binding Domain of Calcineurin Disrupts Calmodulin Binding ad Calcineurin Activation. *Biochemistry* **2008,** *47,* 3085-3095.

203. Clauser, K. R.; Hall, S. C.; Smith, D. M.; Webb, J. W.; Andrews, L. E.; Tran, H. M.; Epstein, L. B.; Burlingame, A. L. Rapid Mass Spectrometric Peptide Sequencing and Mass Matching for Characterization of Human Melanoma Proteins Isolated by Two-Dimensional PAGE. *Proc. Natl. Acad. Sci. U. S. A.* **1995,** *92,* 5072-5076.

204. Qin, J.; Chait, B. T. Identification and Characterization of Posttranslational Modifications of Proteins by MALDI Ion Trap Mass Spectrometry. *Anal. Chem.* **1997,** *69,* 4002-4009.

205. Cohen, S. L. Ozone in Ambient Air as a Source of Adventitious Oxidation. A Mass Spectrometric Study. *Anal. Chem.* **2006,** *78,* 4352-4362.

206. Morand, K.; Talbo, G.; Mann, M. Oxidation of Peptides During Electrospray Ionization. *Rapid Commun. Mass Spectrom.* **1993,** *7,* 738-743.

207. Sommer, S.; Fakata, K. L.; Swanson, S. A.; Stemmer, P. M. Modulation of the Phosphatase Activity of Calcineurin by Oxidants and Antioxidants in vitro. *Eur. J. Biochem.* **2000,** *267,* 2312-2322.

208. Cross, J. V.; Templeton, D. J. Regulation of Signal Transduction Through Protein Cysteine Oxidation. *Antioxid. Redox Signaling* **2006,** *8,* 1819-1827.

209. Baty, J. W.; Hampton, M. B.; Winterbourn, C. C. Proteomic Detection of Hydrogen Peroxide-Sensitive Thiol Proteins in Jurkat Cells. *Biochem. J.* **2005,** *389,* 785-795.

210. Midwinter, R. G.; Cheah, F.-C.; Moskovizt, J.; Vissers, M. C.; Winterbourn, C. C. IκB is a Sensitive Target for Oxidation by Cell-Permeable Chloramines: Inhibition of NF-κB Activity by Glycine Chloramine Through Methionine Oxidation. *Biochem. J.* **2006,** *396,* 71-78.

211. Sethuraman, M.; McComb, M. E.; Heibeck, T.; Costello, C. E.; Cohen, R. A. Isotope-Coded Affinity Tag Approach to Identify and Quantify Oxidant-Sensitive Protein Thiols. *Mol. Cell. Proteomics* **2004,** *3,* 273-278.

212. Shechter, Y.; Rubinstein, M.; Patchornik, A. Selective Covalent Binding of Methionyl-Containing Peptides and Proteins to Water Insoluble Polymeric Reagent and their Regeneration. *Biochemistry* **1977,** *16,* 1424-1430.

213. Degen, J.; Kyte, J. The Purification of Peptides which Contain Methionine Residues. *Anal. Biochem.* **1978,** *89,* 529-539.

214. Gevaert, K.; Van Damme, J.; Goethals, M.; Thomas, G. R.; Hoorelbeke, B.; Demol, H.; Martens, L.; Puype, M.; Staes, A.; Vandekerckhove, J. Chromatographic Isolation of Methionine-Containing Peptides for Gel-Free Proteome Analysis: Identification Of More Than 800 Escherichia Coli Proteins. *Mol. Cell. Proteomics* **2002,** *1,* 896-903.

215. Kuyama, H.; Watanabe, M.; Toda, C.; E., A.; Tanaka, K.; Nishimura, O. An Approach to Quantitative Proteome Analysis by Labeling Tryptophan Residues. *Rapid Commun. Mass Spectrom.* **2003,** *17,* 1642-1650.

216. Lagerwerf, F. M.; van de Weert, M.; Heerma, W.; Haverkamp, J. Identification of Oxidized Methionine in Peptides. *Rapid Commun. Mass Spectrom.* **1996,** *10,* 1905-1910.

217. Jiang, X.; Smith, J. B.; Abraham, E. C. Identification of a MS-MS Fragment Diagnostic for Methionine Sulfoxide *J. Mass Spectrom.* **1996,** *31,* 1309-1310.

218. Betancourt, L.; Takao, T.; Gonzalez, J.; Reyes, O.; Besada, V.; Padron, G.; Shimonishi, Y. The Metastable Decomposition of a Peptide Containing Oxidized Methionine(s) in Matrix-Assisted Laser Desorption/Ionization Time-of-Flight Mass Spectrometry. *Rapid Commun. Mass Spectrom.* **1999,** *13,* 1075-1076.

219. Yang, F.; Stenoien, D. L.; Strittmatter, E. F.; Wang, J.; Ding, L.; Lipton, M. S.; Monroe, M. E.; Nicora, C. D.; Gristenko, M. A.; Tang, K.; Fang, R.; Adkins, J. N.; Camp, D. G.; Chen, D. J.; Smith, R. D. Phosphoproteome Profiling of Human Skin Fibroblast Cells in Response to Low- and High-Dose Irradiation. *J. Proteome Res.* **2006,** *5,* 1252-1260.

220. Beausoleil, S. A.; Villen, J.; Gerber, S. A.; Rush, J.; Gygi, S. P. A Probability-Based Approach for High-Throughput Protein Phosphorylation Analysis and Site Localization. *Nat. Biotechnol.* **2006,** *24,* 1285-1292.

221. Madesclaire, M. Reduction of Sulfoxides to Thioethers. *Tetrahedron* **1988,** *44,* 6537-6580.

222. Houghten, R. A.; Li, C. H. Reduction of Sulfoxides in Peptides and Proteins. *Anal. Biochem.* **1979,** *98,* 36-46.

223. Faucher, A.; Grand-Maître, C. Tris(2-carboxyethyl)phosphine (TCEP) for the Reduction of Sulfoxides, Sulfonylchlorides, N-oxides and Azides. *Synth. Commun.* **2003,** *33,* 3503-3511.

224. Savige, W. E.; Fontana, A. Interconversion of Methionine and Methionine Sulfoxide. *Methods Enzymol.* **1977,** *47,* 453-459.

225. Toennies, G.; Callan, T. P. A Comparison of Oxidative Reactions of Methionine, Cysteine, and Cystine. Determination of Methionine by Hydrogen Peroxide Oxidation. *J. Biol. Chem.* **1939,** *129,* 481-490.

226. Caldwell, K. A.; Tappel, A. L. Reactions of Seleno- and Sulfoamino Acids with Hydroperoxides. *Biochemistry* **1964,** *3,* 1643-1647.

227. Knowles, J. R. The Role of Methionine in α-Chymotrypsin-Catalyzed Reactions. *Biochem. J.* **1965,** *95,* 180-190.

228. Atassi, M. Z. Periodate Oxidation of Sperm-Whale Myoglobin and the Role of the Methionine Residues in the Antigen-Antibody Reaction. *Biochem. J.* **1967,** *102,* 478-487.

229. Clamp, J. R.; Hough, L. The Periodate Oxidation of Amino Acids with Reference to Studies on Glycoproteins. *Biochem. J.* **1965,** *94,* 17-24.

230. Shechter, Y.; Burstein, Y.; Patchornik, A. Selective Oxidation of Methionine Residues in Proteins. *Biochemistry* **1975,** *14,* 4497-4503.

231. Savige, W. E.; Fontana, A., New Procedures for the Chemical Modification of Tryptophan and Sulfur Amino Acids in Peptides and Proteins. In *Peptides, Proceedings, 14th European Peptide Symposium*, 1976; p 135.

232. Burstein, Y.; Patchornik, A. Selective Chemical Cleavage of Trytophanyl Peptide Bonds in Peptides and Proteins. *Biochemistry* **1972,** *11,* 4641-4650.

233. Hachimori, Y.; Horinishi, H.; Kurihara, K.; Shibata, K. States of Amino Acid Residues in Proteins: Different Reactivities with H_2O_2 of Tryptophan Residues in Lysozyme, Proteinases and Zymogens. *Biochim. Biophys. Acta* **1964,** *93,* 346-360.

234. van de Weert, M.; Lagerwerf, F. M.; Haverkamp, J.; Heerma, W. Mass Spectrometric Analysis of Oxidized Tryptophan. *J. Mass Spectrom.* **1998,** *33,* 884-891.

235. Uchida, K.; Kawakishi, S. Identification of Oxidized Histidine Generated at the Active Site of Cu,Zn-Superoxide Dismutase Exposed to H_2O_2:Selective Generation of 2-Oxo-Histidine at the Histidine 118. *J. Biol. Chem.* **1994,** *269,* 2405-2410.

236. Elias, J. E.; Gibbons, F. D.; King, O. D.; Roth, F. P.; Gygi, S. P. Intensity-Based Protein Identification by Machine Learning from a Library of Tandem Mass Spectra. *Nat. Biotechnol.* **2004,** *22,* 214-219.

237. Gibbons, F. D.; Elias, J. E.; Gygi, S. P.; Roth, F. P. SILVER Helps Assign Peptides to Tandem Mass Spectra using Intensity-Based Scoring. *J. Am. Soc. Mass Spectrom.* **2004,** *15,* 910-912.

238. Zhang, Z. Prediction of Low-Energy Collision-Induced Dissociation Spectra of Peptides. *Anal. Chem.* **2004,** *76,* 3908-3922.

239. Zhang, Z. Prediction of Low-Energy Collision-Induced Dissociation Spectra of Peptides with Three or More Charges. *Anal. Chem.* **2005,** *77,* 6364-6373.

240. Narasimhan, C.; Tabb, D. L.; VerBerkmoes, N. C.; Thompson, M. R.; Hettich, R. L.; Uberbacher, E. C. MASPIC: Intensity-Based Tandem Mass Spectrometry Scoring Scheme That Improves Peptide Identification at High Confidence. *Anal. Chem.* **2005,** *77,* 7581-7593.

241. Sun, S.; Meyer-Arendt, K.; Eichelberger, B.; Brown, R.; Yen, C.-Y.; Old, W. M.; Pierce, K.; Cios, K. J.; Ahn, N. G.; Resing, K. A. Improved Validation of Peptide MS/MS Assignments Using Spectral Intensity Prediction. *Mol. Cell. Proteomics* **2007,** *6,* 1-17.

242. Sechi, S.; Chait, B. T. Modification of Cysteine Residues by Alkylation. A Tool in Peptide Mapping and Protein Identification. *Anal. Chem.* **1998,** *70,* 5150-5158.

243. Moritz, R. L.; Eddes, J. S.; Reid, G. E.; Simpson, R. J. S-Pyridylethylation of Intact Polyacrylamide Gels and In-Situ Digestion of Electrophoretically-Separated Proteins: A Rapid Mass Spectrometric Method for Identifying Cysteine-Containing Peptides. *Electrophoresis* **1996,** *17,* 907-917.

244. Shevchenko, A.; Wilm, M.; Vorm, O.; Mann, M. Mass Spectrometric Sequencing of Proteins from Silver-Stained Polyacrylamide Gels. *Anal. Chem.* **1996,** *68,* 850-858.

245. Hunter, E. P.; Lias, S. G. Evaluated Gas Phase Basicities and Proton Affinities of Molecules: An Update. *J. Phys. Chem. Ref. Data* **1998,** *27,* 413-656.

246. Zhang, R.; Sioma, C. S.; Thompson, R. A.; Xiong, L.; Regnier, F. E. Controlling Deuterium Isotope Effects in Comparative Proteomics. *Anal. Chem.* **2002,** *74,* 3662-3669.

247. Lehmann, W. D.; Kruger, R.; Salek, M.; Hung, C.-W.; Wolschin, F.; Weckwerth, W. Neutral Loss-Based Phosphopeptide Recognition: A Collection of Caveats. *J. Proteome Res.* **2007,** *6,* 2866-2873.

248. Rusnak, F.; Mertz, P. Calcineurin: Form and Function. *Physiol. Rev.* **2000,** *80,* 1483-1521.

249. Chin, D.; Means, A. R. Calmodulin: A Prototypical Calcium Sensor. *Trends Cell Biol.* **2000,** *10,* 322-328.

250. Heineke, J.; Molkentin, J. D. Regulation of Cardiac Hypertrophy by Intracellular Signalling Pathways. *Nat. Rev. Mol. Cell Biol.* **2006,** *7,* 589-600.

251. Fujiwara, A.; Kakizawa, S.; Iino, M. Induction of Cerebellar Long-Term Depression Requires Activation of Calcineurin in Purkinje Cells. *Neuropharmacology* **2007,** *52,* 1663-1670.

252. Kissinger, C. R.; Parge, H. E.; Knighton, D. R.; Lewis, C. T.; Pelletier, L. A.; Tempczyk, A.; Kalish, V. J.; Tucker, K. D.; Showalter, R. E.; Moomaw, E. W.; Gastrinel, L. N.; Habuka, N.; Chen, X.; Maldonado, F.; Barker, J. E.; Bacquet, R.; Villafranca, J. E. Crystal Structures of Human Calcineurin and the Human FKBP12-FK506-Calcineurin Complex. *Nature* **1995,** *378,* 641-644.

253. Ye, Q.; Li, X.; Wong, A.; Wei, Q.; Jia, Z. Structure of Calmodulin Bound to a Calcineurin Peptide: A New Way of Making an Old Binding Mode. *Biochemistry* **2006,** *45,* 738-745.